Trailer Sway Control Using an Active Hitch

by

Connor Fry Sykora

A thesis

presented to the University of Waterloo

in fulfillment of the

thesis requirement for the degree of

Master of Applied Science

in

Mechanical and Mechatronics Engineering

Waterloo, Ontario, Canada, 2017

Author's Declaration

I hereby declare that I am the sole author of this thesis. This is a true copy of the thesis, including any required final revisions, as accepted by my examiners.

I understand that my thesis may be made electronically available to the public.

Abstract

The handling and yaw stability characteristics of passenger vehicles are drastically changed when towing a trailer, which can lead to unsafe oscillations in the trailer yaw, known as trailer sway. This thesis examines the feasibility of using lateral articulation of the hitch ball to reduce sway behavior in passenger-sized tractor-trailer configurations. An articulating hitch ball design has the advantage of not being dependent on the trailer being towed, providing stability improvements to the wide variety of trailers that a passenger vehicle may tow over its life cycle.

Changes in the lateral position of the hitch relative to the tractor create dynamic changes to the heading angle of the trailer relative to the tractor, which act as compensating steering inputs into the system. To examine the effectiveness of this method, a linear handling model was developed to predict the system response with different trailer configurations and feedback methods. This model was simulated with various feedback controllers, and the modeling was validated using a model constructed in MapleSim, a high-fidelity multibody simulation tool.

After establishing the required performance characteristics of the active hitch, a prototype was designed, manufactured, and tested in a full scale tractor-trailer combination. The modeling techniques showed good agreement with the physical testing, where the control design of proportional feedback on the trailer articulation angle provided improved yaw stability across many trailer configurations. The simple controller design is adaptable to driving conditions and requires minimal measurements of vehicle states. The performance of the active hitch prototype is best shown in a response to a steering impulse at 65km/h, where a highly unstable trailer causes steady state oscillation without control, and settles in under 4 seconds with control active.

Acknowledgements

It was a pleasure to work on this project under the supervision of Amir Khajepour. His vision for vehicle research provides the entire Mechatronic Vehicle Systems Lab with stimulating, self-driven research projects, which are always nested within the practical constraints of industrial automotive engineering.

I would like to thank Jeff and Jeremy, the MVSL technical staff, for their help in the implementation and testing of my active hitch setup. The technical support in our lab is essential for prompt completion of the short-term projects in the lab, and for maintaining workflow in larger-scale projects.

I would like to acknowledge my fellow graduate students and researchers from the MVSL, who are friendly, knowledgeable, and always willing to engage in some technical discussion. Best of luck in your future endeavors.

Table of Contents

List of Figures

List of Tables

Chapter 1: Introduction

Articulated vehicles refer to any vehicle configurations with pivoting joints, allowing the vehicle to carry a larger payload, while still maintaining the ability to navigate sharp turns. Articulated vehicles typically comprise a **tractor**, which contains the prime mover for the system, and one or more **trailers**, which contain the extra cargo space. These vehicles have widespread use in commercial and passenger vehicle applications. The articulation of the trailer joint introduces new modes of instability. This added instability, coupled with the ubiquity of articulated vehicles in the transportation industry, demands that these systems be studied to determine general trends in stability and to apply appropriate active safety measures.

Trailer sway is characterized by transient oscillations in the trailer articulation angle, which transmit forces to the tractor and the driver, decreasing handling. If these oscillations persist or become divergent, the tires will saturate their lateral handing ability, usually leading to an accident. Most trailer configurations exhibit some level of oscillation at city and highway speeds, so trailer sway is defined loosely in the context of this thesis as oscillations that are potential causes of an accident. Trailer sway occurs when the vehicle is in an understeer configuration, whereas single mass vehicles are inherently stable when they understeer, so the handling characteristics of the tractor cannot be used to predict trailer sway.

To avoid sway, there exist rules of thumb that suggest that passenger vehicle trailers should be loaded such that 10% of the trailer weight is on the hitch ball, although experimental research suggests that the ideal tongue weight is 6-8% [1]. The tongue weight is a primary determinant of trailer stability, along with the overall mass and yaw inertia of the trailer, but these recommendations are not common knowledge, which leads to unsafe towing that greatly increases the risk of an accident.

Current passenger vehicle anti-sway solutions either revolve around passive systems that introduce friction into the trailer joint, or use the trailer brakes to apply differential tractive force to the system. These very different methods leave a middle ground, for an anti-sway system that has higher effectiveness than a passive element, and does not require a modern trailer configuration with sensors, communication channels, and braking.

This thesis describes the modeling, design, manufacturing, and testing of a novel anti-sway concept, called the **active hitch.** The prototype uses a planar linkage that changes the lateral position of the hitch ball to introduce changes in the trailer heading angle. The thesis is divided into four main chapters which document the active hitch development. First, a review of current sway control solutions to determine the benchmark performance for the active hitch, followed by dynamic modeling, control design and simulation of the augmented tractor-trailer system. Using the simulations and current literature, the performance metrics are carried forward to the physical design of the active hitch, including structural components, sensor integration, and the actuation system. Finally, the testing of the completed prototype is discussed, with techniques used to improve performance and the results of the full scale testing using research vehicle platforms.

A top-view graphic of the tractor-trailer configuration is shown in Figure 1.1, contrasted with the final setup used in the experiments:

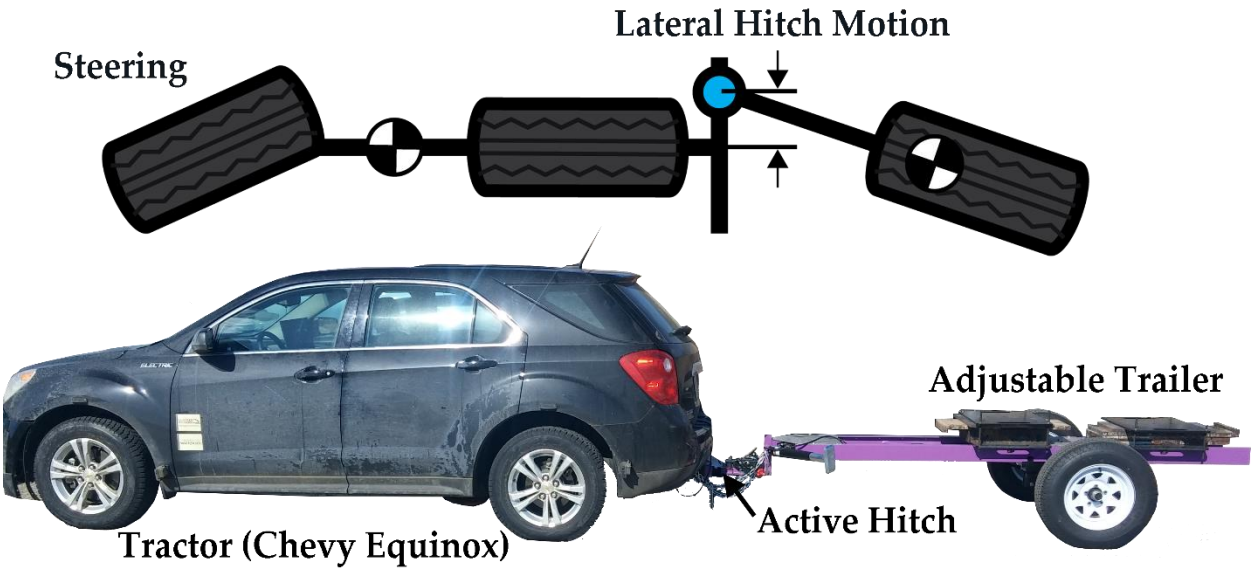

Figure 1.1: Simplified model for active hitch and final testing configuration

The Equinox is used for several projects, but did require modification for this research, whereas the hitch and trailer were designed and built specifically for this research. Based on the effectiveness of active hitch sway control, the prototype hitch may be considered for commercialization, so its features were designed to be as practical as possible for a commercial solution, subject to the time constraints of the project.

Chapter 2: Literature Review

Based on a review of current research in trailer stability, it appears that the use of an active hitch in high speed driving has not been explored. If this thesis can show that sway control via active hitch is feasible, then it will fill a gap in trailer active safety: the active hitch would be able to control a larger variety of trailers, including those that do not have integrated brakes or other electronic systems.

This chapter examines the literature in vehicle stability that are relevant to development of the active hitch. They are subdivided into the following categories:

- Dynamic modeling of vehicle handling, where the standard handling models will be expanded in Chapter 3 to include the active hitch.
- Current methods of sway control in passenger and commercial vehicle combinations, which establish performance goals that the active hitch should meet.
- Low speed maneuvers and trailer backing, which is a popular research category for trailer dynamics, and is a potential auxiliary use for the active hitch.
- Estimation methods in vehicle dynamic control, which allow for additional information to be provided to the controller when limited measurements are available.

The state-of-the-art, both in academic and industrial spaces, helps guide the design of the active controller and its physical layout.

2.1 Tractor-Trailer Modeling

A tractor-trailer often refers to a heavy truck-semitrailer combination, featuring multiple axles on both the tractor (truck or tow vehicle) and the trailer. The terms are used more generally in this section, although this research focuses on passenger vehicle tractors with single axle trailers. Modeling is almost identical between passenger and commercial configurations, and multiple axles can be mathematically reduced to single equivalent axles for direct comparison.

The lateral movement of the active hitch creates dynamic changes in the heading angle of the trailer. This produces lateral forces in the trailer tire, which act to damp out unwanted oscillations in the trailer angle. The heading changes in the trailer are analogous to applying

steering angles to the tractor wheels, so it is appropriate to examine current handling models that are used in yaw control.

A simple model that is ubiquitous in vehicle yaw control is the bicycle model [2]. The bicycle model is a single track model and assumes a linear tire model for the introduction of lateral forces into the system, which allows for various linear-time-invariant state-space formulations of the equations of motion to be derived. A schematic of the bicycle model along with the state space realisation is shown in Figure 2.1 [3]:

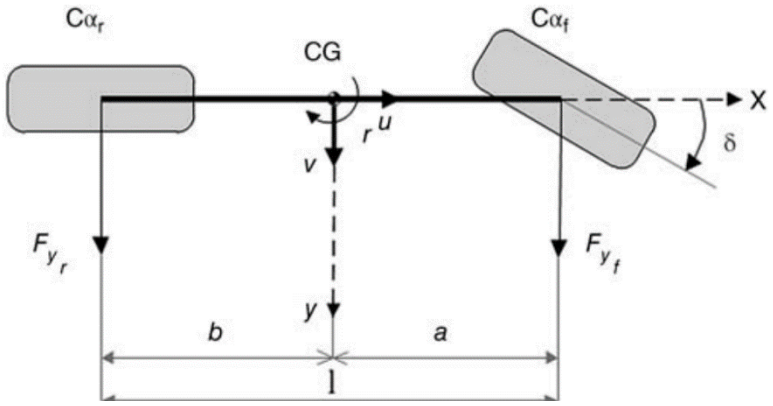

$$\begin{pmatrix} \dot{v} \\ \dot{r} \end{pmatrix} = \begin{pmatrix} -\frac{C_{\alpha r} + C_{\alpha f}}{Mu} & \frac{(bC_{\alpha r} - aC_{\alpha f})}{Mu} - u \\ \frac{(bC_{\alpha r} - aC_{\alpha f})}{I_z u} & -\frac{(b^2 C_{\alpha r} + a^2 C_{\alpha f}}{I_z u} \end{pmatrix} \begin{pmatrix} v \\ r \end{pmatrix} + \begin{pmatrix} \frac{C_{\alpha f}}{M} \\ \frac{aC_{\alpha f}}{I_z} \end{pmatrix} \delta$$

Figure 2.1: Single track linear handling model

The relative simplicity of the model make it extremely useful in model-predictive controllers, where the future behaviour of the model must be predicted for each time step [4]. While the bicycle model does not directly include tractive forces, these forces can be resolved into external torques applied to the vehicle body, allowing for the use of the bicycle model when designing yaw stability controllers based on active braking or torque vectoring. The greatest weakness of the bicycle model is the assumption of a linear tire model. The more accurate tire models are highly nonlinear, and demonstrate that steering has decreasing effectives in applying lateral forces to the system at higher slip angles [5]. For a given normal force, the primary determinant of the lateral tire force is the slip angle, as shown in Figure 2.2.

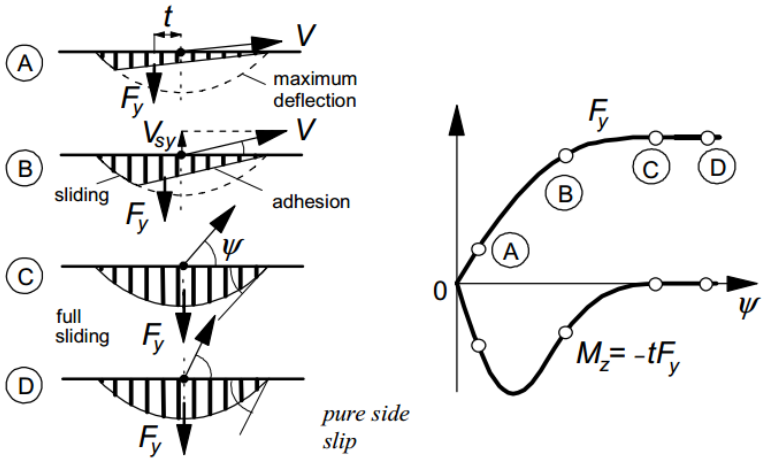

Figure 2.2: Effect of slip angle on tire characteristics [5]

Analysis of the equations of motion in simple handling models also allow certain stability metrics to be established for a vehicle based on its size and inertial parameters [6]. Specifically, the understeer coefficient and steady state gains can be used to predict a vehicle response without having to fully simulate the state-space model. Oversteer vehicles can reach a speed at which no steering input will prevent instability, as shown in Figure 2.3:

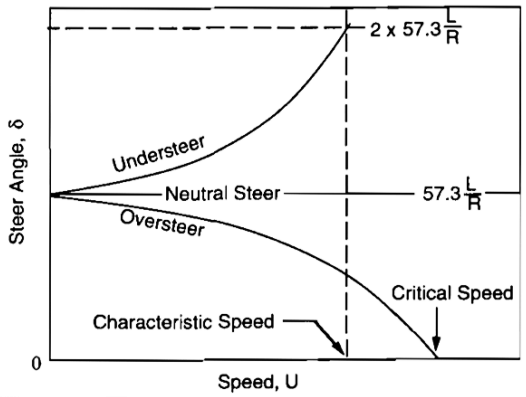

Figure 2.3: Understeer coefficient effects on steering sensitivity [6]

It is important to note that sway behavior occurs when the tractor trailer is understeer, so there is an additional mode of instability introduced when coupling the tractor and trailer. To assess the requirements for the active hitch, the stability of the tractor-trailer systems must be examined. The bicycle model has been extended to include a trailer to study the multibody coupling effects [7]. The tractor-trailer is a multibody system, so the methods for deriving the equations of motion are slightly different than for the lone tractor bicycle model. There have been multiple approaches for deriving the equations, which all result in slightly different state space

realizations. A Newtonian approach uses the method of constructing free-body diagrams and resolving the tractor-trailer constraint through a balance of forces [8]. Alternatively, open chain dynamics can be addressed using a Lagrangian approach, where the kinetic and potential energies of the links (the tractor and trailer) can be used to predict the system dynamics [9], and the constraint equation is solved more implicitly than with the Newtonian approach. This can be used to easily extend the bicycle model to multiple trailers in a single chain [10]. Similar to the case of the lone tractor, the state space realizations can be used to derive static performance and stability parameters like the understeer coefficient and the steady state response to a given steering angle, without requiring full simulation of the equations [11].

2.2 Sway Control Methods

Assuming a tractor will be carrying a similar payload in a particular trailer, the most effective stabilization can be attained by integrating the control action between the tractor and trailer. Direct yaw control (DYC) has been extremely popular in many vehicle systems due to its ability to generate large external moments, and its ability to function outside the typical working region of the tires [12]. DYC, which relies on applying differential brake action or tractive force depending on the detected yaw instability, has been effectively extended to tractor trailer systems, using extra brakes on the trailer [13]. Since the dynamics of the tractor and trailer are highly coupled, it is possible to control the trailer instability indirectly by compensating for yaw oscillations in the tractor. This allows DYC methods to be applied to passenger vehicle configurations, where a certain tractor will be expected to tow a variety of trailers throughout its life [14]. There is also a trend of integrating DYC systems with other controllers and safety systems [15]. These integrated controllers allow other tractor safety systems like ABS or active steering to indirectly stabilize the trailer behavior. In passenger vehicle configurations, DYC control has been implemented in a standalone package that sends braking commands to the trailer brakes based on an inertial measurement unit [16].

Another approach to trailer stability used in passenger vehicles is passive systems. While not nearly as sophisticated as the active methods described above, they have the advantage of being inexpensive and can be installed after-market on nearly any passenger vehicle configuration. Most often, these systems feature some method of restricting the articulation angle of the trailer.

One such example is shown in Figure 2.4, where friction dampers are coupled to the trailer articulation via a second hitch ball, reducing high speed changes in trailer yaw [17].

Figure 2.4: Sway control via friction damping element [17]

The added resistance to trailer articulation also helps to attenuate high frequency disturbances, such as wind loads or uneven road conditions, although these systems are not as effective as active methods in reducing trailer sway. In addition to these industrial solutions, researchers have also proposed alternate hitch designs that can prevent sway passively. One such concept uses two non-parallel planar links to attach the trailer to the tractor, forming a four-bar linkage [18]. A diagram of the setup is shown Figure 2.5:

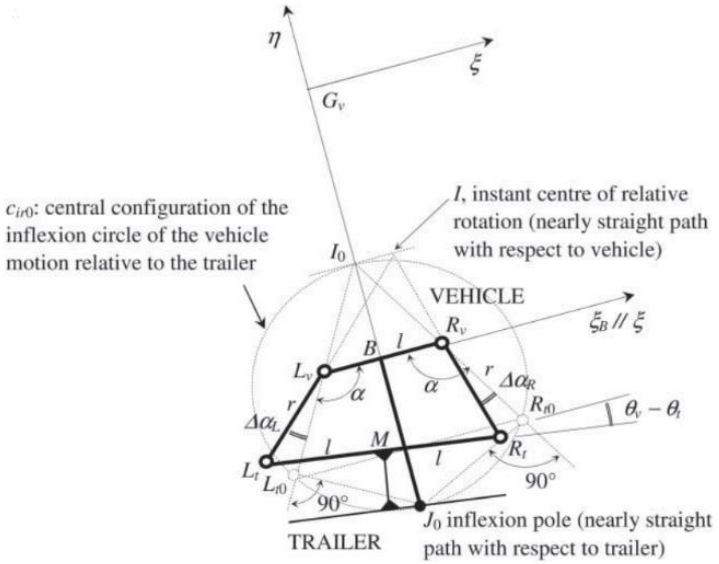

Figure 2.5: Passive sway reduction via four-bar linkage hitch connection [18]

The four-bar linkage kinematics can change the center of rotation of the trailer about the tractor, which can introduce automatic negative feedback to the trailer motion. Different linkage kinematics would be required for different trailers, so this method would lack some versatility. The active hitch design can mimic this effect of changing the instant center with its physical implementation and through control action that creates a nonlinear motion profile.

The articulating hitch point in this thesis is more similar to an active steer-type controller than to DYC, so it is important to also consider the function of active steering controllers. There has been some research into applying steering angles to the trailer axles, but their applications are in low speed maneuvers rather than cruising speeds [19] [20]. Active steering controllers are less jarring to the driver relative to DYC since no harsh tractive inputs are required. However, since active steering controllers depend on the lateral forces provided by the steered tires, they are not as effective as DYC controllers in high slip angle or low road friction scenarios. To compensate for this shortcoming, the two systems have been combined into a hybrid controller that benefits from the appropriate application of both methods [21].

2.3 Low Speed Maneuvers and Backing

Tractor trailer backing up maneuvers are inherently unstable, and can easily lead to low speed jackknifing in the hands of an unskilled driver. While it is out of the scope of this thesis, the active hitch controller has potential for use in a low speed backing scenario, since the small changes in trailer angle can correct the heading before it diverges to jackknifing.

Methods for controlling backing maneuvers often involve some form of predictive control, which determines the optimal path to follow in order to achieve some desired change in orientation [22]. Since these methods attempt to define optimal behavior given a large solution space, the solutions tend to involve intelligent systems applications of optimization, namely genetic algorithms [23]. The intelligent systems are combined with more traditional techniques like model predictive control or sliding mode control to produce robust, hybridized control systems. An active hitch method for controlling backup maneuvers was developed using a fuzzy logic controller [24]. The controller is formulated as a line follower, where the hitch movements supplement the steering inputs required to follow the path. This controller relies on a pre-

determined path, which is similar to industrial solutions for backing [25]. These controllers are limited to situations where the driver intends to perform a particular maneuver.

While the backing controllers mostly use steering of the front tractor wheels to maneuver, active hitches have also been used in low speed applications to reduce off tracking in semi-trailers [26]. This active hitch configuration could be used for high speed sway reduction, although the effect size would likely be small because of the long wheelbases of semi-trailers. The off tracking reductions were made based on approximately 0.2m of hitch travel. Considering the size of semi-trailers relative to those towed by commercial vehicles, it is promising that relatively small hitch movements can create large changes in stability. Off tracking in semi-trailers has also been examined using an active steering solution [20].

2.4 Estimation

One of the goals of the active hitch controller is to use as few measurements as possible to stabilize the trailer sway. Additionally, the controller should function without knowledge of the trailer configuration. The specific geometric and inertial parameters of the trailer have a large effect on its stability, and without knowing the specific parameters, the controller must be functional over a large range of behavior. Estimation techniques can be used to solve both these problems, where different types of observers can be used to guess vehicle states, as well as configuration parameters.

To estimate the unmeasured states of a tractor-trailer system, a model of the vehicle handling can be combined with an observer. These observers use statistical models to predict the missing states. The observers require a relatively accurate vehicle model to correctly predict the missing states. When the vehicle model is not known, intelligent systems can be used to identify states. Neural networks can mimic an unknown system model in a black-box sense. The model for the tractor-trailer handling can be combined with a genetic evolution method to determine which model can most accurately predict the tractor and trailer states [27].

These intelligent techniques can also be used for system identification. This allows the unknown parameters of the vehicle model (masses, wheelbases, etc.) to be estimated. This is particularly relevant to the active hitch design, since the trailer parameters will not be explicitly provided to

the controller. In addition to its use as an observer, Kalman filters can also be used for system identification in vehicle handling models [28]. As with state estimation, parameter estimation of vehicle handling models are well suited to intelligent techniques like genetic algorithms [29]. Hybrid systems have been employed in the mass estimation of vehicles, where the different observer techniques provide checks on each other [30]. The trailer mass is highly variable in passenger vehicles, so the active hitch system could use mass estimation for automatically identifying the dynamics of different trailers. In addition to passenger configurations, mass identification techniques have been successfully employed in semi-trailer configurations, where the variance in payload is also extreme [31].

2.5 Summary

Current literature in handling models for tractor-trailer configurations indicate that it should be reasonably straightforward to incorporate the active hitch, building on the previous models. In high speed sway control, DYC methods offer effective damping at the cost of increased complexity, while commercial passive solutions are simple to implement, but lack the same effectiveness. This leaves a middle ground for the active hitch controller: maintain some of the effectiveness of DYC methods, while being as versatile as the passive methods. Where there are gaps in the knowledge of the vehicle system required to apply the control action, intelligent systems and other observers can be employed to ensure that the active can operate with as few direct measurements as possible. The use of the active hitch for backing assistance is not included in the scope of this thesis, although current research on using mobile hitches and steerable trailer wheels suggest that the active would be well-suited for future research in backing control.

Chapter 3: Control Design and Simulation

Since the idea of trailer stability control via active hitch is relatively unexplored in current literature, dynamic modeling and simulation of the system is required before designing a prototype hitch. The accuracy of the simulation techniques developed in this chapter will be validated through the physical testing of the hitch as discussed in chapter 5, and will be derived based on previous research in trailer stability as discussed in chapter 2. The major components of the theoretical and simulation development are as follows:

- The requirements and goals of the feedback controller.
- Multibody dynamic modeling of the tractor-trailer system, based on an extension of the "bicycle" handling model.
- Simulation of the extended bicycle model and feedback controller in MATLAB.
- High-fidelity simulation of the system in MapleSim, using custom MapleCar modules.

The results of the simulations will be combined with recommendations from literature to inform the design of the hitch system as described in chapter 4.

3.1 Control Design Overview

The high-level goal set at the beginning of this project is to develop a mechanism that allows the hitch point to move laterally to reduce trailer sway, which can be used on a variety of tractor-trailer configurations. Therefore, the control design must function with limited sensing, and must be robust to changes in tractor trailer lateral dynamics. For a standalone system, the active hitch may not have access to measurements taken by the tractor, so the sensing should be designed such that it can be contained within the hitch system. Despite limited sensing, the active hitch system should be able to adequately control stable and unstable trailer configurations, where the stability of those configurations is also dependent on the overall vehicle speed.

The obvious measurements to make using the active hitch are the lateral position of the hitch ball, and the trailer yaw angle relative to the tractor. These measurements can be made using simple sensors that are easy to package within a standalone system. Using numerical differentiation, the rates of change in these positions can also be estimated. If these

measurements cannot provide the basis for an effective controller, an important variable to measure is the tractor longitudinal speed. It is an essential factor in vehicle yaw dynamics, as critical speeds establish the point at which mathematically unstable system response occurs.

Assuming no further knowledge of the system, a simple feedback controller can articulate the hitch based on an error signal. Since sway behavior is characterized by yaw oscillations between the tractor and trailer, it is intuitive to choose the trailer angle as an error signal. The limitation of using the trailer angle is that during a turn maneuver, the trailer will settle to a nonzero angle based on the system dynamics, and so the hitch position will not always return to zero. It is therefore useful to use the relative angular rate of the trailer as an error signal, since a stable trailer will follow the yaw rate of the tractor, resulting in zero difference in yaw rates.

The use of the trailer angle and yaw rate as error signals sets the basis for a PD-type feedback controller for the active hitch system. More complicated model-predictive controllers were simulated based on an extended bicycle model (discussed further in section 3.2). This control model requires measurement of additional system states, and the increase in performance was not significant enough to be justified, since the active hitch would be less of a standalone system if it required multiple measurements from the tractor. Different types of intelligent controllers were also considered in simulation. Controllers based on fuzzy inference or neural networks do not require extensive system knowledge, and can adapt to varying conditions. Further discussion on the use of intelligent systems in the controller design is provided in section 3.2.6.

3.2 Dynamic Modeling

To model the multibody dynamics of the tractor-trailer combination, a lateral handling model was developed. The active hitch is concerned primarily with yaw dynamics, so a state space realisation was developed based on the bicycle handling model described in section 2.1. The bicycle model is used widely in vehicle dynamics modeling, and is used to simply describe the response of a vehicle to steering inputs [2]. The bicycle model assumes a single track (one tire per axle) and ignores the effect of weight transfer in the tires during lateral maneuvers. It has been derived for use in lone tractor configurations, and research on tractor-trailer yaw stability have extended the model to include the trailer. Since the model is derived into a linearized state space representation, it can easily be implemented in MATLAB, and can make use heuristics and

methods from classical control theory. The low computational load in simulating state space representations allows for rapid iteration of different controller designs and maneuvers, which can later be implemented in high-fidelity simulation or in physical tests. Bicycle models usually retain accuracy within 10% of an experiment, as long as the wheel sideslip angles are lower than 10° [15].

3.2.1 Extended bicycle model

The following state space realization further extends the bicycle model to include the dynamics that are introduced by a moveable hitch ball. The base assumptions for a bicycle model are as follows:

- Planar motion (bounce, pitch, and roll motions are ignored)
- Single track (effects of vehicle width are ignored)
- Constant longitudinal velocity (to avoid non-linearity in the vehicle sideslip definition)
- Small angles (trigonometric simplification for wheel & vehicle sideslip, trailer angle, steering)
- Linear tire model (lateral force from tire is proportional to the sideslip angle)
- Small angular rates (products of angular rates have negligible effect on results)
- Three axle (front tractor, rear tractor, trailer)

A schematic of the extended bicycle model is shown in Figure 3.1:

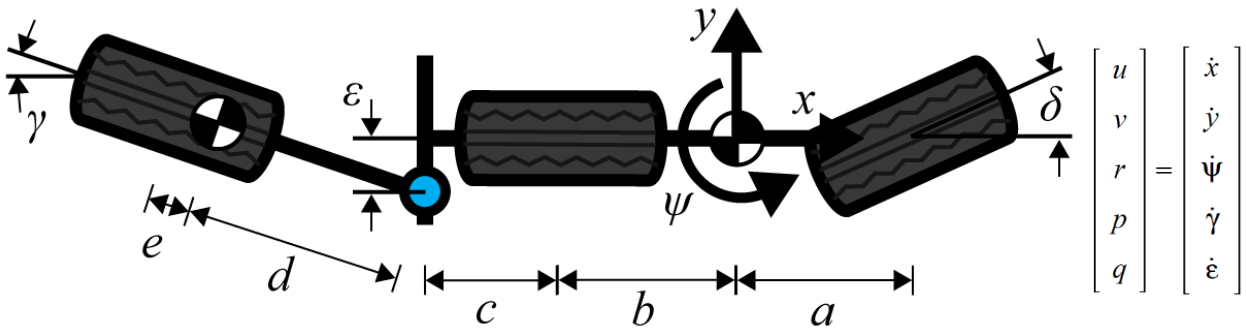

Figure 3.1: Extended bicycle model diagram, including alternate naming for rates of change

Derivation of the base bicycle model consisting of the lone tractor results in two degrees of freedom: the local lateral position y, and the global tractor yaw ψ. The local coordinate system is located at the vehicle center of mass. Local coordinates can be transformed back into global coordinates to produce the position and orientation of the vehicle at any time. The two degrees of

freedom result in two system states: the vehicle lateral velocity v and the yaw rate r. The variable names are changed to be consistent with literature, and the state space realization is a 2x2 system matrix, with its one input being the steering angle δ. The extension of the vehicle model introduces the trailer angle γ and the hitch lateral position ε as degrees of freedom. The hitch position is treated both as an input and a degree of freedom, with results in the final state space realisation comprising of a 4x4 system matrix with two inputs: the steering angle and the hitch position. The names of the variables are chosen to be consistent with literature.

The geometric parameters a, b, c, d, e remain constant based on the tractor-trailer combination, as well as the inertial properties m_1, m_2, J_1, J_2, corresponding to the tractor and trailer masses and yaw inertias (measured about their respective mass centers).

Current literature on tractor-trailer modeling uses two main methods to derive the equations of motion. The first is a Newtonian approach, which involves creating free-body diagrams to resolve the forces, and using constraint equations to connect the two bodies. The second method is Lagrangian, which relies on balancing kinetic and potential energies in the system. The second method was chosen because it does not require calculation of the reaction force in the hitch; since the hitch is being driven as an input, the reaction force along that degree of freedom is not explicit. The reaction force can be calculated independently using the Newtonian approach. The Lagrange energy method as described in [9] uses an equation for each degree of freedom in the system, which are arranged by state variable and converted into a state space model:

$$\frac{\mathrm{d}}{\mathrm{d}\,t}\frac{\partial K}{\partial \dot{z}_i} - \frac{\partial K}{\partial z_i} + \frac{\partial V}{\partial z_i} = Q_i \tag{3.1}$$

The left-hand side of the equation contains the differentiation of kinetic and potential energies K and V with respect to the state variables z_i. There is no potential energy term in this case. The right hand side considers the external forces that are acting directly on the degree of freedom. In the bicycle model, the only external forces are lateral forces in the tires, which will be derived later. The kinetic energy in the system is based on the global translational and rotational speeds of the tractor and trailer:

$$K = \frac{1}{2}\cdot J_1 \cdot r_1^{\,2} + \frac{1}{2}\cdot J_2 \cdot r_2^{\,2} + \frac{1}{2}\cdot m_1 \cdot \left(\dot{X}_1^{\,2} + \dot{Y}_1^{\,2}\right) + \frac{1}{2}\cdot m_2 \cdot \left(\dot{X}_2^{\,2} + \dot{Y}_2^{\,2}\right) \tag{3.2}$$

To be compatible with the lateral forces from the tires, the global translations in the kinetic energy formula must be converted into the local frame, which is centered on the tractor center of mass and rotates with the tractor. The trailer rotational rate is translated simply by adding the relative trailer yaw rate p to the global tractor yaw rate ($r_1 = \dot{\psi}$). Based on the diagram on the previous page, the localized kinetic energy is resolved to:

$$K = \frac{1}{2} J_1 \cdot r^2 + \frac{1}{2} J_2 \cdot (r+p)^2 + \frac{1}{2} m_1 \cdot \left(u^2 + v^2\right) + \frac{1}{2} m_2 \left(\left(u + d\sin(\gamma)(r+p) - \varepsilon r\right)^2 + \left(v - (b+c)\, r - d\cos(\gamma)(r+p) + q\right)^2 \right) \tag{3.3}$$

The left-hand side of equation (3.1) also needs to be transformed into local frame, which is centered at the tractor CG and rotates with the tractor. This only applies to the tractor lateral velocity and yaw states, since the trailer angle and hitch position are already defined in terms of the local coordinates. The lateral velocity transformation is found as follows:

$$\begin{bmatrix} LHS_{X_1} \\ LHS_{Y_1} \end{bmatrix} = \begin{bmatrix} \frac{\mathrm{d}}{\mathrm{d}t}\frac{\partial K}{\partial \dot{X}_1} - \frac{\partial K}{\partial X_1} \\ \frac{\mathrm{d}}{\mathrm{d}t}\frac{\partial K}{\partial \dot{Y}_1} - \frac{\partial K}{\partial Y_1} \end{bmatrix} = \begin{bmatrix} \frac{\mathrm{d}}{\mathrm{d}t}\left(\frac{\partial K}{\partial u}\cos\psi - \frac{\partial K}{\partial v}\sin\psi\right) \\ \frac{\mathrm{d}}{\mathrm{d}t}\left(\frac{\partial K}{\partial u}\sin\psi + \frac{\partial K}{\partial v}\cos\psi\right) \end{bmatrix} = \begin{bmatrix} \cos\psi & -\sin\psi \\ \sin\psi & \cos\psi \end{bmatrix} \begin{bmatrix} \frac{\mathrm{d}}{\mathrm{d}t}\frac{\partial K}{\partial u} - r\frac{\partial K}{\partial v} \\ \frac{\mathrm{d}}{\mathrm{d}t}\frac{\partial K}{\partial v} + r\frac{\partial K}{\partial u} \end{bmatrix} \tag{3.4}$$

The first term is the planar rotation matrix that transforms the global translational speed into u and v. Applying similar transformations to the local yaw component results in the following expressions for the left-hand side of the Lagrange equation:

$$\begin{aligned} LHS_y &= \frac{\mathrm{d}}{\mathrm{d}t}\frac{\partial K}{\partial v} + r\frac{\partial K}{\partial u} \\ LHS_\psi &= \frac{\mathrm{d}}{\mathrm{d}t}\frac{\partial K}{\partial r} - v\frac{\partial K}{\partial u} + u\frac{\partial K}{\partial v} \end{aligned} \tag{3.5}$$

The right-hand side of the Lagrange equation introduces external forces into the model via the following equation [9]:

$$Q_i = \sum_{k=1}^{n} \left(F_k \frac{\partial T_k}{\partial z_i} \right) \tag{3.6}$$

For each state variable i, all external forces F_k are multiplied with the points of application of the forces T_k, differentiated with respect to the corresponding degree of freedom. The points of application are the centers of the three tires, which are transformed into local coordinates using

the same method used in calculation of the kinetic energy equation. After trigonometric simplification (small angle assumption), the quantities $\partial T_k / \partial z_i$ result in constant terms.

The forces F_k are derived based on the linear tire model from [2]. The linear tire model assumes that the lateral force is proportional to the tire slip angle. True tire behavior is much more complicated, but the assumption of linear behavior is generally valid for slip angles less than 5° [3]. The slip angles for each wheel are determined by the ratios of lateral and longitudinal speed of the tires, combined with any deviation in tire orientation relative to the local frame (steering angle, trailer angle). Since the longitudinal speed is assumed to be constant, the resultant forces are resolved as linear combinations of the state variables. The resultant lateral force inputs are simplified to the following:

$$\begin{aligned} F_{front} &= C_1\left(\delta - \frac{v + ra}{u}\right) \\ F_{rear} &= C_2\left(-\frac{v - rb}{u}\right) \\ F_{trailer} &= C_3\left(\gamma - \frac{v - (b + c + d + e)r - (d + e)p + q}{u}\right) \end{aligned} \tag{3.7}$$

Now that the components of the left-hand and right-right hand side of equation (3.1) have been adjusted to reflect the parameters of the extended bicycle model, the equations can be expanded and re-combined into a state-space realization. The expansion of the Lagrange equations results in more terms than a typical state space realization:

$$M\begin{bmatrix} \dot{v} \\ \dot{r} \\ \dot{p} \\ \dot{\gamma} \end{bmatrix} = F\begin{bmatrix} v \\ r \\ p \\ \gamma \end{bmatrix} + S_1\begin{bmatrix} \delta \\ \varepsilon \end{bmatrix} + S_2\begin{bmatrix} \dot{\delta} \\ \dot{\varepsilon} \end{bmatrix} + S_3\begin{bmatrix} \ddot{\delta} \\ \ddot{\varepsilon} \end{bmatrix} \tag{3.8}$$

The time-derivatives of the states are multiplied by the mass coupling matrix M, which represents the multibody interactions of the tractor and trailer. The terms arise from taking time-derivatives on the left-hand side of the Lagrange equation:

$$M = \begin{bmatrix} m_1 + m_2 & -m_2(b+c+d) & -m_2 d & 0 \\ -m_2(b+c+d) & J_1 + J_2 + m_2(b+c+d)^2 & J_2 + m_2 d(b+c+d) & 0 \\ -m_2 d & J_2 + m_2 d(b+c+d) & d^2 m_2 + J_2 & 0 \\ 0 & 0 & 0 & 1 \end{bmatrix} \quad (3.9)$$

The forcing matrix F contains the terms that represent the tire forces, as well as first-order terms derived from the kinetic energy equation:

$$F = \begin{bmatrix} \frac{-C_1 - C_2 - C_3}{u} & \frac{-C_1 a + C_2 b + C_3(b+c+d+e)}{u} - (m_1 + m_2)u & \frac{C_3(d+e)}{u} & C_3 \\ \frac{-C_1 a + C_2 b + C_3(b+c+d+e)}{u} & \frac{-C_1 a^2 - C_2 b^2 - C_3(b+c+d+e)^2}{u} + m_2(b+c+d)u & \frac{-C_3(b+c+d+e)(d+e)}{u} & -C_3(b+c+d+e) \\ \frac{C_3(d+e)}{u} & \frac{-C_3(d+e)(b+c+d+e)}{u} + m_2 d u & \frac{-C_3(d+e)^2}{u} & -C_3(d+e) \\ 0 & 0 & 1 & 0 \end{bmatrix} \quad (3.10)$$

The input matrices S group the extra terms resulting from steering inputs and the hitch inputs. Since the hitch movement is also a degree of freedom of the system, time derivatives of the hitch position appear as inputs:

$$S_1 = \begin{bmatrix} C_1 & 0 \\ aC_1 & 0 \\ 0 & 0 \\ 0 & 0 \end{bmatrix}, \quad S_2 = \begin{bmatrix} 0 & -\frac{C_3}{u} \\ 0 & \frac{C_3(b+c+d+e)}{u} - m_2 \cdot u \\ 0 & \frac{C_3(d+e)}{u} \\ 0 & 0 \end{bmatrix}, \quad S_3 = \begin{bmatrix} 0 & -m_2 \\ 0 & (b+c+d)\, m_2 \\ 0 & m_2\, d \\ 0 & 0 \end{bmatrix} \quad (3.11)$$

To isolate the time derivatives of the system states, the matrices can be multiplied by the inverse of the mass coupling matrix. The derivatives of the hitch input are not resolvable within the system states, since the hitch position dynamics are not affected by the other system states.

The hitch kinematics are assumed to be only affected by the input of hitch positions, due to the nature of actuating the hitch. As discussed later in chapter 4, the hitch will be driven either by a ball screw drive electric actuator, or by a hydraulic flow valve. In both cases, the actuator behaves like a worm-sprocket gear mesh, where the worm can force the sprocket to move, but

not vice-versa. To make the time derivatives of the hitch input implicit in the state space model, the following method from [32] is used on the state space representation:

A state space model with the form $\dot{x} = Ax + Bu + D\dot{u}$ commonly arises in electric circuit design, where derivatives of the inputs have a dynamic effect on the system states. A modification to the realisation can eliminate the derivatives; Setting $x' = x - Du$ and differentiating with respect to time results in a new realisation:

$$\begin{aligned} \dot{x'} &= (\dot{x}) - D\dot{u} = (A\{x\} + Bu + Du) - D\dot{u} \\ &= A\{x' + Du\} + Bu = Ax' + (AD + B)u \end{aligned} \tag{3.12}$$

This no longer depends on the derivatives of the inputs. This method only functions for first derivatives of the inputs, so the second derivative effect of the hitch accelerations (matrix S_3) must be neglected to form the final state space realization. Simulations of applying pre-defined hitch inputs in MATLAB showed that the results were negligibly different when neglecting the hitch accelerations (<1% change in steady state values, damping ratio, natural frequency). These simplifications lead to the final form of the state space model, where the system states are modified, and the system outputs are the original vehicle states:

$$state\ equation: \begin{bmatrix} \dot{v}' \\ \dot{r}' \\ \dot{p}' \\ \dot{\gamma}' \end{bmatrix} = M^{-1}F \begin{bmatrix} v' \\ r' \\ p' \\ \gamma' \end{bmatrix} + M^{-1}\left(FS_2 + S_1\right) \begin{bmatrix} \delta \\ \varepsilon \end{bmatrix} \tag{3.13}$$

$$output\ equation: \begin{bmatrix} v \\ r \\ p \\ \gamma \end{bmatrix} = \mathbf{I_4} \begin{bmatrix} v' \\ r' \\ p' \\ \gamma' \end{bmatrix} + M^{-1}S_2 \begin{bmatrix} \delta \\ \varepsilon \end{bmatrix} \tag{3.14}$$

$\mathbf{I_4}$ is a 4x4 identity matrix. Since the matrix S_2 has zeros in its first column, the modified states are equal to the original states when the hitch position is static. In the case where the hitch is static, the mass and forcing matrices are identical to similar derivations in tractor-trailer stability literature [33] [10].

3.2.2 System matrix stability

The extended bicycle model can be used to assess which parameters in a tractor-trailer system have the greatest effect on system stability. The linear state space equations produce oscillations in the system that can be analyzed using pole plots. For a given system matrix, the eigenvalues λ predict a second-order response of the system to input, where the imaginary component indicates the oscillation frequency, and the real component indicates the exponential envelope of the response:

$$x(t) \approx e^{-\omega_n \zeta t} \sin\left(\omega_n \sqrt{1-\zeta^2}\, t\right), \quad \omega_n = |\lambda|, \qquad \zeta = {-Re(\lambda)}/{|\lambda|} \tag{3.15}$$

For state matrices with multiple eigenvalues, the eigenvalue with the largest real part will dominate the behavior and the system will behave similar to a second order system, since the exponential terms with smaller real components will decay much more quickly. Even in cases where the dominant pole assumption is less accurate, the eigenvalue with the largest real part is still the primary cause of sway instability in the tractor-trailer system.

For the extended bicycle model, the eigenvalues of the matrix $M^{-1}F$ in equation (3.13) were calculated for the predicted range of trailer characteristics that may be used in simulation and testing. The properties of the tractor are fixed for the eigenvalue study, and are based on the parameters of the Equinox test platform, supplemented with data from [34] and [35]. The input parameters are presented in TABLE 3.I:

TABLE 3.I: EIGENVALUE STUDY PARAMETERS

Parameter	Symbol	Value(s)	Unit
Tractor mass	m_1	2000	kg
Tractor yaw inertia	J_1	3500	$kg\ m^2$
Front cornering stiffness	C_1	90000	N/rad
Rear cornering stiffness	C_2	120000	N/rad
Tractor CG to front axle	a	1.26	m
Tractor CG to rear axle	b	1.6	m
Rear axle to hitch	c	1.1	m
Trailer mass range	m_2	500 to 1000	kg
Trailer yaw inertia	J_2	800 to 1600	$kg\ m^2$
Trailer wheelbase range	$d+e$	1 to 3	m
Trailer tongue weight range	$e/(d+e)$	-20 to 30	$\%\ of\ m_2$

The production Equinox is designed to tow trailers in this mass range, but may be capable of towing trailers up to 1600kg. The cornering stiffness for the trailer is difficult to predict, since cornering properties of low-cost wheels are tested less often, and change based on vehicle and road parameters. As an approximation, the cornering stiffness is roughly proportional to the normal force on the tire [6], so for each combination of parameters, an estimated trailer cornering stiffness is calculated. The results are not highly sensitive to the estimated value, where changes of ±25% to the estimation yielded similar stability regions. The eigenvalue study was performed for low speed (40km/h) and high speed (110km/h) cases, with the resulting eigenvalues plotted in Figure 3.2:

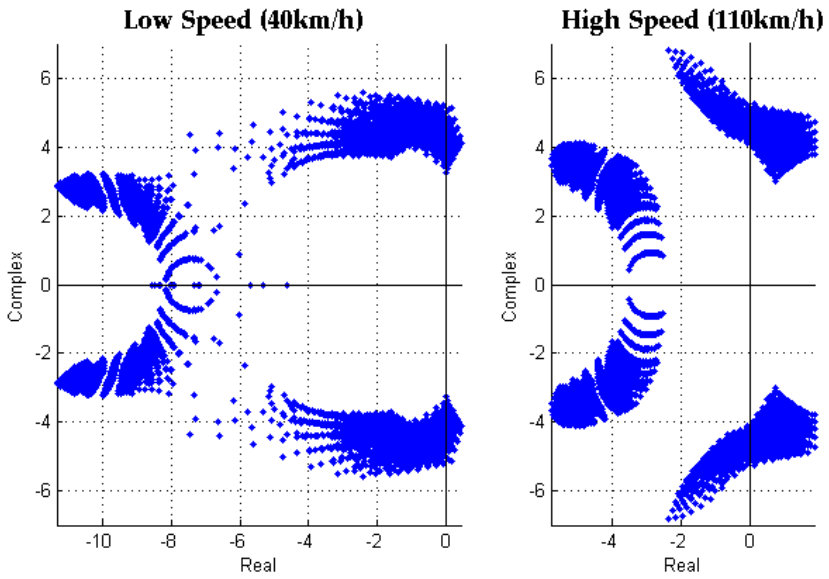

Figure 3.2: Eigenvalues of the system matrix for expected range of trailer configurations

At both low and high speed, the system produces two complex conjugate pairs of eigenvalues. In the high speed case, the distinct regions of eigenvalues show that there is always a dominant set of poles. In the low speed test, the regions are less distinct, but any overlap is far enough left on the real axis that the effects are very quickly damped out of the system.

Using the region of dominant eigenvalues, the damped oscillation frequency of the trailer during sway can be predicted, so that the active hitch can be designed appropriately. The eigenvalue plots predict a maximum oscillation frequency of 6.5 rad/s (1 Hz). In a limit condition, the active hitch should be able to travel across its entire range of motion to keep up with the trailer. The range of motion of the hitch is predicted to be ±10cm, which must be traveled in 0.5s based on the oscillations of the trailer. By predicting a sinusoidal hitch motion from end to end, the

maximum required speed would be in the range of 60cm/s. This range can be reduced by ignoring eigenvalues that have a sufficiently negative real part. For example, real parts smaller than -2 will damp to <10% in one second, which is short relative to the expected oscillation frequencies. For this reason, oscillations that decay in less than a second will not be considered as sway behavior. This peak speed is only required at one instant during the sinusoid, so when designing the active hitch, a speed limited, acceleration limited profile can be used to approximate the sinusoid, where the peak speed is 95% of a pure sinusoid. This reduction, along with the exclusion of values that decay in less than a second, the maximum speed metric for the hitch is set at **45cm/s.** Further discussion on the speed capabilities on the hitch is provided in section 4.2.

To supplement Figure 3.2, each parameter of the system matrix was examined individually for its effect on the overall sway stability. A quantitative list of individual effects is presented in TABLE 3.II:

TABLE 3.II: PARAMETRIC STUDY RESULTS

	To Improve Sway Stability
Tongue Weight $\left(e/d+e\right)$	Increase
Rear Corner Stiffness Ratio $\left(C_2/C_1\right)$	Increase
Trailer Corner Stiffness Ratio $\left(C_3/C_1\right)$	Increase
Hitch Length (c)	Decrease
Trailer Mass (m_2)	Decrease
Trailer Yaw Inertia (J_2)	Decrease

Results from this study are intuitive, and the inertial parameter effects match the experimental results from [1]. The cornering stiffness of the rear tire C_2 is included in the analysis, since varying trailer masses and tongue weights will change the weight loading on the rear wheels of the tractor, which in turn affects the wheel cornering stiffness, in addition to the inertial effects.

3.2.3 Sensitivity to steering input

When deriving vehicle system stability through simple handling models, the responsiveness of the vehicle to inputs can be assessed in terms of the understeer coefficient and the steady state

gains. In this case, both methods can be examined using only the steady-state components of the system response. Examining the final values that the states approach during a static input of steering gives a prediction of how sensitive the vehicle system is to varying steering inputs.

Assuming the transient behavior is eventually damped out, and assuming no inputs from the hitch, the state rates are eliminated and the state equation (3.13) simplifies significantly to:

$$0 = F\begin{bmatrix} v_{ss} \\ r_{ss} \\ p_{ss} \\ \gamma_{ss} \end{bmatrix} + S_1\begin{bmatrix} \delta \\ 0 \end{bmatrix} \tag{3.16}$$

The understeer coefficient is a measure of how the vehicle steady states change with speed. Ideally, vehicles traveling at high speed would require equal or greater steering input to navigate a constant turn of the same radius. This corresponds to neutral steer and understeer cases. For oversteer vehicles, steering sensitivity increases nonlinearly at higher speeds, which can diverge and cause a spinout [6].

The steady state gains follow from the steady state form of the state equation:

$$G = F^{-1}(-S) \quad , \quad G = \begin{bmatrix} \frac{v_{ss}}{\delta} & \frac{r_{ss}}{\delta} & 0 & \frac{\gamma_{ss}}{\delta} \end{bmatrix}^T \tag{3.17}$$

In this case, the understeer coefficient k_{us} can be formulated such that the denominators of the steady state gains approach zero as the coefficient times the square of the velocity approaches the wheelbase of the tractor. This formulation is based on the critical speed of the vehicle, where spinout occurs for any steer input. It is important to note that in tractor-trailer configurations, sway instability can occur well below the critical speed of the system, so this method is only used to examine the steering response of the system. It is still important to consider the steady state gains, since the addition of the trailer has significant effects on handling. The formulation of the understeer coefficient with a trailer was derived as:

$$k_{us} = \frac{m_1 l_2 \left(bC_2 - aC_1\right) - m_2 e \left(c\left(C_1 + C_2\right) + l_1 C_1\right)}{C_1 C_2 l_1 l_2} \tag{3.18}$$

In this case, l_1 , l_2 are the wheelbases of the tractor and trailer, $(a+b)$ and $(d+e)$. The first term of the understeer coefficient is identical to the lone tractor configuration [3], so the second term can be used to examine the effects of adding a trailer. In general, the second term indicates that the tractor-trailer configuration will always be more oversteer than the lone tractor assuming a positive value for e, and therefore more sensitive to speed changes. The steady state gains in equation (3.17) can now be simplified to:

$$\frac{r_{ss}}{\delta} = \frac{u}{u^2 k_{us} + l_1}$$

$$\frac{v_{ss}}{\delta} = \frac{u\left(-u^2\left[\frac{m_1 a l_2 + m_2 e(l_1 + c)}{C_2 l_1 l_2}\right] + b\right)}{u^2 k_{us} + l_1} \tag{3.19}$$

$$\frac{\gamma_{ss}}{\delta} = \frac{-u^2\left(\frac{m_1 a l_2 + m_2 e(l_1 + c)}{C_2 l_1 l_2} - \frac{m_2 d}{C_3 l_2}\right) - l_2 - c}{u^2 k_{us} + l_1}$$

The most important effect to note is that if the trailer tongue weight is zero, the steady state handling of the tractor will be unaffected by adding a trailer. This occurs because when the trailer center of mass is directly above the axle, there is no moment applied to the hitch once the transient effects are damped out. Additionally, the tractor steady state behavior is unaffected by the trailer yaw inertia and the trailer cornering stiffness, although these parameters have a significant effect on the transient response of the system.

3.2.4 Closed loop stability

For a single-input-single-output system, a root locus is a useful tool to show the effect of a proportional feedback control applied to system [36]. For a multi-input-multi-output system like the tractor-trailer formulation, an analogous state space version of the root locus technique can be performed: set the desired input (the hitch position in this case) to a negative proportional feedback vector, multiplied by all system states $u = -Kx$. With the hitch input formulated in terms of the system states, a new system matrix is derived based on the chosen values of K:

$$A_{closed} = A_{open} - BK \tag{3.20}$$

In this case, the system states were augmented with equation (3.12) to remove the input derivatives, so some addition manipulation is required to define the closed system matrix such that the feedback is acting on actual states (yaw, lateral velocity, etc.). The row vector K_p assigns a gain to each original state, and the vector B_2 represents the second column of the matrix $M^{-1}S_2$ from the output equation (3.14), corresponding to the implicit effect of hitch speed. The column vectors B_δ , B_ε represent the first and second columns of the matrix $M^{-1}(FS_2 + S_1)$ from the state equation (3.13), corresponding to the effects of steering and hitch inputs.

The closed-loop system matrix can now be formulated, using θ and θ' as shorthand for the original and transformed system states:

$$\dot{\theta}' = M^{-1}F\theta' + M^{-1}\left(FS_2 + S_1\right)\begin{bmatrix}\delta\\ \varepsilon\end{bmatrix}, \quad \varepsilon = -K_p(\theta) = -K_p\left(\theta' - B_2\varepsilon\right)$$
$$\dot{\theta}' = M^{-1}F\theta' - B_\varepsilon\left(\frac{K_p}{1 - K_pB_2}\right)\theta' + B_\delta\delta \qquad \therefore A_{closed} = M^{-1}F - B_\varepsilon\left(\frac{K_p}{1 - K_pB_2}\right) \tag{3.21}$$

The system matrix now contains the effect of the controller, so the eigenvalues can be examined for different values for K_p. For root locus, the feedback gain is altered to show how the poles (system eigenvalues in this case) vary with feedback size. When examining different feedback gains, it was found that placing a feedback term on the tractor yaw rate or on the trailer yaw rate provided little to no reduction in instability. The root locus plots for the two states that make use of feedback are shown in Figure 3.3:

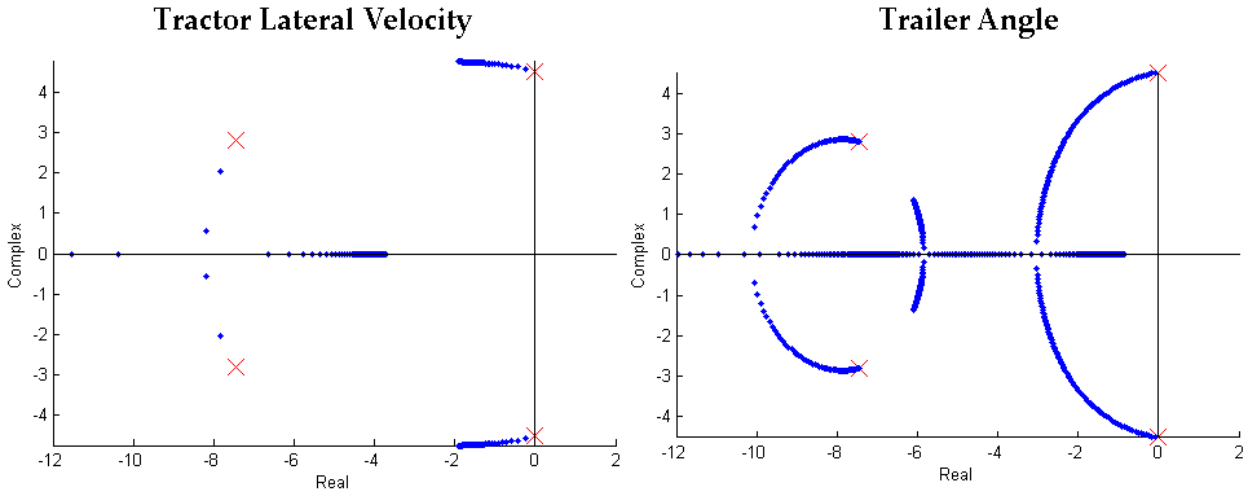

Figure 3.3: Root locus plots for proportional feedback acting on different states

The tractor-trailer configuration for this comparison was chosen such that the open loop ($K = 0$) dominant eigenvalues are on the complex axis, indicated with red "X" marks. Increasing the feedback gain shows a clear decrease in the real eigenvalue components, so the state space model predicts that the active hitch can be used to reduce sway. The eigenvalue study shown in Figure 3.2 can be repeated to show the effect of negative feedback. The high-speed (110km/h) eigenvalue study is shown in Figure 3.4:

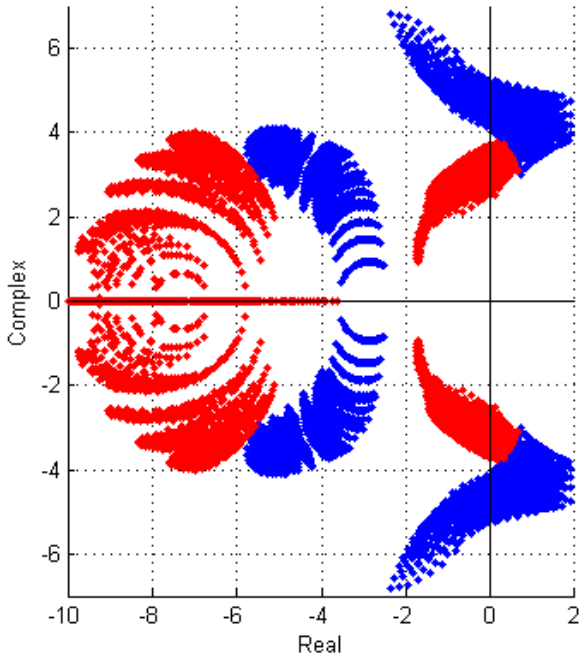

Figure 3.4: Eigenvalues for different trailers at 110km/h, showing open-loop (blue) and closed loop (red) response

The previous figure shows the resulting stability improvement for a unity feedback gain acting on the trailer angle ($\varepsilon = -\gamma$). The simple controller results in a significant reduction in positive real eigenvalues, and significant reduction in the oscillation frequency of the trailer. At this speed, the controller is not able to stabilize every trailer configuration. The same control gain applied to the tractor lateral velocity results in slightly higher stability, however the required control action to achieve the higher stability is almost 5 times higher. By setting a negative feedback gain acting on the trailer yaw rate, some marginal increases in stability are possible, but are mainly applicable to cases where the open loop response has a negative real eigenvalue component. For these reasons, and since the controller is meant to be as standalone as possible, the feedback will be based on the trailer angle instead of the tractor lateral velocity.

3.2.5 Simulations in MATLAB

MATLAB has several tools for analyzing and simulating LTI state-space equations, solved either in discrete or continuous time. The model was first solved in continuous time to ensure that the model is stable in continuous time. Subsequent simulations were performed in discrete time, so that additional elements could be added, like state measurement noise, actuation delays, and more complicated steering sequences.

Several maneuvers were performed on different tractor-trailer combinations to assess potential control solutions. Initial simulations verified the stability plots from the previous section:

- The most efficient error signal to use is the trailer angle.
- Using the trailer yaw rate as a supplemental error signal (PD controller) marginally increases settling time, but has a narrow margin of usefulness.
- Using the tractor states as error signals are not as effective for reducing sway even when the measurements are perfectly accurate. In physical setups, even taking these measurements is a less accurate and requires increased actuation effort for a standalone hitch system.
- The feedback controller is able to decrease sway in marginally stable and unstable tractor-trailer combinations, although certain maneuvers result in an unrealistically high actuation of the hitch.

As discussed in section 3.1, using the trailer angle as the error signal has the drawback that the hitch will not settle to its neutral position. In light of the MATLAB simulations, this effect may be to the benefit of the hitch controller: if the controller is reaching its physical limit during a constant steer maneuver, there will be additional travel available in the other direction when the driver changes the steering direction. Another downside to this error signal is that at low speeds, the trailer will be very stable, yet the trailer angles will be relatively high, causing unnecessary actuation and possible stalling. This can be mitigated by setting a lower bound on the trailer yaw that warrants a reaction from the hitch, or by decreasing the feedback gain at lower speeds, which is discussed further in section 3.2.6.

One of the simulation benchmarks is step steering input to a marginally stable tractor-trailer configuration. At 60km/h, a trailer approximately half the weight of the tractor is loaded such that the center of mass is directly above the axle. The resulting simulation is shown in Figure 3.5:

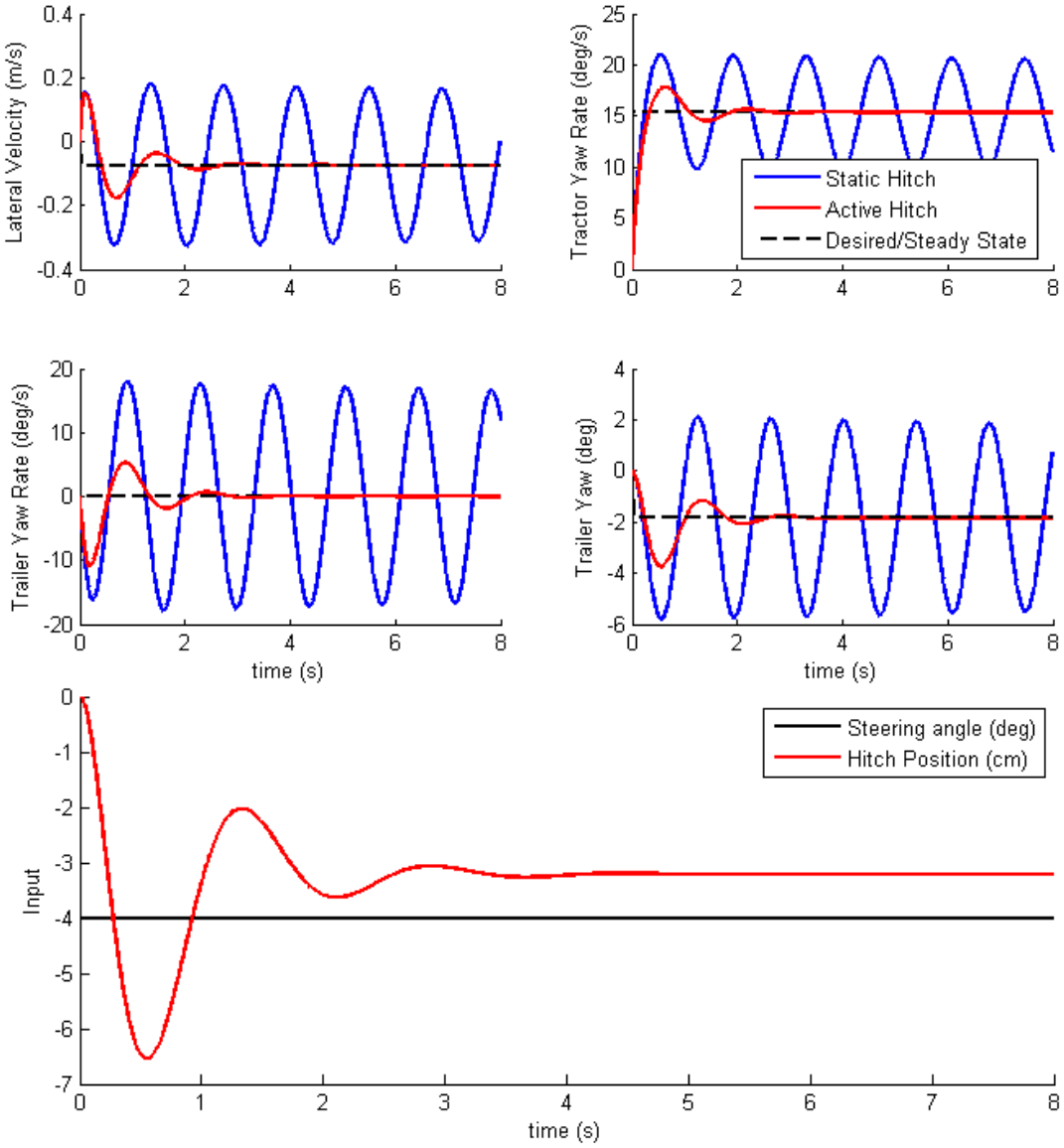

Figure 3.5: System response to step steering input

The desired state values are calculated using the derived parameters for steady state gains discussed in section 3.2.3. All the vehicle states oscillate about the steady-state value, with the same oscillation frequency and exponential envelope, which demonstrates that there is one highly dominant pole in the system response. This particular maneuver only requires a maximum hitch speed of 20cm/s, and can damp out steady oscillations in approximately 2 seconds.

The oscillations in the trailer are within the linear region of the tires, so this simulation represents a realistic case where sway motion is occurring at a small amplitude, but the motion is definitely felt by the driver as indicated by the change in yaw rate of the tractor. If the driver reacts to the sway with additional steering input, resonance can easily occur. The driver would likely respond to the sway with steering at the same natural frequency, resulting in the following response pictured in Figure 3.6:

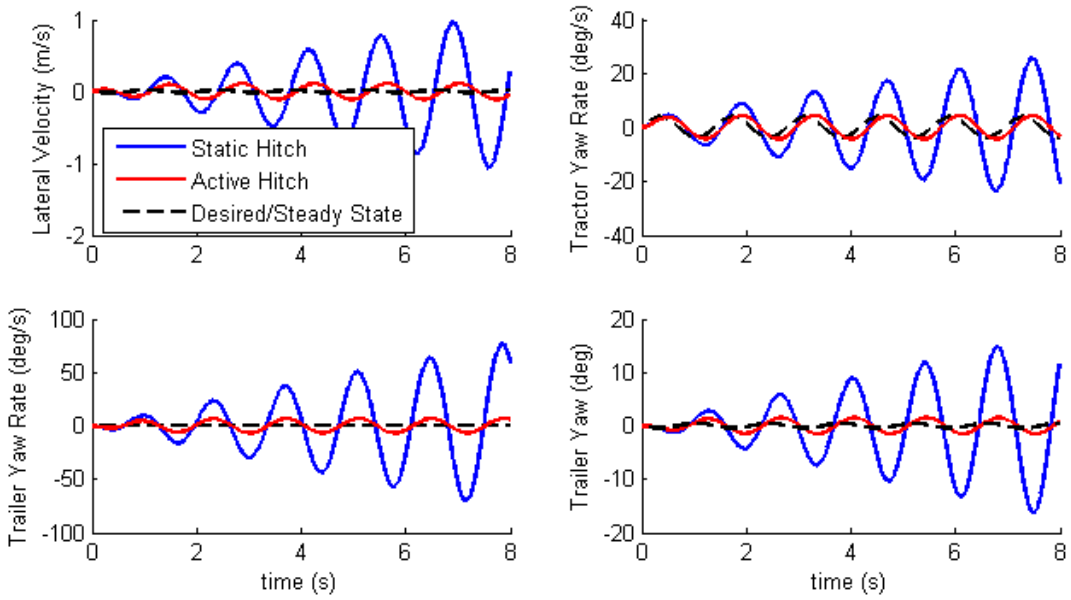

Figure 3.6: Resonance created for a sinusoidal driver input of ±1°

When a driver experiences sway, it is a natural reaction to respond with steering inputs at the natural oscillation frequency, causing resonance. The active hitch maintains the steady oscillations introduced by the steering without diverging.

The stability improvements provided by the active hitch are consistent across many simulations. Since this is a linear model, the system response scales linearly with the severity of steering inputs. Changes in the vehicle parameters have a nonlinear effect on the system response, although all responses resemble the second-order-system behavior driven by the dominant pole of the system matrix.

During simulation, it was noted that the natural frequency of the trailer decreased slightly when applying proportional gain, and increased slightly when applying derivative gain. This is supported by the root locus analysis performed on the system matrix. It requires higher force to actuate a system at a different frequency than its open loop natural frequency. Noting this,

derivative feedback was used to maintain the natural frequency of the system, which resulted in faster settling times without any increase in the required hitch range of motion. This technique does have practical limitations, since there are many values for the derivative gain increases the system instability, and since the rate of change of the trailer angle is harder to measure accurately in a standalone hitch system.

The double lane change represents high-speed object avoidance. In a tractor-trailer configuration, this rapid change in steering almost definitely leads to a crash. The reaction of the hitch controller to a double lane change with a different trailer combination is shown in Figure 3.7:

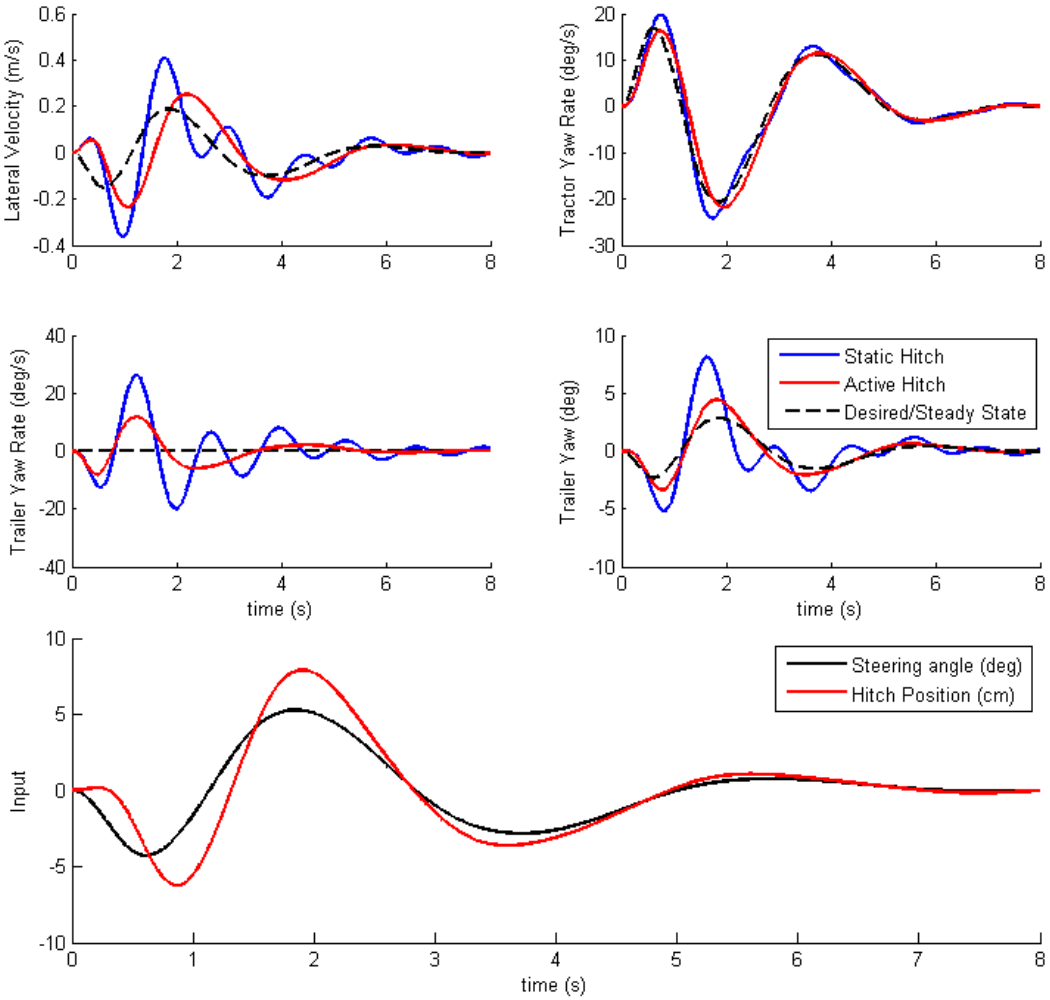

Figure 3.7: Double lane change simulation

With only knowledge of the hitch angle, the controller can track the desired steady states, while eliminating transient oscillations. The trailer slip angle is high enough in the open loop case that the trailer would have a more violent reaction with a nonlinear tire model. So the double lane

change maneuver is not as accurate in this simulation, but can still show the points at which the sway motion becomes dangerous.

An additional set of simulations was performed to assess the sensitivity of the controller to noise and delay in the trailer angle measurement and the hitch actuator. A delay was placed on the actuation of the hitch, and a normally distributed signal noise was added to the measurement of the trailer angle. The measurement noise did not affect the proportional action, but the derivative action became significantly less useful in the presence of measurement noise. On average, delays of 0.25s or greater cause the proportional controller to become unstable. A comparison of the perfect actuation and the noisy, delayed actuation is shown in Figure 3.8:

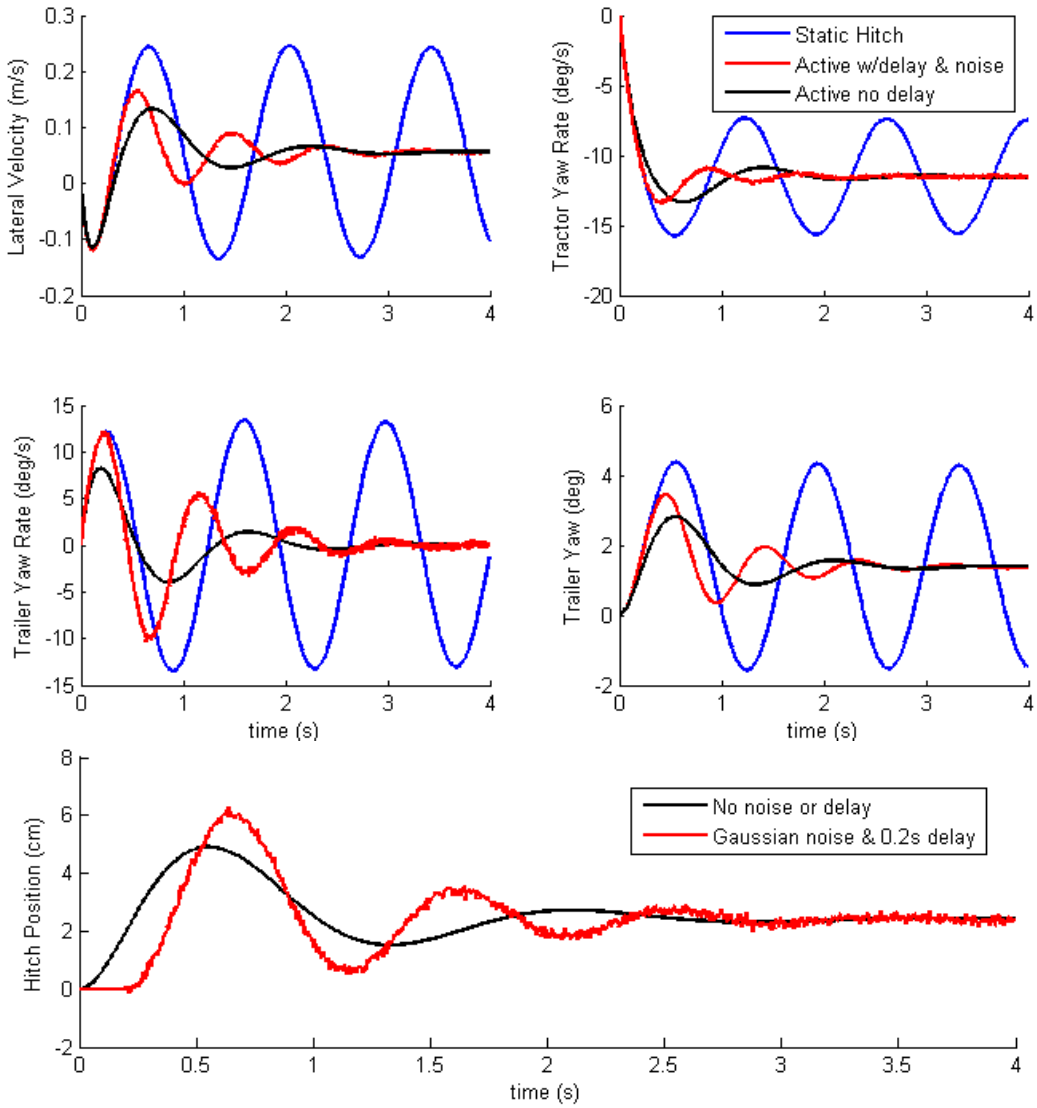

Figure 3.8: Effect of measurement noise and actuation delay

The effect of delay is more severe during more complex steering maneuvers. Different methods that are used to deal with noise and delay in the physical setup are discussed in section 5.2.2, along with the feasibility of using derivative action.

The MATLAB state space simulations were used to define a realistic range of motion for the active hitch. This decision is mitigated by practical considerations: namely that the first prototype is required to attach to a production hitch tube. The desired actuation range is set at ±**10cm** for the prototype discussed in Chapter 4, although a greater range of motion can be implemented by creating a customized mount for different vehicle frames. The force required is discussed in the context of high-fidelity simulation in section 3.3.

Feedback gain resonances were found to not have an effect on the system stability, since the gains required to create resonances are orders of magnitude higher than the gains that cause the controller to exceed its practical position and speed requirements. Since the specific actuation method for the hitch was not finalized until later in the design process, actuator dynamics were not considered in the model. Resonance between the actuation and the open system dynamics are discussed in the context of the final test setup in section 5.2.2.

3.2.6 Gain tuning

Since the primary controller design is based on simple feedback on the trailer angle measurements, it is difficult to experiment with more advanced control designs for the active hitch. Even in simple proportional controllers, the use of gain scheduling techniques can help set the controller feedback appropriately for different maneuvers. Two such methods for adjusting the feedback gain were considered and simulated using the MATLAB model for the tractor-trailer system.

The first gain scheduling technique uses the longitudinal speed of the tractor to set an appropriate gain. As discussed in section 3.2.3, the sensitivity of a vehicle system to steering input does not scale linearly with speed. The understeer coefficient and the steady state gains as derived in equations (3.18), (3.19) indicate that the feedback gain may not strictly increase for higher speeds, since more understeer configurations are likely to produce more extreme sway responses. Additionally, higher gains increase the actuation effort of the controller past the practical limits

of the hitch, and may overdamp the system in cases where the trailer is relatively stable, and may even result in feedback instability.

A brute-force approach was employed to estimate appropriate gains at different speeds. Iterating through a variety of trailer configurations, the response was measured over a range of feedback gains. The gain that resulted in the fastest settling time was recorded for the particular configuration. The gains for a particular speed were weighed based on the largest hitch motion required and averaged to give one gain recommendation for that speed. This process was repeated over a range of speeds, and a polynomial fit was applied to the results. The resulting gain schedule curve is presented in Figure 3.9:

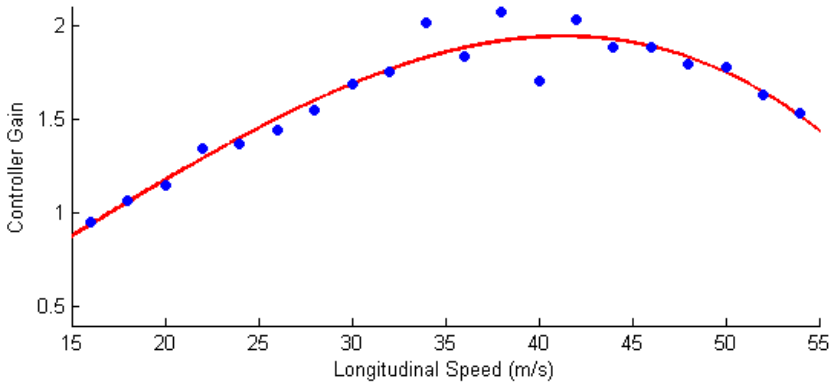

Figure 3.9: Gain tuning for vehicle speed

As predicted, gains initially increase to respond to the increased demand of higher speed, but eventually peak due to the increasing controller effort required to support the higher gains.

When plant dynamics are not explicitly known, or if state measurements are limited, heuristics can be employed to control systems using fuzzy logic. To experiment with the use of intelligent control systems in this application, a gain tuning method based on [37] was constructed and implemented in the MATLAB model. The tuning method assigns a linguistic value to different values of the error signal and its first derivative, and uses fuzzy inference rules to assign a change in the proportional feedback. An example of one of the 25 rules is as follows:

$$IF\ e(t)\ is\ negative\_small\ AND\ \Delta e(t)\ is\ zero\ THEN\ \Delta K\ is\ positive \tag{3.22}$$

The values in the membership functions were chosen based on typical values from previous simulations and from PID controller tuning heuristics. The resulting system responses for a steady steering input at 72km/h and a nominal gain of 1 is shown in Figure 3.10:

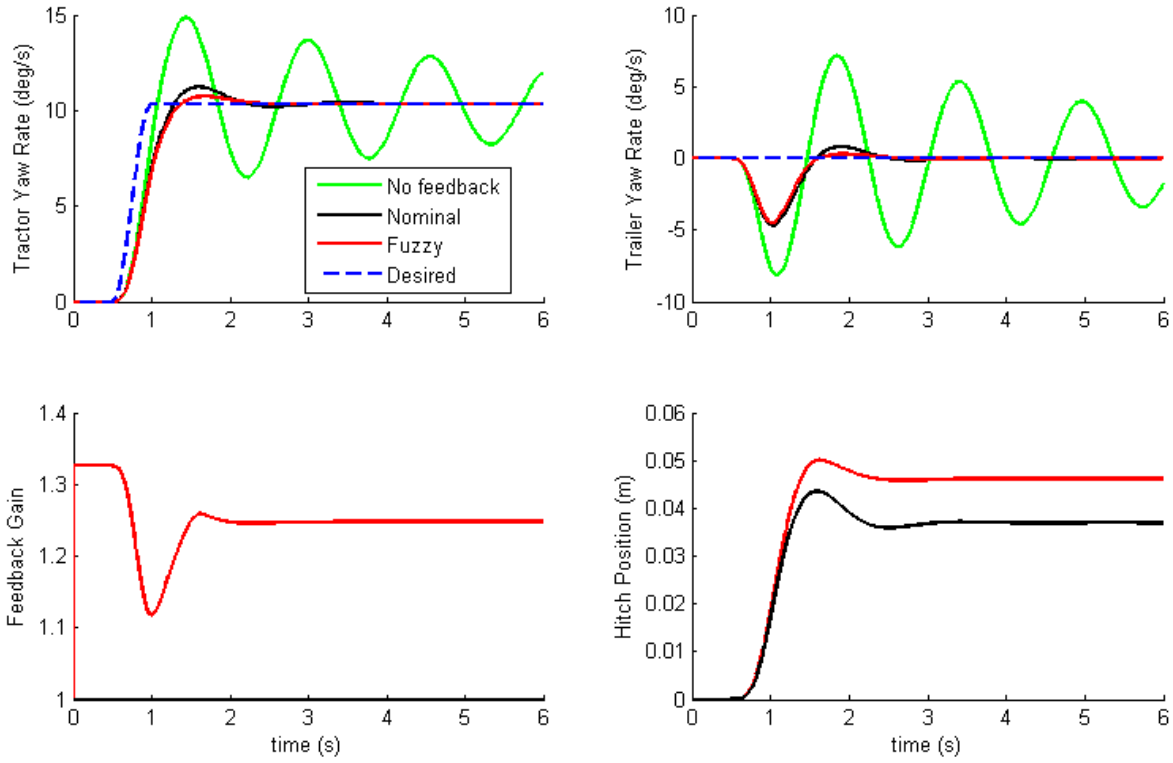

Figure 3.10: Results of fuzzy gain scheduling

In this case, the fuzzy tuning rules to not provide a significant advantage over the nominal setting. The overshoot in yaw rates are reduced, but at the cost of additional hitch motion. This marginal increase in performance, when combined with the added difficulty of assessing the stability of a nonlinear controller, resulted in the decision to not include fuzzy gain scheduling in the full scale testing of the active hitch.

3.3 Multibody Modeling in MapleSim

The most important weakness of extended bicycle model is the interaction of the tires with the road. In reality, the tire lateral force is a function of the slip angle, as well as the normal force. The lateral force that can be provided is eventually saturated, leaving a constant force of sliding friction as the only lateral force. Additionally, the weight transfer during lateral acceleration changes the cornering stiffness of the tires in a non-conservative way; the nonlinearity of the tires causes the total cornering force to be reduced. The weight transfer effect is worsened by travel of the suspension.

Once the control design for the active hitch was validated on the bicycle model in MATLAB, some supplemental simulations were required to account for the weaknesses of the model. For simulation tools like CarSim [38], the simulations are driven by a library of vehicle dynamics equations that are a balance of complexity and ease of calculation for the computer. Since sway control via active hitch is a novel concept, there is limited support for its dynamic simulation. As a result, it was beneficial to use a multibody solver to incorporate the active hitch. Multibody solvers treat an entire system as a chain or rigid or flexible bodies, and applies general kinematic and dynamic equations to simulate the chain.

MapleSim is a multibody solver based on the Maple mathematical tools, and uses concepts from linear graph theory to resolve dynamic and constraint equations for the various bodies [39]. It has a lower learning curve than solvers like Adams and comes with various prebuilt vehicle modules, and so is well suited for construction of a custom vehicle configuration. In addition to the built-in components, MapleSim allows for custom libraries of components to be created. For the active hitch, a custom trailer component was created that incorporates suspension, measured angles and accelerations in the vehicle frame, and can articulate the position of the hitch ball. This module, among others, is part of an effort by students in the MVSL to create a library of vehicle subsystems for rapid construction of models. The simulations of high-fidelity vehicle models in MapleSim are used to examine the extra effects that are not accounted for in the extended bicycle model developed in section 3.2.1, namely:

- Nonlinear tire behavior
- Weight transfer due to lateral accelerations
- Additional weight transfer due to suspension
- Lateral forces in the hitch connection
- Longitudinal dynamics (acceleration, braking)
- Terrain changes (low friction, slopes)
- Reactive steer inputs from the driver

The measurements or variables can be probed and plotted in a results menu, along with a 3D animation of the vehicle configuration. The animation allows the user to verify that the model is responding realistically, and can animate reaction forces. The layout of the tractor trailer model is presented below in Figure 3.11:

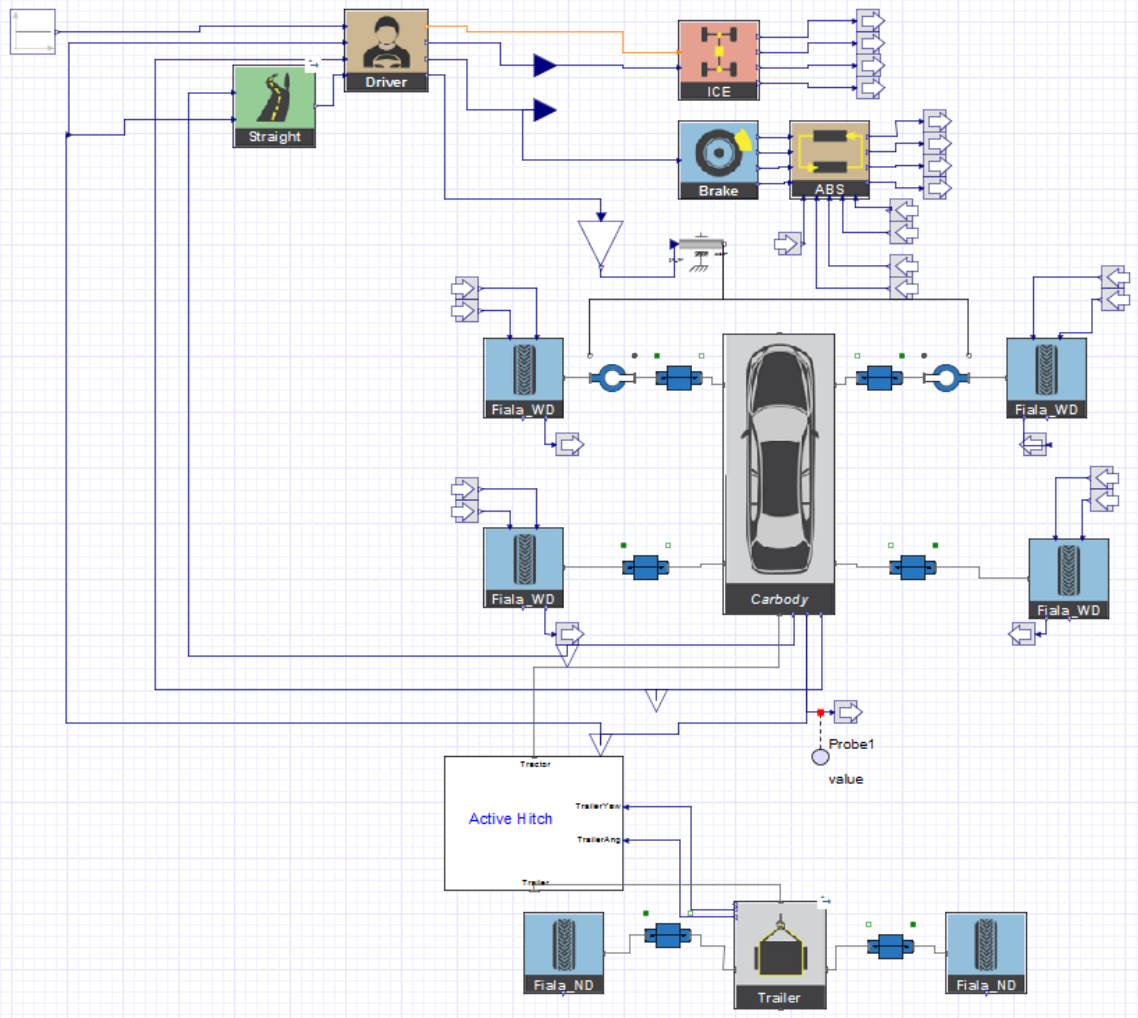

Figure 3.11: MapleSim component model of active hitch setup

The model uses an IC engine to drive the tractor with the driver acting as a cruise controller, with an ABS module so that the driver can stay within a region of maximal tire traction during handling maneuvers. Road profiles are based on waypoints, and are followed by the driver using a basic line follower controller for steering. When the road profile is suppressed, manual steering inputs can be used as in the MATLAB bicycle model. When attempting to simulate a full suspension setup, there were considerable increases in the required simulation time and the frequency of errors in the simulation, so the standard wishbone suspensions where switched for equivalent prismatic springs with damping. The Fiala tire model is used to represent the nonlinear behavior [40]. The inertial properties of the tractor-trailer combination were similar to those used in the MATLAB simulations. To compare with a simple steering maneuver at constant speed, the results from a steering impulse on a standard road is shown in Figure 3.12:

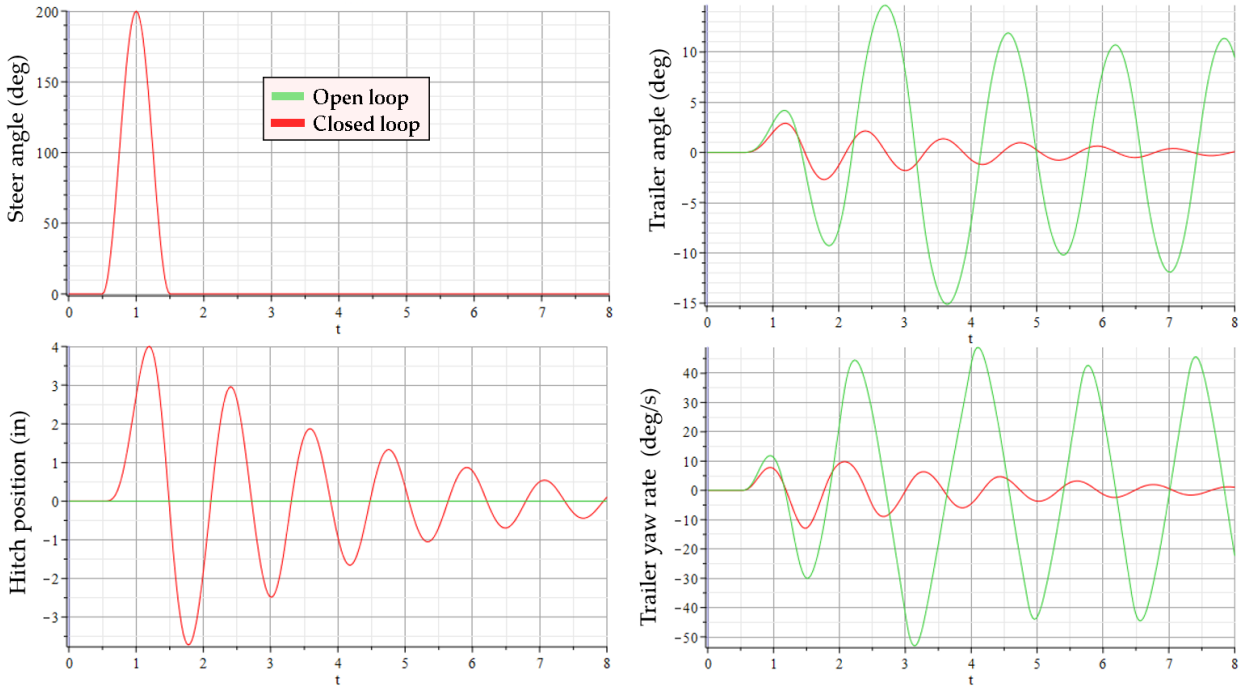

Figure 3.12: Steer impulse, 65km/h, unstable trailer configuration, open loop (green) and with active hitch (red)

The steer angle in the above figure is the driver's steering wheel input, and not the steering of the tires. The nonlinear effect of the tires is clearly visible; the trailer yaw rate (bottom right of the figure) resembles a saw tooth wave rather than a pure sinusoid, which indicates the constant friction force that would be present when the tires are saturated. The active hitch, using proportional control only, is able to keep the trailer tires from leaving their linear region, drastically improving the safety of this maneuver. At 4inches of travel (10cm), the hitch is at its practical limit, and does not stabilize the motion nearly as quickly as when only considering linear dynamics. As with the MATLAB simulations, using a derivative gain yielded marginal improvements to the controller, but was less effective since the natural frequency of the trailer when the tires are becoming saturated is significantly lower than when they remain within a mostly linear region.

In addition to constant speed maneuvers, the longitudinal dynamics of the tractor-trailer combination were tested using the MapleSim model. Since the forces that the tire generates must be shared between lateral cornering forces and longitudinal tractive forces, any braking or accelerations lead to earlier saturation of the tires. Since the trailer is not modeled with brakes, there will be no longitudinal forces and the cornering ability of the trailer tires will help the trailer follow the tractor, even if the tractor may be sliding.

One example of a longitudinal maneuver is a brake on grade with lateral disturbances. The vehicle is traveling at 100km/h down a 10% grade (5.7° slope). A small lateral disturbance is provided via a very small steering impulse, and the tractor applies 0.5g of braking force, assisted by ABS. The driver attempts to follow a straight road during the braking. The resulting hitch articulation and the lateral force on the hitch ball are plotted in Figure 3.13:

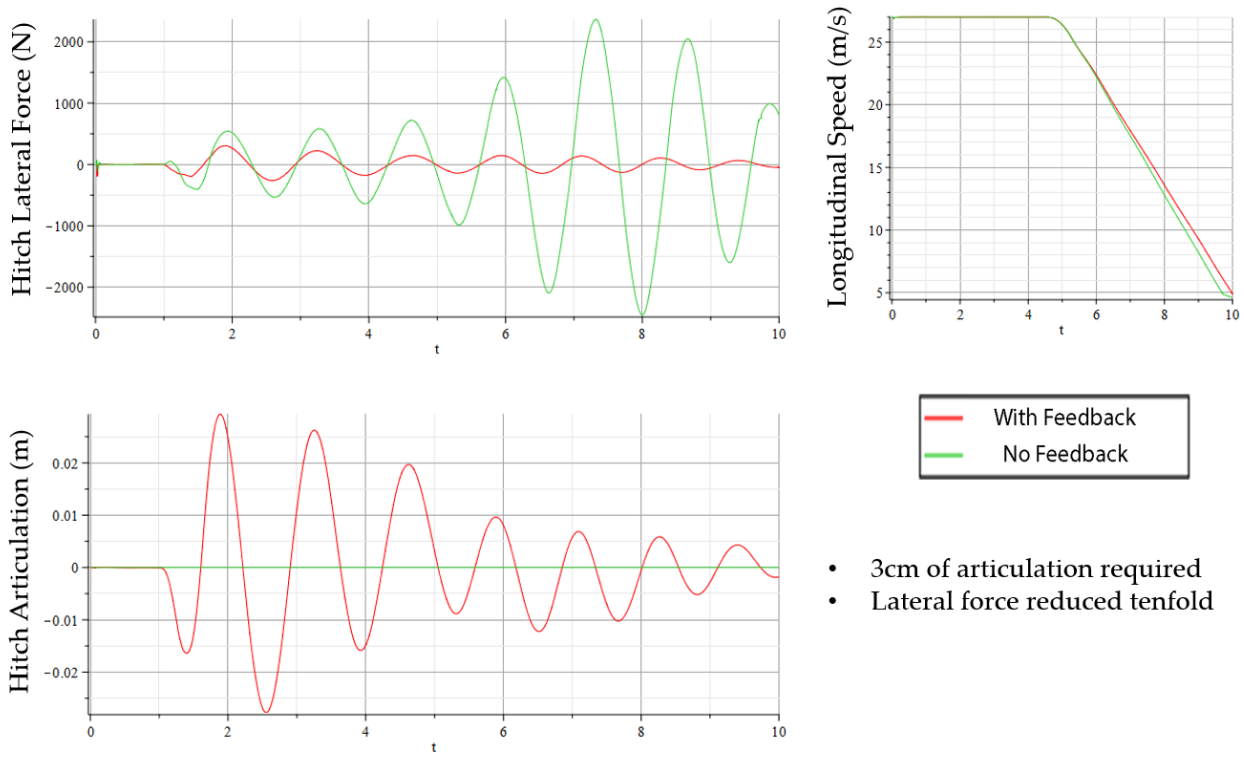

Figure 3.13: Brake on slope maneuver

As expected, the hitch lateral force follows the oscillatory behavior of the other trailer states. The peak lateral force found in double lane change and steady turn maneuvers was approximately 3000N. The intervention of the active hitch reduced the peak lateral force tenfold, while only requiring a third of its available travel. This maneuver shows that even if speed is reduced, the oscillations in the trailer can continue to rise. The extra longitudinal friction from the tires causes the tractor-trailer to decelerate slightly faster, which means that the active hitch also reduces the overall rolling resistance of the system.

The MapleSim model had issues solving consistently, but was nonetheless a useful tool for iterating controllers though a variety of trailer sizes. The hitch movement and force data collected from the studies served as design benchmarks for designing the hitch prototype discussed in the following chapter.

Chapter 4: Design of Active Hitch Components

Carrying forward from the simulations of active hitch dynamics, this chapter comprises the work required to create the physical active hitch setup that has been implemented in full-scale testing. Specifically, this chapter discusses the design and manufacture of the primary mechanism, as well as the selection of the auxiliary components needed to actuate the mechanism. Extra systems that were used in the test setup (custom test trailer, test tractor, electronic hardware implementation) are discussed in chapter 5.

The overall guidelines for design of the mechanism were based on the results achieved through simulation, limited by practical/structural restraints. To demonstrate potential use as an aftermarket solution, the mechanism and accompanying power pack should be mounted on available hitch hardware. Figure 4.1 shows the hitch that was purchased for use on the test vehicle, which represents a typical medium-duty hitch attachment.

Figure 4.1: Class III hitch component, compatible with Equinox SUV [41]

The hitch ball should be able to laterally move **10cm** in either direction. This metric was chosen based on favorable simulation results presented in section 3.2, showing that significant sway reductions were possible over this range of motion, without requiring unreasonable actuation speed or an excessively bulky mechanism. These practical limitations are discussed in more detail in the structural analyses of the mechanism.

The power pack should be able to drive the hitch ball laterally at **25cm/s**, while the components support a simultaneous lateral load of **3000N** and a vertical load of **1500N**. It should also be capable of peak lateral speed of **45cm/s** for approximately **0.5s (1350W peak power)**. As with the previous item, these metrics were derived from simulations of the controller during harsh maneuvers by noting the speed of the control input and the lateral reaction from the hitch.

4.1 Mechanism Design

During the conceptual design of the mechanism, a linear actuator was chosen as the prime mover for the hitch ball. A linear actuator, either actuated electrically or hydraulically, allows precise movement that can support the reaction forces of the trailer on the hitch. Both types of linear actuator have some type of mechanical locking which prevents the trailer forces from driving the hitch: electric actuators use worm gears that cannot be driven by the meshing spur gear, and hydraulic power loops generally feature components that can only be driven one way. This feature allows the hitch mechanism to remain stationary when not powered. Two configurations of the actuator were considered for more detailed consideration: in-line and planar linkage. Schematics of the two configurations are shown in Figure 4.2:

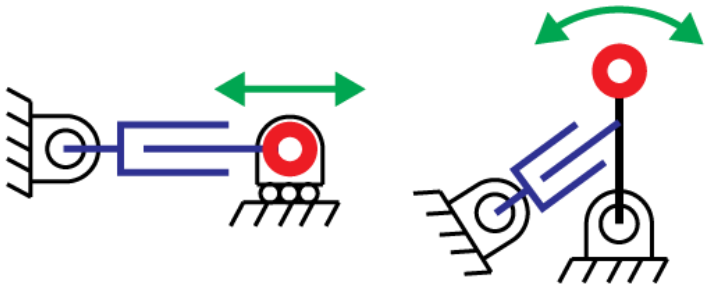

Figure 4.2: Schematic of in-line configuration (left) and planar linkage configuration (right)

The in-line configuration creates pure lateral motion of the hitch ball (illustrated in red), by restricting motion on a linear guideway. The actuator can be placed to one side, or be incorporated into the guideway, such as in CNC machine rails. The linkage configuration relies on the rotation of a pivoting linkage, and therefore produces a component of longitudinal motion. The major advantages and disadvantages of each method are listed in TABLE 4.I.

TABLE 4.I: COMPARISON OF CONFIGURATIONS

	In-line	**Planar Linkage**
Pro	• Pure lateral motion • Small longitudinal profile • More symmetric structural components	• Robust rotating connections • Small lateral profile • Variable performance based on placement of actuator
Con	• Linear slides are not robust • Linear bearings prone to binding • More expensive	• Longitudinal motion of hitch • Nonlinear mapping from actuator length to hitch position • Longer linkage must be stronger to withstand trailer tongue weight

Both configurations were investigated for compatibility with industrial actuation solutions. Hydraulic and electric solutions for the in-line configuration presented practical problems:

- Linear guides were unable to support the multiple loading conditions from the trailer without significantly more expensive components.
- Linear guides are more prone to the ingress of dust and water during testing.

Rectifying these problems requires a more specialized design of the components, greatly increasing design and manufacturing time. The linkage configuration is therefore more appropriate for a first design to determine if active hitch stabilization is effective in practice.

4.1.1 Linkage kinematics

The kinematics of the hitch linkage were designed to minimize the overall size of the mechanism (subject to the system requirements), and to create a nearly linear relationship between actuator movement and hitch lateral movement. This section will only deal with the linkage kinematics, although the process of designing the hitch involved several iterations through kinematic, structural, and component selection.

A basic MATLAB script was created to simulate the motion profile of different configurations. Inputs for the script were the desired lateral hitch ball travel, the locations of the rigid supports, the length of the control arm (distance from the hitch ball from the main pivot point), and the location where the actuator connects to the control arm. The script performs the inverse kinematic calculations to find the required range of motion for the actuator, calculates the rate of change of the actuator with respect to the hitch ball, and calculates the force on the actuator for a given lateral force on the hitch ball (hereafter referred to as the **force multiplier**). The script performs forward kinematic calculations to confirm the results of the inverse kinematics. Figure 4.3 on the following page shows the parameters that are used to perform the kinematics calculations.

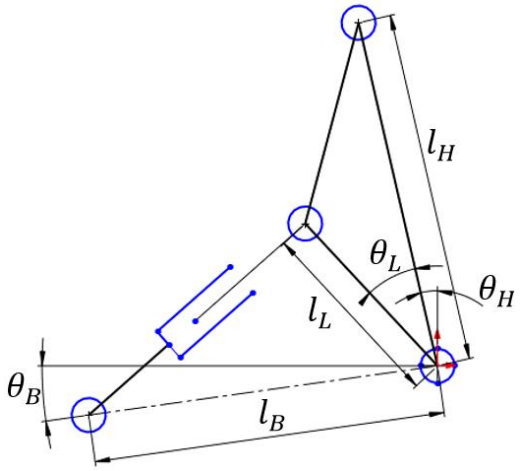

Figure 4.3: Kinematics Diagram

The trigonometric equations that define the linkage kinematics reveal that the rate of change of the actuator length ball with respect to the hitch ball movement $\frac{dl_{ac}}{dy_H}$ is the inverse of the force multiplier at a given hitch position.

$$\theta_H = \sin^{-1}\left({}^{y_H}/_{l_H}\right) , \quad \frac{d\theta_H}{dy_H} = \frac{1}{l_H}\sqrt{\frac{1}{1-y_H^2}} \tag{4.1}$$

The actuator length l_{ac} forms a triangle with l_B and l_L. The opposite angle θ_{ac} is used with the cosine law to find l_{ac}:

$$\theta_{ac} = 90° + \theta_B - (\theta_H + \theta_L) , \quad \frac{d\theta_{ac}}{dy_H} = \frac{d\theta_H}{dy_H} \tag{4.2}$$

$$l_{ac} = \sqrt{l_B^2 + l_L^2 - 2l_B l_L \cos(\theta_{ac})} \tag{4.3}$$

$$\frac{dl_{ac}}{dy_H} = \frac{d\theta_{ac}}{dy_H}\frac{dl_{ac}}{d\theta_{ac}} = \frac{1}{l_H}\sqrt{\frac{1}{1-y_H^2}} * \frac{l_B l_L \sin(\theta_{ac})}{\sqrt{l_B^2 + l_L^2 - 2l_B l_L \cos(\theta_{ac})}} \tag{4.4}$$

And using statics to get the force multiplier $\frac{F_{ac}}{F_y}$ at a given hitch positon, first take the sum of moments about the central pivot to find the force acting perpendicular to line l_L:

$$\frac{F_l}{F_y} = \frac{l_H}{l_L}\cos\left(\sin^{-1}\left({}^{y_H}/_{l_H}\right)\right) = \frac{l_H}{l_L}\sqrt{1-y_H^2} \tag{4.5}$$

Again using cosine law, the angle δ between the perpendicular line to l_L and the axis of the actuator is calculated, and this angle can be used to project the force perpendicular to l_L onto the actuator axis:

$$\delta = \frac{pi}{2} - \cos^{-1}\left(\frac{l_{ac}^2 + l_L^2 - l_B^2}{2 l_{ac} l_L}\right) = \sin^{-1}\left(\frac{l_{ac}^2 + l_L^2 - l_B^2}{2 l_{ac} l_L}\right) \tag{4.6}$$

$$\frac{F_{ac}}{F_y} = \frac{F_L}{F_y}\frac{1}{\cos(\delta)} = \left(\frac{l_H}{l_L}\sqrt{1 - y_H^2}\right)\sqrt{\frac{1}{1 - \left(\frac{l_{ac}^2 + l_L^2 - l_B^2}{2 l_{ac} l_L}\right)^2}} \tag{4.7}$$

The second term can be expanded and re-simplified by using the definition of l_{ac} from equation (4.3):

$$\frac{F_{ac}}{F_y} = \left(\frac{l_H}{l_L}\sqrt{1 - y_H^2}\right)\sqrt{\frac{l_B^2 + l_L^2 - 2 l_B l_L \cos(\theta_{ac})}{l_B^2 \sin^2(\theta_{ac})}} \tag{4.8}$$

The above is the inverse (or negative inverse) of equation (4.4), so by creating a nearly linear relationship between actuator movement and hitch movement, the actuator will also have a nearly constant force multiplier for different hitch positions.

In order to minimize the overall size, and also to create a consistent force multiplier, the following heuristic rules were used to determine the final layout of the mechanism:

- For compactness, maximise the ratio between actuator motion range and actuator total length.
- To ensure small variations in the actuator axis angle, restrict endpoints of actuator motion to have the same actuator angle.
- Define a ratio of total lateral hitch travel to total actuator motion and chose the value that best balances resultant trade-offs (higher ratio puts more force into actuator but is slower).

These heuristics were implemented in a CAD model of the linkage with various actuators and sizes, which defined the kinematics from Figure 4.3 to be used in the MATLAB script. The final configuration combines packaging constraints with the kinematic performance requirements, and is shown in Figure 4.4. The figure shows the linkage dimensions, the mapping of actuator movement to lateral hitch ball movement, and how the force multiplier changes at different actuator positions (equivalent to the rate of change of the mapping curve).

Dimension	Value
Linkage Length (l_H)	20.89cm
Outboard actuator attachment (l_L)	8.26cm
Base Length (l_B)	30.95cm
Linkage internal angle (θ_L)	17.3°
Base angle offset (θ_B)	4.0°
Actuator range of motion (Δl_{ac})	8.89cm

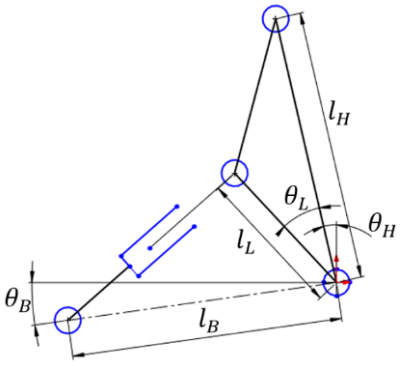

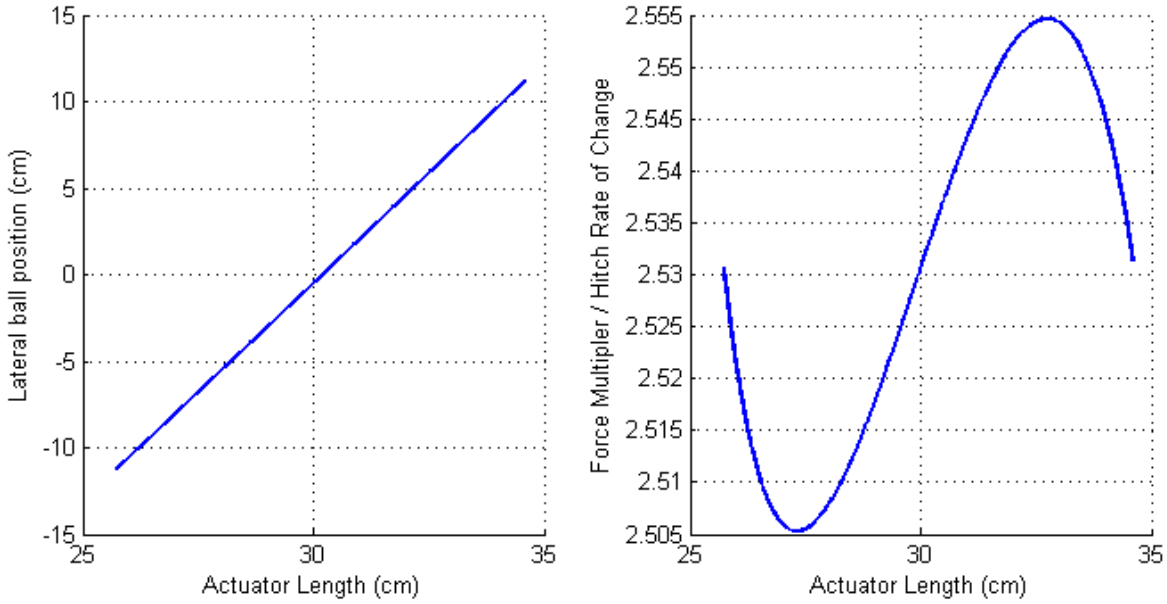

Figure 4.4: Kinematic characteristics

The motion profile is nearly linear; there is a variation of **<1%** between the peak rate of change and the average value of **2.53(cm/cm)**. The rate of change is also nearly symmetric about the midpoint of the hitch motion, so the performance will be even in both directions, despite the asymmetry of the actuator placement.

Since the hitch ball will travel around a circular path, it will experience a change in longitudinal position of **3.29cm.** Further reduction of this unwanted motion would result in a longer linkage, which results in greater moments transferred to the mechanism and to the hitch mounts. The axis of the actuator deviates in direction by **<3°** throughout the motion, allowing it to be packed more tightly with the rest of the assembly. When the hitch ball position is centered, the direction of the actuator axis is perpendicular to the line l_L, which means that the axial force in the actuator will not transfer excessive off-axis forces into the linkage and the mounting bracket.

4.1.2 Structural components

The linkage kinematics presented in the previous section were finalized based on manufacturing and structural considerations. Since the hitch linkage and supporting components are relatively small compared to most passenger vehicles, weight savings are not of primary concern when designing the structural components. The main two goals for creating a practical setup are manufacturability and robustness, which are elaborated below:

- **Manufacturability**: This goal covers the ease of manufacturing, as well as the overall cost and timeline required for the manufacture. Typically in manufacturing for research projects, the highly customized nature of the projects require specialized and expensive manufacturing methods, such as CNC machining. The expense of this type of manufacturing can be reduced at the cost of degrading quality of the parts. The goal of using the low cost manufacturing methods results in projects that can be manufactured quicker, and with more direct involvement from the researchers. Additionally, low cost methods are attractive to industrial partners, as the manufacturing cost would scale more reasonably if the project is considered for commercial use.
- **Robustness**: This refers to the linkage's ability to withstand a harsh loading conditions which are common in trailering components. In addition to withstanding expected loading cases, the structural components should be adaptable to unforeseen cases. In a manufacturing sense, robustness entails the system's ability to be improved or reworked during manufacturing without compromising the fundamental attributes of the design.

The linkage design consists of three primary mechanical parts: the linkage arm, the actuator, and the support bracket which attaches to the vehicle hitch via a mating square tube. A rendering of the structural components are shown in Figure 4.5:

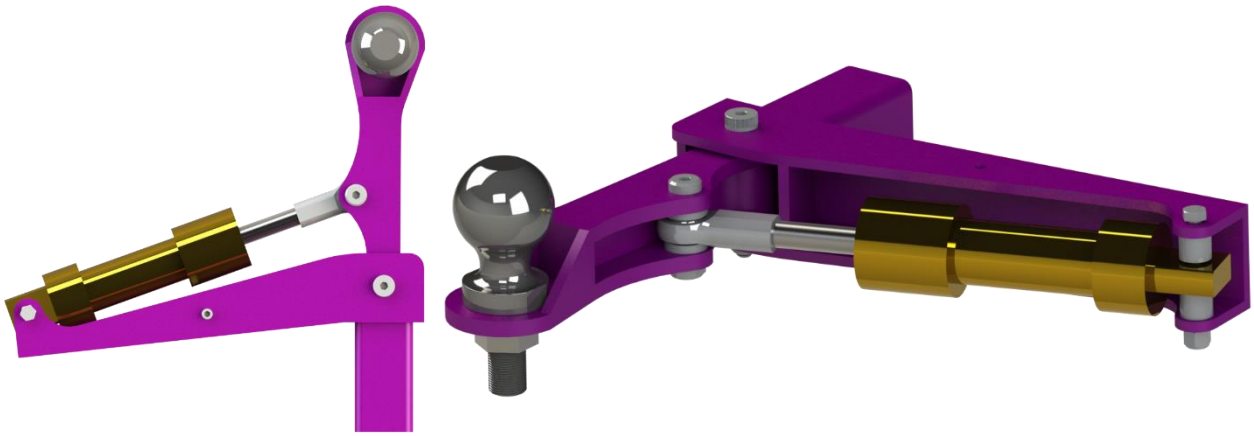

Figure 4.5: Mechanism structural components: top planar view (left), isometric view (right)

The actuator pictured is a 1500psi rated hydraulic cylinder, whose selection and properties will be elaborated when discussing the power pack. The linkage is supported by SAE grade 8 fasteners, and are sized such that the fasteners have a safety factor of approximately double the safety factor of the main components. To facilitate motion of the linkage, the actuator is attached to the linkage arm via a rod end, which is rated for 10000lbs of static loading. The main pivot is comprised of a shoulder bolt that interfaces with two flanged oil-impregnated bushings, which are pressed into the linkage arm. The flanges reduce friction along the pivot and the clamping surfaces, as shown in Figure 4.6:

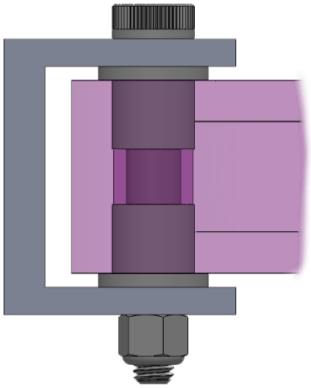

Figure 4.6: Section view of pivot, showing bracket, shoulder bolt, bushings, linkage arm (transparent)

The bushings are rated for a combined dynamic loading of 3000lbs while rotating at 60rpm, which is adequate for the kinematic requirements of the linkage.

The structural components are made of mild steel plate, and are cut into sections using a laser cutter. This method of manufacturing is extremely fast and low-cost when compared to machining parts from single billets. Despite mild steel not having the tensile strength or hardness of higher-carbon alloys, the lower cost of manufacturing using hot-rolled steel allows the hitch to achieve greater structural integrity at lower cost. Another advantage of mild steel is that it is less susceptible to alterations in structural properties during heating, from welding or cutting operations. Since the sections are welded together, the lower degree of heat-treating results in consistent properties throughout the structure. This allows the structural performance to be analyzed by relatively simple tools, and increases the confidence in consistent manufacturing of the components. The configuration for the linkage arm is based on an I-beam, which is suited for multi-axis bending loads, with a possible exception of twisting loads. Alternative designs based on structural tubes were considered, but eventually rejected since the actuator and hitch ball attachments place crushing loads on the tube walls.

The combination of laser cutting and welding of steel plate is prone to issues in dimensional accuracy. It is important to consider how the pieces will tend to warp during welding, and design appropriate jigging to minimize this effect. The linkage arm and the bracket use perpendicular connections wherever possible, to best make use of the two-dimensional nature of the cut parts. The components were created using as few individual pieces as possible, to prevent excessive buildup of dimensional errors. Finally, the component pieces were designed using self-aligning tabs, so minimal jigging is required to maintain dimensions. The tabs are placed in regions that experience lower relative stress as determined by FEA studies, so the material discontinuities are less likely to develop cracks or micro-yielding. The individual sections of the structures are illustrated in Figure 4.7:

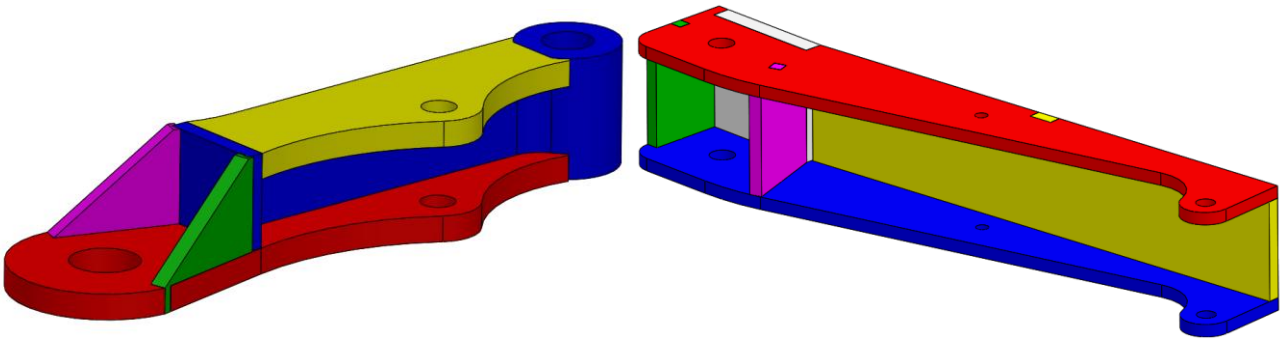

Figure 4.7: Welded sections of the linkage arm (left) and mounting bracket (right)

In addition to the alignment tabs, bolts and spacers were used to help maintain concentric holes. The spine of the linkage arm (pictured in blue on the left graphic) is an exception that required more complicated machining due to its increased thickness, and its surface requirements for press-fitting the bushings. In addition to being water jet cut, two milling operations and reaming operation on the pivot hole were required. The additional machining operations only required 3 hours of machining time, a time that would have been much shorter in the hands of an experienced machinist. The spine was designed as such in an effort to lower the number of segments, and to help the shear forces transfer across the top and bottom plates with minimal discontinuities. This decision improved the strength of the structure, but would not be ideal for producing multiple units. An alternative design would extend the top and bottom plates (red and yellow in the left graphic) over the pivot hole and into the front gussets, reducing the thickness and additional machining on the spine.

In an effort to make the components as consistent as possible in terms of structural properties, all seams between individual pieces were welded by the University of Waterloo machine shop. To ensure full penetration of welds, the plates were pre-chamfered to allow more weld material into the seams, and TIG beads of approximately 0.25” diameter were maintained to reduce stress concentration and to input adequate heat. The manufactured structural components are shown in Figure 4.8, a picture of the hitch linkage mounting on the test vehicle during initial testing:

Figure 4.8: Structural components mounted on test vehicle hitch

The desired dimensional accuracy was achieved; all fasteners fit snugly in the concentric holes and between the shear plates, and the bushings were a loose interference fit on the linkage arm. The main pivot can be easily moved by hand with virtually zero play, although there was approximately ±0.125” of vertical play at the hitch ball after preparing and painting the structural parts. The hitch tube mates with the vehicle hitch via a loose sliding fit, and is fastened with a 5/8” grade 8 bolt.

4.1.3 Finite element analysis

In order to arrive at the final shape of the linkage arm and bracket, iterations of the design were subjected to simulated load cases using finite element analysis (FEA), performed using Solidworks Simulation [42]. Solidworks has basic tools for FEA, but lacks many advanced features that are present in ANSYS or other dedicated FEA software. In this case, the use of Solidworks for FEA was justified for two reasons:

1. The majority of the 3-D modeling in this project was done using Solidworks. The ease of use in creating models and immediately having them available for simulation cases allows for rapid iteration of potential design concepts.
2. The expected loading cases for this design are within the capabilities of Solidworks Simulation, which is optimized for fast static studies of isotropic structures. The analysis of the active hitch mechanism does not include high impact simulations, and is based primarily on the oscillatory forces that are transferred from the trailer during harsh driving maneuvers. The frequency of these oscillations is low enough that static analysis yields reasonably accurate results, and shock/safety factors can be applied to account for the inaccuracy of static methods. Although the parts are formed from welded pieces, selection of materials and welding techniques yield a part that is mostly isotropic, within the accuracy of the solver. Furthermore, it was an auxiliary goal of the FEA studies to ensure that the weld locations experienced lower stress than the shear plates.

As stated in the beginning of this chapter, the lateral load applied to the system is 3000N, representative a harsh steering maneuvers found in simulation. The vertical load of 1500N represents a tongue weight of 20-30% on a light or medium duty trailer. The benchmark loading is applied to the parts as they would be in assembly. Figure 4.10 and Figure 4.9 show the application of loads in the finite element model:

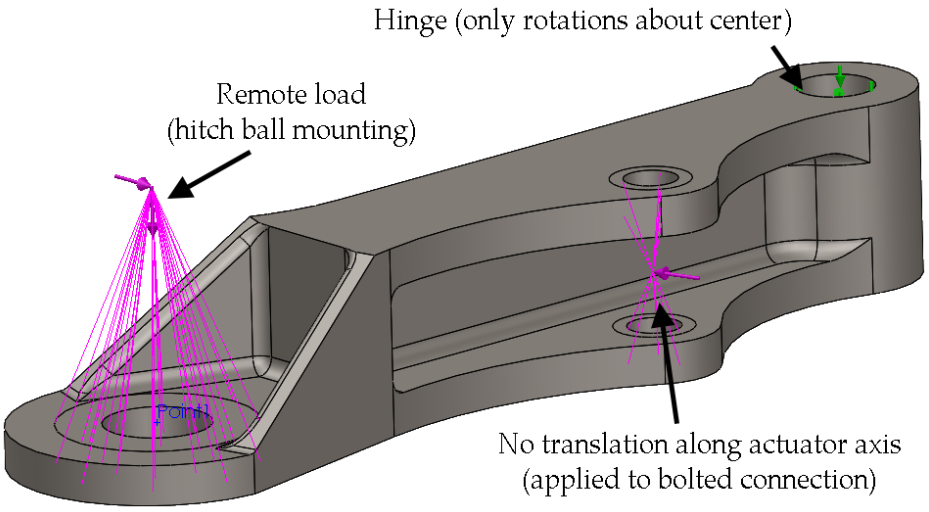

Figure 4.10: Boundary conditions on finite element model (linkage arm)

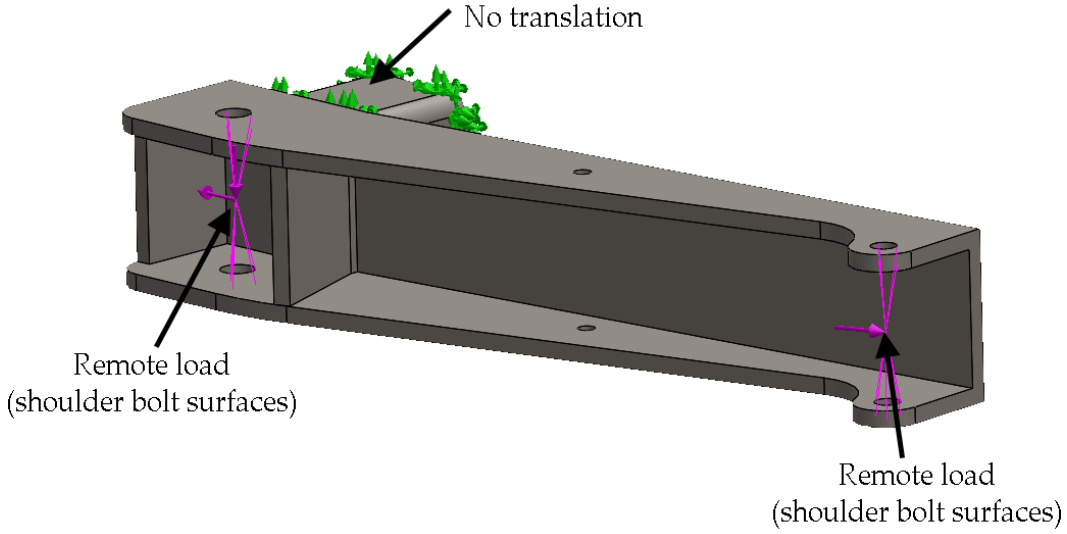

Figure 4.9: Boundary conditions on finite element model (support bracket)

Using remote loads, typical boundary conditions (forces, fixed displacements) can be applied to the parts to simulate a more complicated connection that is not present in the model (bolts, pins, etc.). The remote loads also apply the moments caused by the remote point of force application by the hitch ball. The finite element mesh uses tetrahedral elements with an average element

edge size of 0.15in, with finer mesh controls placed on the connection surfaces for higher accuracy. The mesh study reports that 98% of the elements used have an aspect ratio of less than 3, which contributes to more accurate results.

Based on the manufacturing of the components, the solver used material properties for ASTM A36 Steel, which is typical for structural sheet metal [43]. Since the solver is meant primarily for use in the linear elastic range of the material, the condition for failure will be exceeding the yield stress of the material of 250MPa. This criterion is measured using Von-Mises stress, which is a single measurement of a material stress subject to multi-axis loading. The Von-Mises criterion was developed to describe yield failure in ductile materials like structural steel [44].

For the linkage arm, the benchmark loads were applied in different orientations based on the different mechanism positions expected during testing. The first loading case is with the linkage in the central position, representing when the controller is turned off. The two loads were reversed to create four subcases based. The loading that is applied at both ends of the actuator range of motion was also simulated, since the system dynamics dictate that the trailer will place the highest loads at the peaks of the oscillation, where the mechanism is near its peak movement. Due to the design of the kinematics, the load cases produce very similar FEA results. For the purposes of being concise, only the two most relevant loading cases are shown on the following page, as determined by maximum stresses and most different loading orientations.

The two most extreme and distinct cases are illustrated in Figure 4.11. For both cases, the vertical load is considering a positive tongue weight, since the simulations for negative tongue weight yielded nearly identical results.

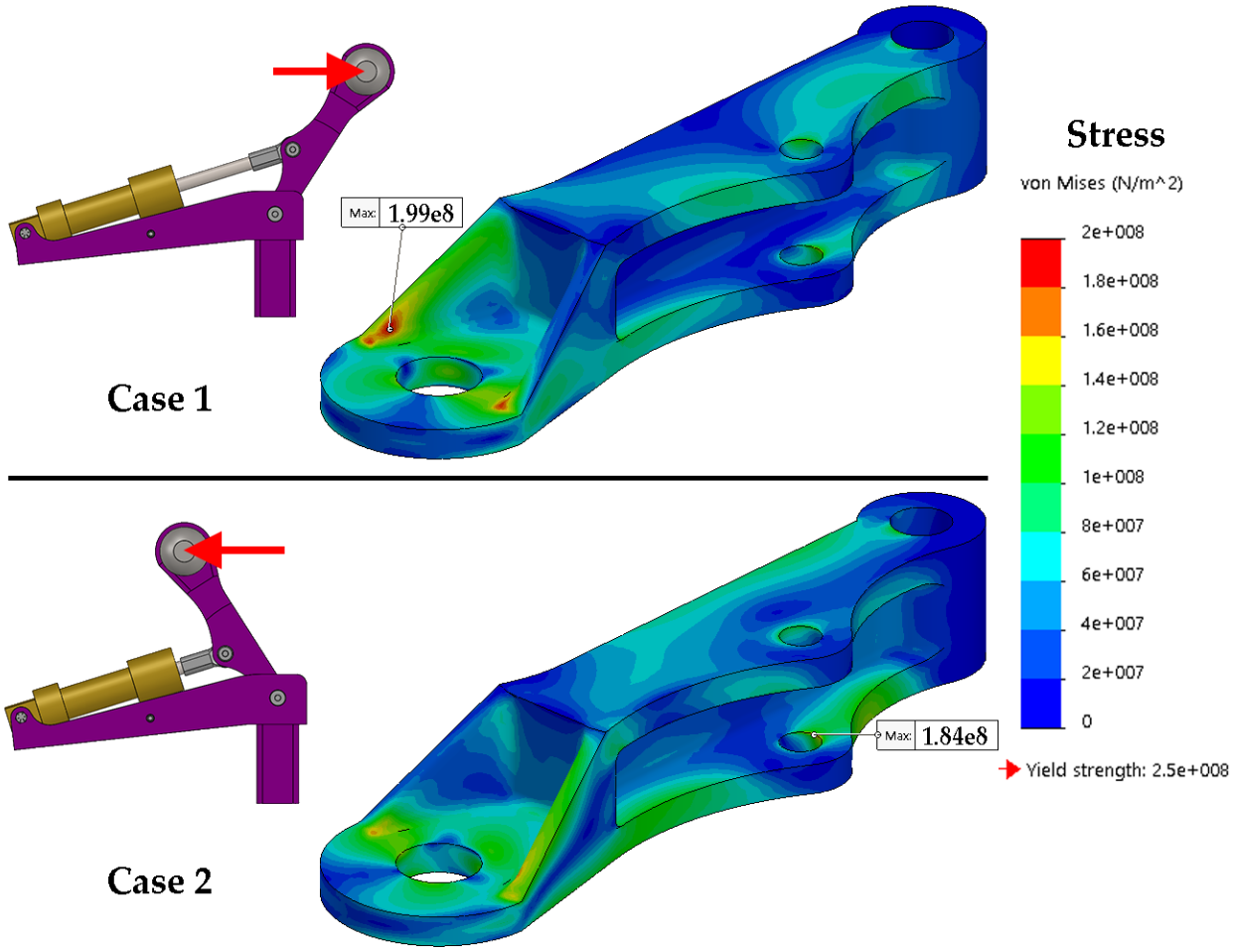

Figure 4.11: Linkage stress plots for motion limit cases

Important note: The maximum stress is lower than the yield stress of the material, but not low enough to achieve a safety factor of 2 or higher, which is used to account for shock loading, inaccuracy of the model, or other unexpected loads. This is a mistake on the part of the author, as the finite element studies were conducted using the incorrect set of material properties, an error which was not discovered until the parts were already being fully tested. It is possible that the finite element model is overestimating the stresses, since the stresses at the area of application of boundary conditions are often unreliable [45], and that real structures with stress concentrations tend to re-distribute stresses through micro-yielding, without damaging the overall structure [46]. At the end of testing, there was ~2mm of plastic deformation detected near the hitch ball mounting hole, which further indicates that the structure requires re-design for future iterations.

Using statics equations, the loads placed on the hitch ball were transferred through the linkage arm and into the support bracket. Using the force ratio derived in section 4.1.1, a load of 7600N was applied to the outboard bolted connection, along the cylinder axis. Due to the clevis and rod ends used for mounting, the applied force is treated as purely axial. The bending and twisting moments of 315Nm and 165Nm, respectively were applied onto the pinned (shoulder bolt) connection at the main pivot, along with the 1500N vertical force and the lateral force of 4600N from balancing lateral forces between the hitch ball and the actuator. In the case of the bracket, the maximum stress occurs when the orientation of the actuator axis is most different from the part geometry, causing more bending and less pure tension. This case occurs when the hitch ball is in the center position. As with the linkage, reversing the loads yielded nearly identical results, so only one test case is shown below:

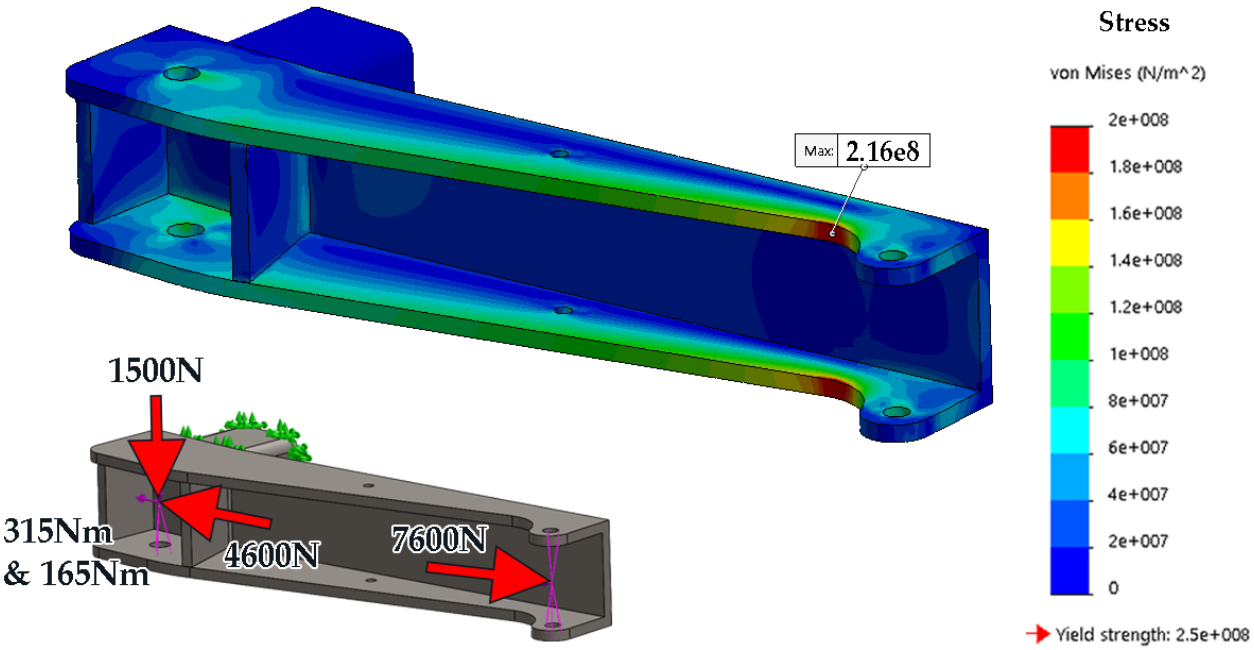

Figure 4.12: Support bracket stress plot for worst-case loading

As with the linkage, the maximum stress is below the yield strength, but is not adequate for the recommended safety factor, based on the same error in selection of material properties described on the previous page. In future iterations of the active hitch setup, it will be an easy matter to adjust the structure to accommodate heavier loads. In the case of the bracket, simply increasing the thickness of the main shear plates by 1/16in results in a 25% reduction in maximum stress,

and requires no rework on the assembly other than lengthening the shoulder bolt. Further potential structural reworks are discussed in chapter 6.

The deformation in the assembly does not exceed 1mm, as shown in Figure 4.13:

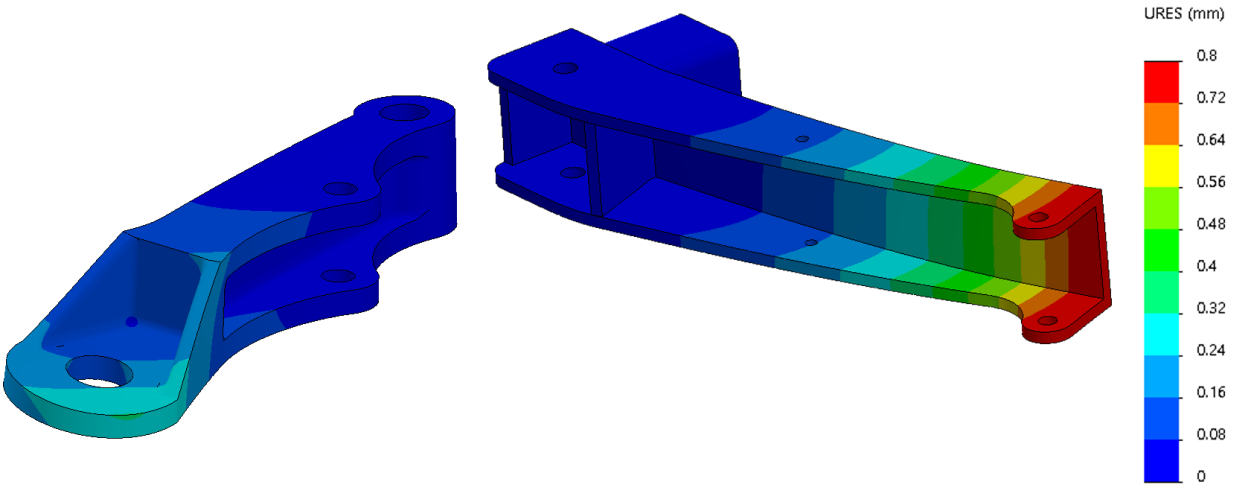

Figure 4.13: Resultant displacements under static compression of actuator (deformation scaling: 40)

The deformations are exaggerated to show how the parts deflect. The larger deformation occurs in the bracket shear plates, and will likely combine with some axial deformation of the actuator. The total deformation under load is less than the expected deviation in hitch position caused by play in the mechanical connections, which is common in trailering components (despite efforts to minimize play). Since there are sensors installed on the hitch mechanism to measure the position of the linkage, the deformation under load can be measured during full scale testing. Because the hitch linkage extends further in the longitudinal direction than a standard hitch ball, there is approximately 20% of extra moment applied to the OEM hitch mount, lowering its effective load rating. This is not an issue for this research given the trailer that is used, but this extra moment is an important consideration when paring the hitch with OEM hitches in a commercial application.

4.1.4 Sensor packaging and auxiliary components

Treating the active hitch as a planar system, there are only two measured degrees of freedom required to control the linkage: the movement of the linkage relative to the tractor, and the yaw of the trailer relative to the hitch. The roll and pitch behavior of the trailer will affect the measurement of the trailer yaw of only two sensors are used, so the placement of the sensors is designed to minimize the extra effects.

The sensors are hall-effect based rotary position sensors, manufactured by Delphi [47]. The sensors were chosen for low cost and robustness in harsh outdoor environments, which results in their use in many automotive chassis applications. They have a rotation range of approximately 100°, and can easily be fitted with custom mounting to attach to various chassis linkages. They are also spring-loaded to decrease mechanical play during hitch movement. Since the sensors have a limited range of motion, they are meant to be configured into four bar linkages, where the sensor rotation acts as the follower, and the suspension component acts as the crank.

The configuration of sensors is shown along with the customized mounting for the sensors in Figure 4.14, which also highlights the four-bar linkages that were analysed:

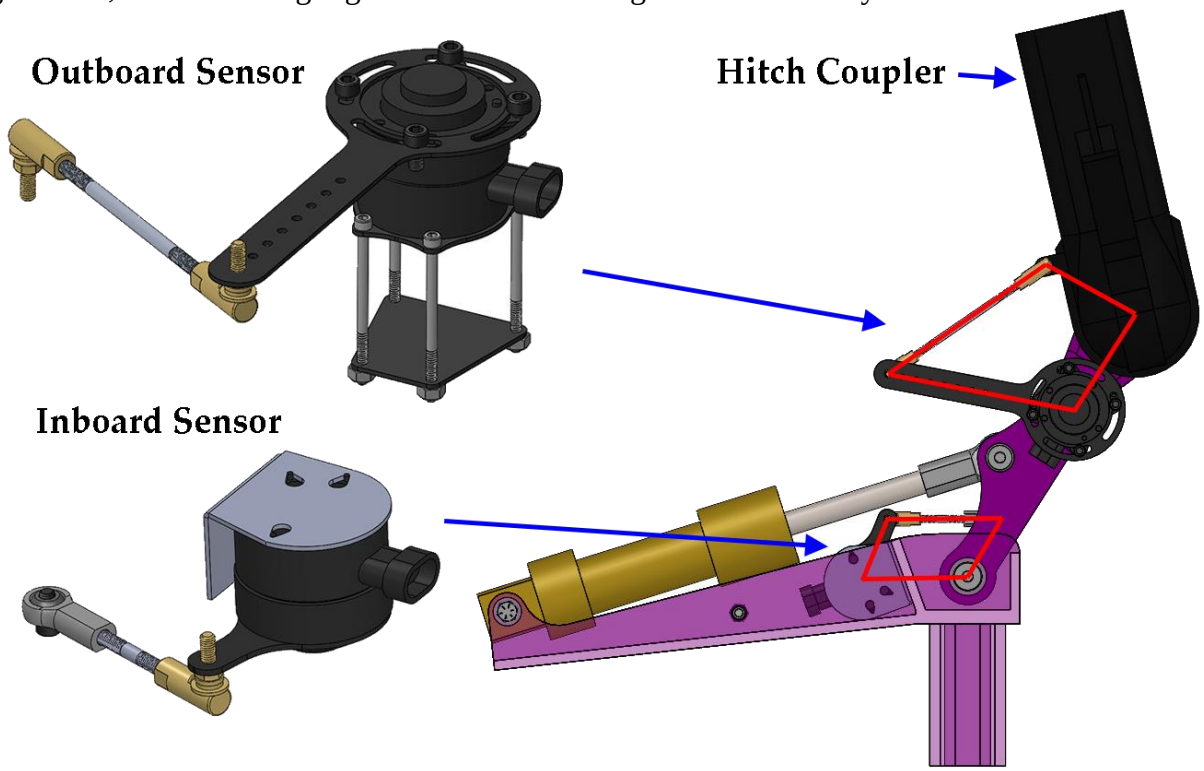

Figure 4.14: Sensor placement (four bar linkages highlighted in red)

The custom mounting and linkage arms for the sensors are laser cut from 1/16in sheet. The inboard sensor is bolted to the inside of the structural bracket. The outboard sensor is clamped onto the end of the hitch arm, where the bolts index on the curvature of the hitch arm, preventing sliding. The outboard sensor plates also have slots and indexed holes, so that the plates can accommodate mounting to different hitch couplers.

The previous figure also shows how the active hitch attaches to the hitch coupler on the test trailer. Since the outboard sensor link must be attached to the same spot on the coupler each time the trailer is attached, this particular method of measurement is not viable for commercial use. More sophisticated methods of sensing the trailer position were considered, such as ultrasonic sensing and customized hitch balls, but were deemed less practical and beyond the scope of the research. A more versatile method for sensing the hitch position should be of primary concern to future development of the active hitch as a commercial product.

Once the structural components of the active hitch were designed, a MATLAB script was created to simulate the motion profiles of four bar linkages. These simulations were used, along with packaging constraints imposed by the 3-D model, to place the two sensors in locations that could measure the range of possible trailer motions, and that would have a reasonably linear mapping from the follower angle to the crank angle. Given the crank angle θ, a set of trigonometric equations can be set up to describe the positions of the links in terms of the unknown follower and rocker angles ψ and ϕ [48]:

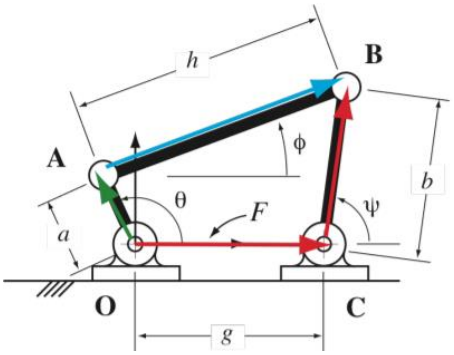

$$\mathbf{A} + (\mathbf{B} - \mathbf{A}) = \mathbf{C} + (\mathbf{B} - \mathbf{C}),$$

$$\begin{Bmatrix} a\cos\theta \\ a\sin\theta \end{Bmatrix} + \begin{Bmatrix} h\cos\phi \\ h\sin\phi \end{Bmatrix} = \begin{Bmatrix} g \\ 0 \end{Bmatrix} + \begin{Bmatrix} b\cos\psi \\ b\sin\psi \end{Bmatrix}.$$

Figure 4.15: Four bar linkage loop equations [48]

The inboard sensor linkage measures the position of the hitch ball. The only goal in designing the inboard linkage is to make it as close to a parallel linkage as possible. A parallel linkage would have identical angles for the crank and follower, resulting in a 1:1 mapping of the sensor angle to the angle of the main structural arm. The sensor is able to mount firmly within the shear plates on the structural bracket, but is not a perfectly parallel linkage. The range of motion for the inboard linkage is illustrated in Figure 4.16 on the following page, along with the mapping from the sensor angle to the hitch arm angle:

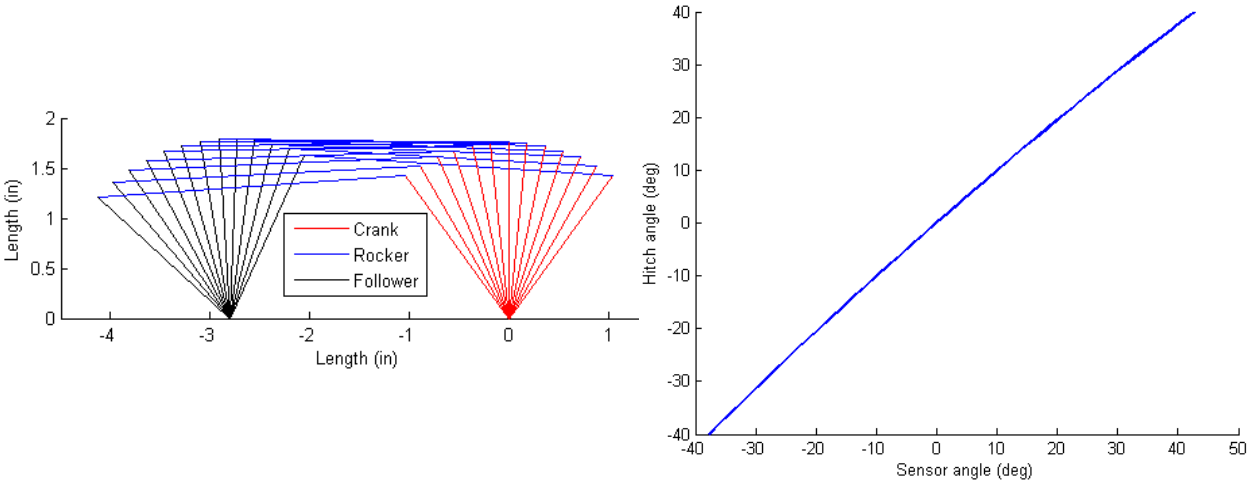

Figure 4.16: Inboard sensor linkage kinematics

The profile is mostly linear; the rate of change between the sensor angle and the hitch angle varies from 0.9 to 1.15 at the extremes. Achieving the benchmark motion range for the active hitch requires ±29° on the hitch arm, and the actuator range of motion allows for some extra travel (33° for 12.5cm of lateral motion).

The outboard sensor linkage has more design requirements due to being directly attached to the trailer. The angle of the trailer is measured relative to the hitch arm, which can be added to the arm angle to get the actual trailer angle. The trailer is permitted ±90° of rotation relative to the hitch arm without damaging the sensor, which covers the most extreme maneuvers, since the control law dictates that the hitch arm will orient in the same direction as the hitch angle, so the relative angle will be lower. Additionally, the following design features were implemented for the outboard linkage:

To minimize the effect of pitch and roll, the follower and rocker links are made as long as possible, while avoiding self-intersection of the linkage. Based on the part geometry, the trailer can roll by approximately 20° before the rolling accounts for 1% of the measured yaw rate. In order to cover the 180° range of the crank, the ratio between the crank and the follower must be lowered since the sensor is limited to around 100°. The outboard sensor kinematics are presented in Figure 4.17 on the following page:

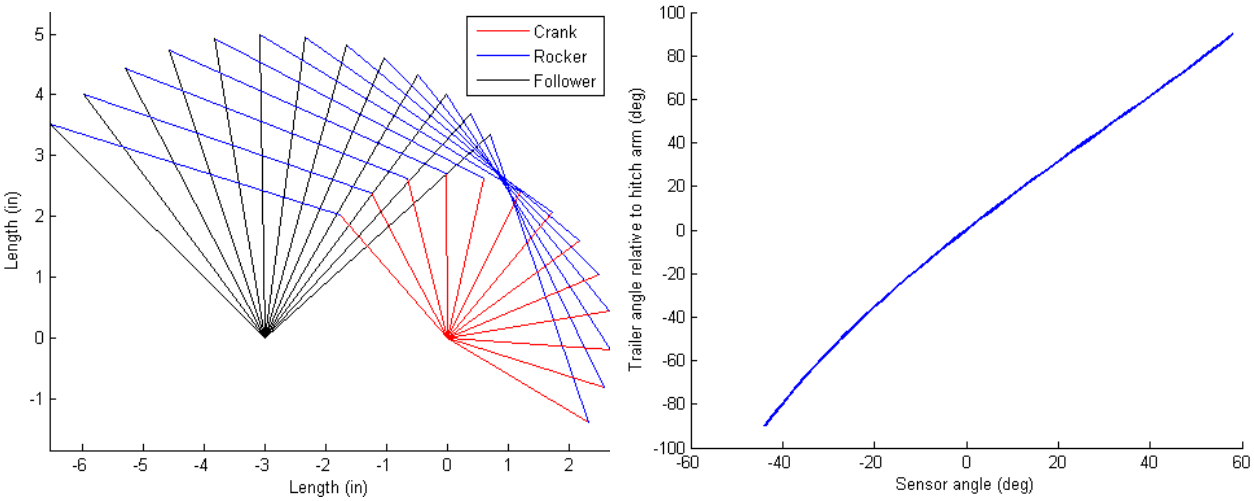

Figure 4.17: Outboard sensor linkage kinematics

Due to the more diverse constraints on the outboard linkage, the motion profile is fairly nonlinear, where the rate of change between sensor angle and relative trailer angle varies from 1.5 to 2.9. From the motion profiles, a lookup table was generated for each sensor, so they could be calibrated on the final assembly to measure the hitch position and the trailer yaw angle.

In order to protect the sensors and the actuator during testing, a sheet metal cover was manufactured. It is attached at the main assembly at the main pivot, the outboard actuator bolt, and a third bolted connection through the center of the shear plates on the structural bracket. The cover is made more rigid through a combination of bends and welds, which can provide some additional stiffness to the main structure.

4.2 Power Pack

The active hitch system is powered by a hydraulic power loop. Based on the simulations, and estimating the power consumption of the auxiliary components, the power pack is designed to deliver peak power of **1500W**, whereas the low duty cycle results in an average estimated consumption of **500W** (this estimation was never verified during testing). In the initial design phase, a fully electric solution was considered to reduce the total number of components, and to be more suitable for a standalone aftermarket product. The main reasons for choosing a hydraulic system are as follows:

Standard industrial setups for electric linear actuators are slower and weaker mechanically than a similarly sized hydraulic system. While it is possible to achieve similar performance from an electrical hitch actuator, there would be a significant increase in cost of components and mechanical design to create a feasible solution. Based on the timeline of the project, a hydraulic system is more realistic.

While one of the goals is to make the system attractive as a commercial solution, the primary goal is to verify that active hitch control is an effective method for reducing sway in passenger-sized vehicle configurations. To this end, a hydraulic setup is far more robust for dealing with a prototype design for research, and components can more easily be upgraded without fundamental changes to the mechanical design.

A simplified layout of the components required to drive the hitch is shown in Figure 4.18. It serves to enumerate the main components of the system, and does not reflect specific routing of hydraulic lines (tank, pressure) or driving electronics.

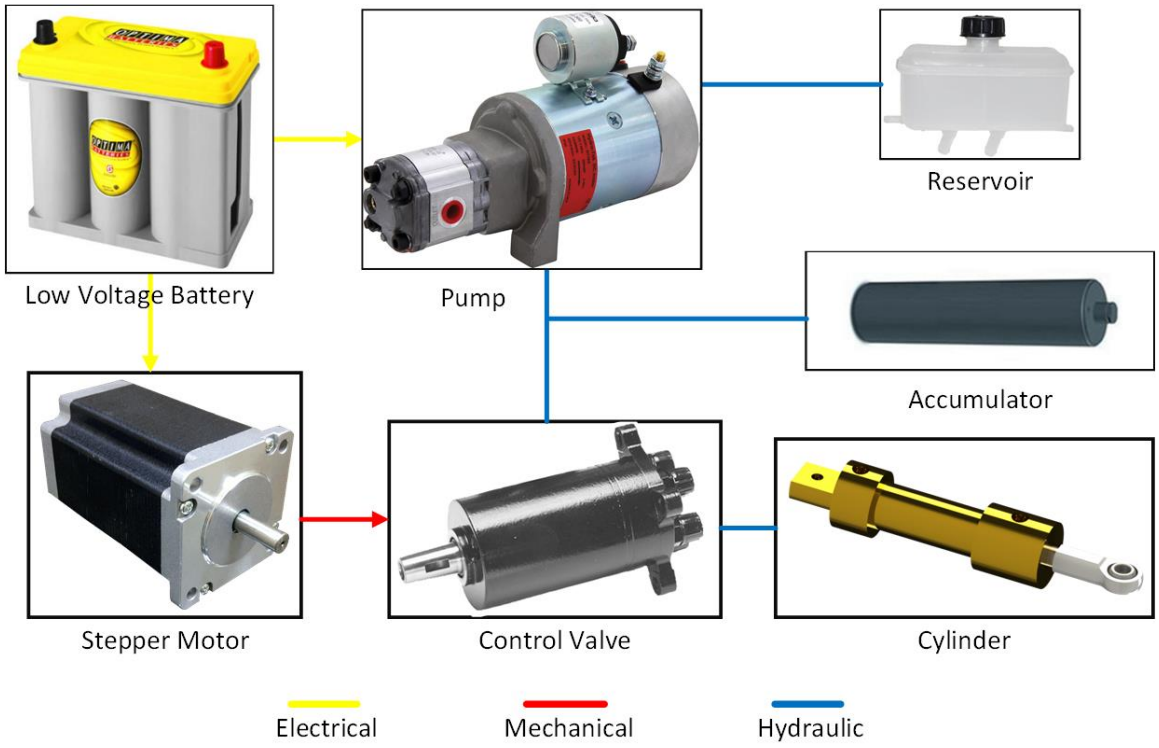

Figure 4.18: Simplified diagram of actuation power loop

The power loop uses a high-performance car battery as the primary power source [49]. The battery drives the pump motor and the stepper motor, which in turn drive the hydraulic loop. The

battery charge is maintained through power from the high voltage pack of the test vehicle. Justification for the selected components is elaborated in the following subsections.

4.2.1 System performance requirements

In keeping with the dynamic requirements proposed at the beginning of this chapter, the hydraulic system must be able to actuate the hitch ball against 3000N of lateral force at 25cm/s, with 45cm/s peak. The speed benchmark is based on the capability of the system to complete a sine wave oscillation that covers the entire range of motion of the hitch, while matching the natural oscillation period of a typical tractor-trailer configuration. Simulation of different configurations resulted in selecting a benchmark oscillation period of 1.4s, which is characteristic of smaller trailers towed by mid-size tractors. The benchmark motion profile is illustrated in Figure 4.19:

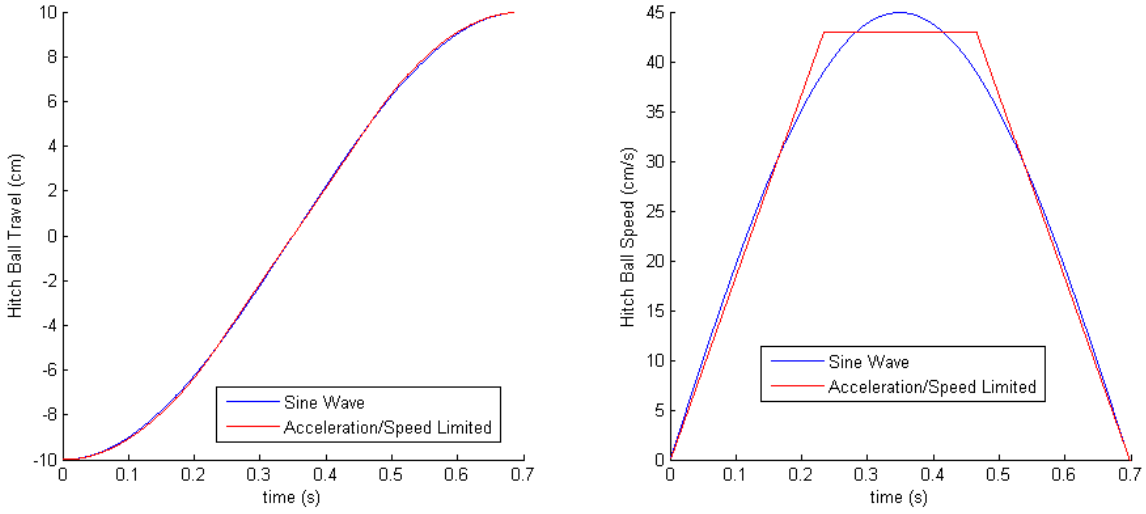

Figure 4.19: Benchmark Motion Profile

The above figure shows a comparison of the pure sine wave motion with an equivalent acceleration and speed limited profile. The limited profile is split evenly in time into two periods of constant acceleration and one period of constant speed. This provides a close match to the pure sine wave, and is a common method for selection of hydraulic and electric actuators. In this case, the limits are used to select a motor drive that can supply a given torque and maximum rotation speed, and to select a flow valve with an appropriate flow rate limit.

For this hydraulic system, achieving the required lateral force is determined by its ability to maintain pressure in the line, and for the cylinder to have a sufficient bore size to translate the

system pressure into a lateral force. In practice, the performance is limited by the ability of the pump and accumulator to maintain reasonable system pressure when the cylinder is moving at its top speed.

4.2.2 Hydraulic cylinder

A high-pressure brass cylinder was purchased from Cylinders & Valves, Inc [50]. It was selected in conjunction with the kinematic design of the hitch mechanism, and serves as a mechanical stop to prevent the mechanism from damaging itself. As discussed in section 4.1.1, the motion/force ratio between the hitch ball and the cylinder is 2.53, so the cylinder must support the scaled force and speed limits of **7590N** and **17.8cm/s**, respectively. The specifications of the cylinder as well as derived performance parameters, are listed in TABLE 4.II.

TABLE 4.II: HYDRAULIC CYLINDER SPECIFICATIONS

Bore Diameter	1.5in
Piston Diameter	0.625in
Stroke (total travel)	3.5in
Rated Pressure	1500psi
Length when Retracted	10in
Push & Pull Force	2650/2190 lbs (**11800/9810 N**)
Push & Pull Speed (5.3 GPM peak flow)	11.5/14.0 in/s (**29.2/35.6 cm/s**)

The flow limit of 5.3GPM is based on the maximum operating flow rate of the valve, which is discussed further in section 4.2.3. The smaller bore was selected so that the mechanism could be as compact as possible while achieving the required performance. All hydraulic cylinders have asymmetric performance, due to the piston creating different effective areas for extension and retraction. Therefore, the weaker performance in each case is used for design purposes; extension is slower, retraction supports less force.

4.2.3 Driving components

The maximum system flow rate of 5.3GPM comes from the performance limit of the flow valve [51]. The OSPM 32 PB valve diverts flow through the cylinder ports, allowing reciprocal motion of the hitch. The valve is powered by a NEMA 42 stepper motor [52]. This particular motor was selected out of convenience rather than peak performance, since the supporting electronics and

hardware for this type of motor were already installed in the test vehicle during manufacturing. Since the valve delivers 32cc/rev, the benchmark maximum hitch speed requires the stepper motor to rotate 382RPM peak. This rotation rate is typically achievable by stepper motors of this size, further discussion of motor performance is provided in the testing chapter.

The pump is a standard configuration of a 1.6cc/rev gear pump, driven by electric motor. Pressure in the system is regulated by a gap-action controller, which attempts to keep the pressure in the range of 1300-1500psi, the rated pressure for the cylinder. This motor/pump combination can nominally supply 1.1GPM at 1500 psi [53]. This is equivalent to moving the hitch ball only 16cm/s, while supporting the required 3000N lateral force.

This shortcoming in performance is addressed by including and accumulator on the pressure line [54]. The 0.25 gallon capacity accumulator can be charged by the pump, and can deliver stored fluid at up to 100GPM, which is far in excess of the 5.3GPM limit of the valve. Combining the pump and the accumulator, the system is able to produce the full speed hitch movement at a 20% duty cycle, and can maintain the full speed movement for 3.5s. Simulation results have shown that the active hitch can remove transient oscillation in approximately 3s, where the full speed movement is only required for the first oscillation period of the transient response.

The hydraulic components are routed using a combination of flexible hose and aluminum piping. Both types of selected tubing are rated to 3000psi, which is well above the expected maximum pressure in the system. Tubes were sized based on the SAE ARP994, a standard dealing with best-practice for hydraulic components [55]. The primary concern for correctly sizing tubing is preventing cavitation and excessive head loss.

$$\frac{P_1}{\rho g} + \frac{V_1^2}{2g} = \frac{P_2}{\rho g} + \frac{V_2^2}{2g} + \left(\frac{fL}{D} + \Sigma K\right)\frac{V^2}{2g} \tag{4.9}$$

The extended Bernoulli equation that includes head loss (where f and K represent friction/loss factors of particular fittings or tubing material) shows that higher flow velocity will result in a pressure drop. If the pressure is low, such as at the inlet of the pump, vapor cavities can form, which damage the components when they collapse. The head loss is also a function of velocity squared, so larger tubes will prevent excessive head loss for a given volumetric flow rate. Based on these principles, ARP994 recommends maximum fluid velocities of 15-20ft/s in pressure

lines, 10-15ft/s in tank lines, and 5ft/s in suction lines. Combining these recommendations with the maximum achievable flow of 5.3GPM, the tubes in this hydraulic system have a 3/8in inner diameter, with a larger 1/2in hose for the suction line at the pump inlet.

4.2.4 Physical packaging

The power pack is physically split between the front and rear of the Equinox. The battery, reservoir, accumulator, and pump are located in the front of the vehicle. The tubing is routed through the vehicle under-tray to the remainder of the components, which are mounted to the hitch via a welded bracket on the hitch. This is not ideal for a standalone system; the components were only split in this way because of practical constraints on the test setup. The components at the front of the vehicle were being used for other research projects at the time of testing, and there was little room remaining behind the hitch since the Equinox has custom components installed in that area to cool the high voltage battery pack. Based on the amount of room forward of the hitch on a production vehicle, it is reasonable to assume the entire power pack could be packaged forward of the hitch. The underside of the rear of the test vehicle is pictured in Figure 4.20, containing the flow valve and the stepper motor:

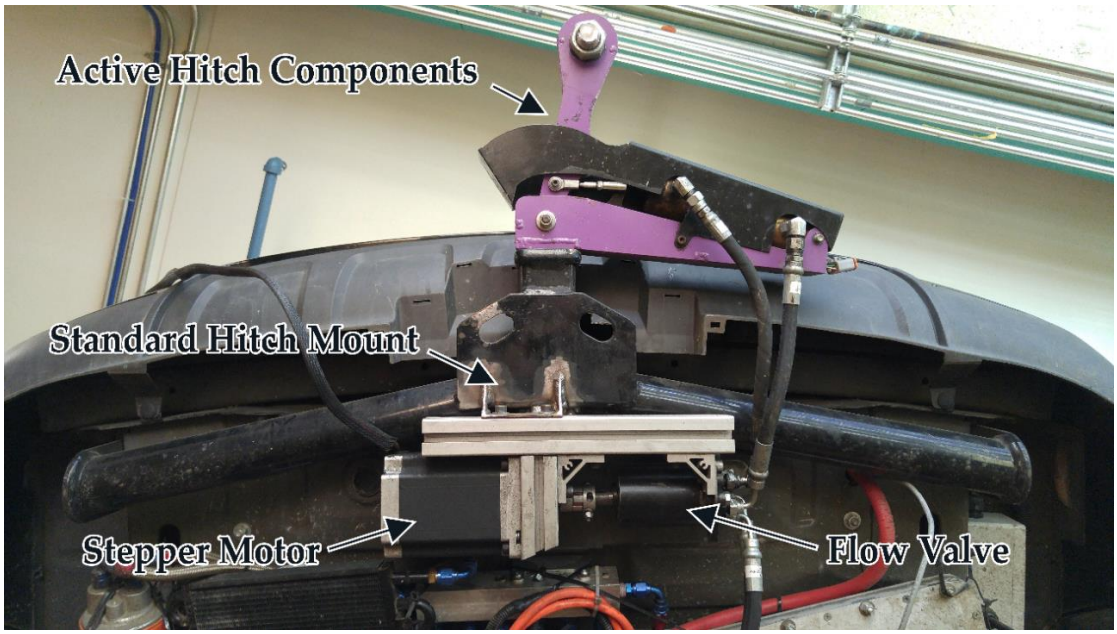

Figure 4.20: Packaging of power pack components on hitch

The performance of the power pack and the hitch linkage are discussed in more detail in the following chapter, which covers the process of experimental testing.

4.2.5 Reverse configuration concept

For potential commercialization of the active hitch, it may be desirable to reverse the configuration of the active components, where the actuation and the system power pack would be contained on the trailer. An example of this reverse configuration is shown in Figure 4.21, where the power pack would be packaged rear of the actuation components.

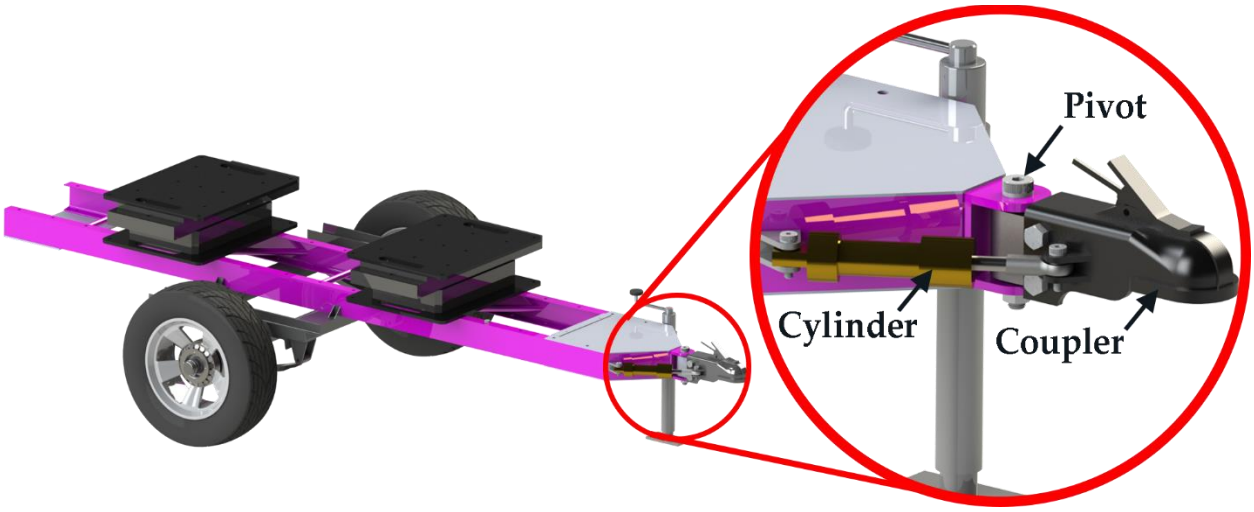

Figure 4.21: Reverse linkage configuration on test trailer

This configuration has the disadvantage of losing versatility; the active hitch would be contained on a single trailer. The reverse configuration has the advantage of increased passive stability; the trailer wheel base would be increased to package the active hitch, where longer wheelbases have more damped oscillations. In addition, the hitch ball on the tractor side could be packaged closer to the rear axle of the tractor, where smaller distances from hitch ball to rear axle are also more stable. The measurement of the trailer states is also easier when the entire active setup is packaged on the trailer, and the active hitch control can be more easily hybridized with differential braking of the trailer wheels.

Chapter 5: Experimental Testing

To validate the performance of the active hitch, sway behavior was induced in a full scale test setup and compared against the simulation results. The test setup comprises a combination of purpose built and existing lab equipment to capture the required data. This chapter describes the test equipment, the techniques used to capture data, and the final testing results.

5.1 Test Equipment

This section describes the components that are required to assess the performance of the hitch. The primary pieces of test equipment are the test trailer, the test tractor, and the test track.

5.1.1 Test trailer

A custom trailer was designed and manufactured for use in testing. Since the hitch controller is meant to function on a variety of trailers, the test trailer was designed so that it could simulate that variation in trailer configurations. Full-scale vehicle testing also emphasizes the need for auxiliary systems to ensure the safety of the test driver. The completed trailer is pictured in Figure 5.1:

Figure 5.1: Test trailer

The following features of the test trailer will be elaborated throughout this section:

- Inertial properties can be adjusted to vary the trailer dynamics, which can be determined using the 3D model (adjustable mass, mass center, yaw inertia, wheelbase).
- Relatively compact, to decrease damage in the event of accidents at the track, and ease in transport of equipment.
- Equipped with brakes, to be activated once trailer instability becomes unmanageable.
- Equipped with inertial sensing to compliment the measurements from the active hitch.

The main structural components of the trailer are formed with welded sections of 4”x7.25 structural channel, also supported by round tubes. The two main structural components are the spine and the axle carrier, pictured in Figure 5.2:

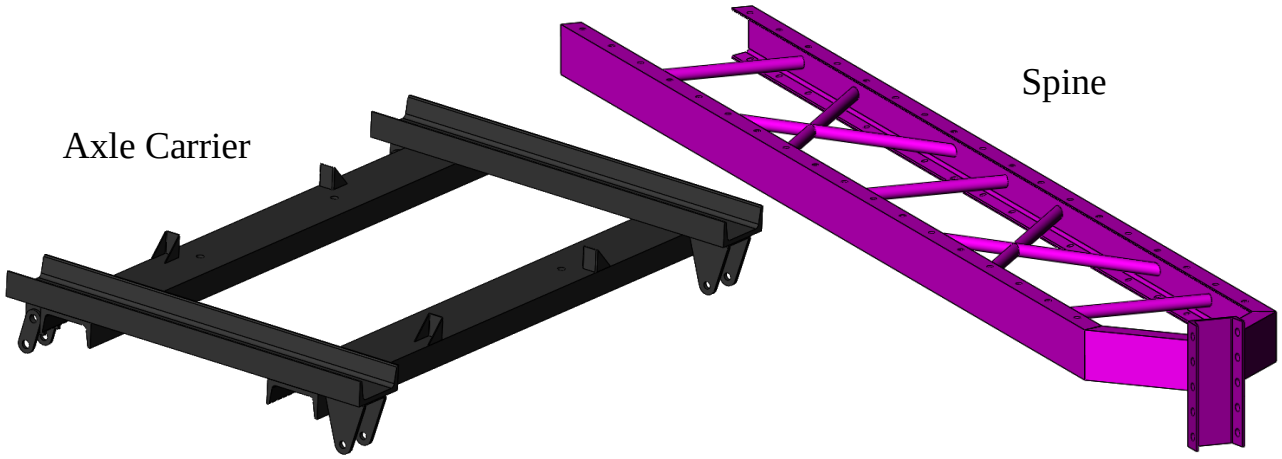

Figure 5.2: Trailer structural components

The spine has indexed holes drilled every 6 inches, which allows the axle carrier to be fastened to the spine at a variety of positions. This is used to change the mass center and the overall wheelbase of the trailer. The wheel base can reasonably vary from 50 to 90 inches. The indexed holes are also drilled through the top surface of the spine, so that the same adjustments can be made to the placements of the weight carriages. There are two weight carriages so that for a given mass center, the yaw inertia can be adjusted independently. The weight carriages are laser cut plates, which use threaded rods to fasten a variable weight to the trailer spine. The variable weights are pieces of scrap steel, and the combined weight of the carriages and the steel weights is approximately 500kg, depending on the trailer configuration being tested. Both the weight

carriages and the axle carrier use small bent sheet metal brackets to maintain alignment during the adjustment of the trailer inertial properties.

Since the control design of the active hitch is based on isolated yaw motion, the structural components were designed to minimize roll and pitch motions in the trailer. To ensure the structural components were suitable for safe use on the test track, FEA studies were performed similar to the studies performed on the hitch components. From static loading cases from the weights and from the lateral loads transferred from the trailer suspension, the structural components achieve a safety factor of greater than 2 on total trailer masses up to 1000kg. Trailer configurations of greater weight were not considered for this project, since the same unstable behavior can be achieved with a relatively small trailer, which would cause less damage in the event of an accident. In addition to the application of static loading, simplified frequency/modal studies were performed to ensure that the various resonant frequencies of the structure would not interfere with the measurement of the trailer yaw. Since the structure is comprised of common structural members, the trailer spine can be broken into beam-type finite elements. These simplified elements can achieve reasonable accuracy and can more quickly asses the various mode shapes. The weight carriages were added at various positions, and the lowest-frequency mode shapes were recorded for bending (in the pitch and yaw axes), as well as torsion. The vibration mode that produced the lowest natural frequency is presented below:

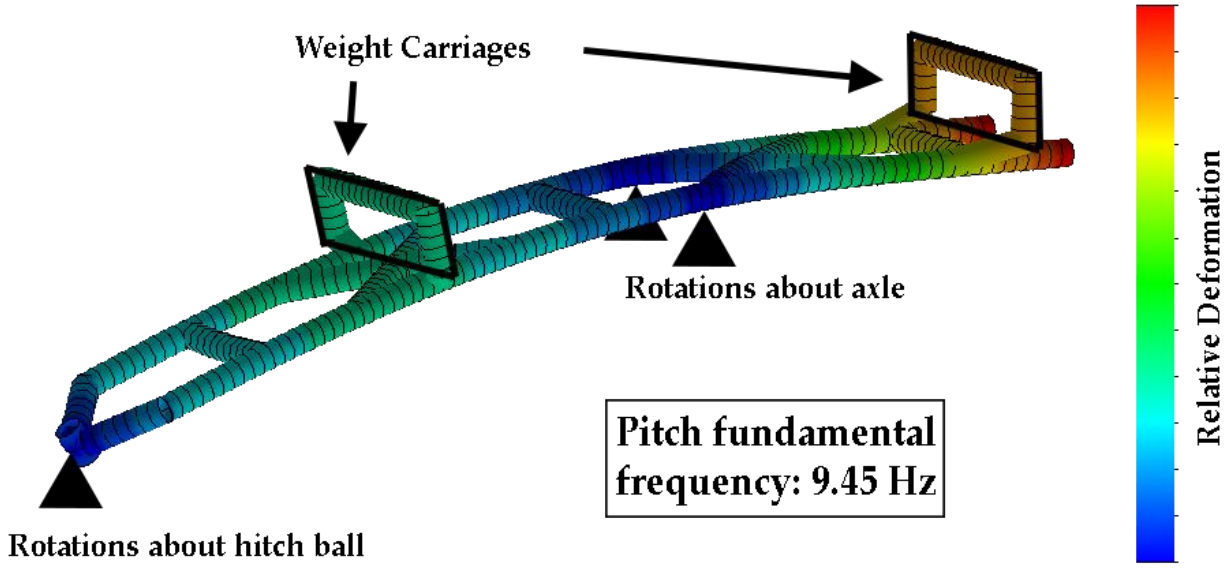

Figure 5.3: FEA frequency study (pitch motion simulated with beam elements)

The suspension on the trailer is comprised of two 1750lb capacity leaf springs, which brings the axle capacity to 3500lbs (1590kg). The equivalent stiffness of the springs is not provided by the supplier, so a simplified calculation is performed based on the stiffness of laminated beam elements, which estimates the leaf spring stiffness at 20275N/m. Assuming a maximum trailer mass of 1000kg, basic calculations can be applied to find the bounce/pitch natural frequency and the roll natural frequency [6]. The pure bounce motion of the trailer is estimated to be a minimum of 1.01Hz, assuming pure vertical motion, which is a typical bounce frequency for passenger vehicles. The wheelbase is long enough across the possible trailer configurations that the pitching motion is unlikely to create a noticeable change in the yaw angle measurement. The 3D model of the trailer is used to calculate the rotational inertias about the principal axes, which results in a worst case roll frequency of 1.86Hz. The trailer was designed with the intention of minimizing roll inertia, so that the trailer yaw would be as isolated as possible during lateral motions.

A limitation of the prototype active hitch structure is a lack of vertical adjustability. The difference in height of the hitch on a small passenger vehicle and a truck can lead to unwanted tilting in the trailer if the heights of the hitch coupler and ball do no match. The test trailer uses an adjustable coupler, which can be translated vertically by 6 inches. The coupler is rated for heavy use well above the expected trailer weight, supporting up to 5000lbs of tongue weight. The coupler is shown in its lowest position in Figure 5.4:

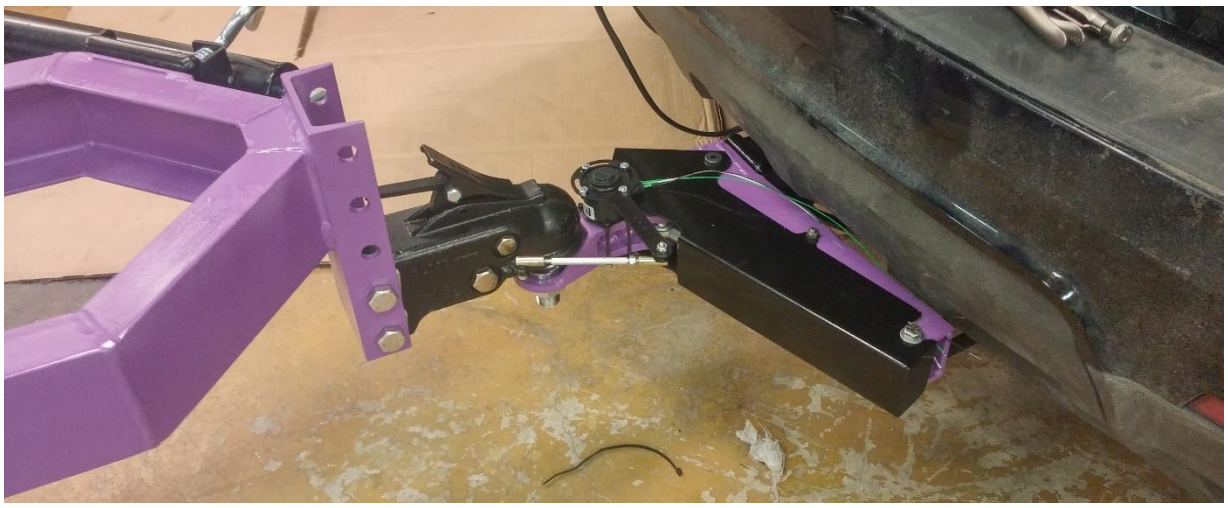

Figure 5.4: Coupler positioning, including attachment of trailer angle sensor

The suspension, axle, hubs, wheels, and brakes were purchased as a kit from Cerka [56]. The wheels are sized at 205/75R14, and the track width of the trailer is 1.32m. The drum-style brakes are actuated via a PWM signal, which causes a brake shoe to press against the drum. There is a basic relay control circuit for the brakes: if the braking on the tractor or the trailer angle reaches a threshold value, a baseline brake force is applied to both trailer wheels, as well as a differential force based on the trailer angle, which creates a restoring yaw moment. The brakes deactivate once the vehicle comes to a stop.

Inertial sensing is achieved through an automotive grade Inertial Measurement Unit (IMU), manufactured by RaceGrade [57]. The sensor sends 3-axis accelerations and 3-axis angular rates over the vehicle CAN bus. This sensor is not intended to be part of a standalone active hitch system. The IMU was included in the trailer design to ensure that the kinematics sensors are reporting reasonable trailer yaw data. The IMU is self-contained for outdoor use, and is mounted to the trailer via and adjustable plate, so that the sensor is as close to the trailer mass center as possible.

5.1.2 Test tractor

The test tractor is a highly modified 2011 Chevrolet Equinox. It serves as a test platform for multiple projects in the Mechatronics Vehicle Systems Lab, and is pictured performing a high speed double lane change in Figure 5.5:

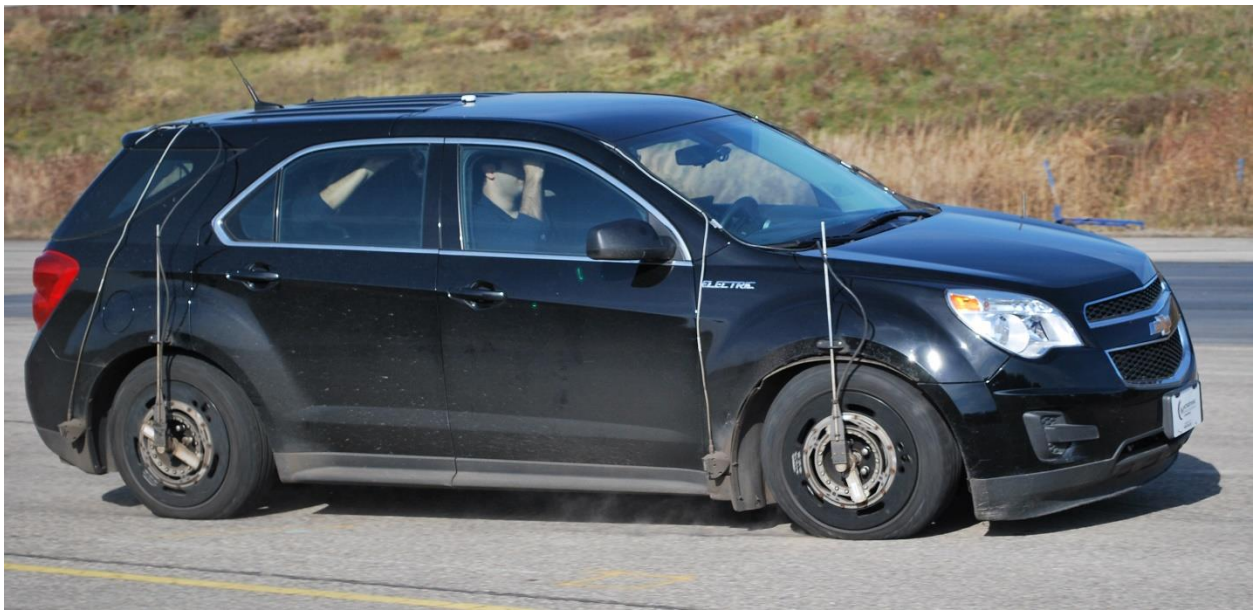

Figure 5.5: Equinox test platform

Major features of the Equinox are listed below:

- Each wheel is controlled independently, which allows for simulation of different driveline configurations and traction control algorithms.
- Brake and steer by wire for consistent maneuvers and path following.
- Full access to vehicle CAN bus for design of diagnostic and control systems.
- Wheel sensors that can be used to measure wheel speed and slip conditions.

The measurement of vehicle states and the execution of driving routines on the Equinox is achieved using a dSPACE MicroAutoBox II [58]. This prototyping unit runs automatically, taking the role of the Vehicle on-board ECUs. It can connect to a laptop to modify the vehicle routines in real-time, to tune the control system performance. The control algorithms can be imported from Simulink, which are stored on the memory and continue to run without the laptop. The AutoBox also contains the required I/O for function with the active hitch electrical components; it features analog and digital inputs and outputs to drive control components and take measurements from sensors. It also communicates with the production CAN bus, and can run 4 CAN networks at varying speeds.

The primary measurements used in control of the active hitch are the kinematics sensors discussed in section 4.1.4. Additional measurements are taken to verify the function and change the controller performance during different maneuvers. The equinox internal measurements (accelerations, angular rates) are taken from a navigation unit [59], which supplements the built-in inertial measurements from the AutoBox. The active hitch algorithm also uses the longitudinal velocity and steering input from the equinox, to ensure that maneuvers are performed consistently.

The equinox has a fully electric powertrain, powered by a 400V battery pack. In order to drive high current components on the active hitch, the low voltage battery is supplemented by power from the high-voltage pack, which is stepped down using a DC/DC converter, and AC power is provided to the stepper motor through an inverter. Additional fusing, relays, and contactors are used to route high current components and increase safety.

5.1.3 Control architecture

The final active hitch controller is based on the feedback control model discussed in section 3.1. The physical step for the controller uses the electronic components on the test equipment, as well as the specific electronics required to operate the active hitch. A simplified schematic in Figure 5.6 shows how the control action affects the system dynamics, and how measurements feed back into the control action:

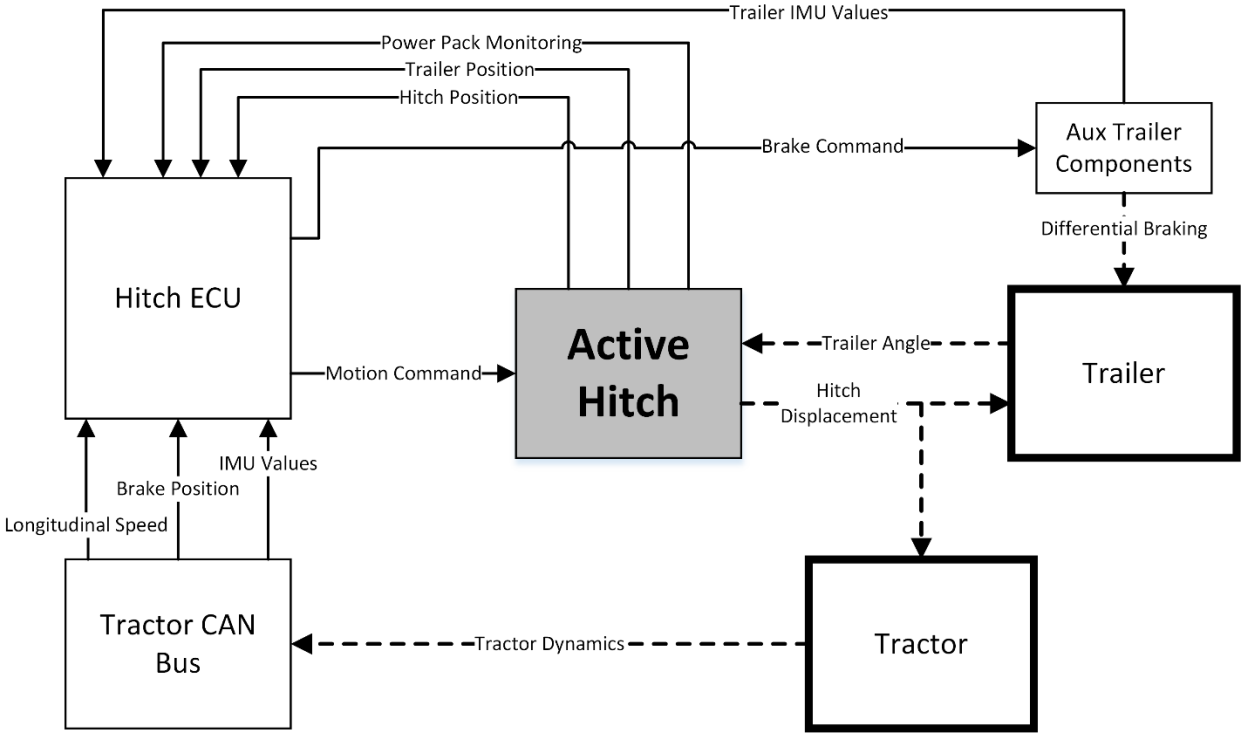

Figure 5.6: High-level control schematic

The solid lines correspond to measured signals, and dotted lines correspond to physical movement or forces. This schematic represents a non-exhaustive number of possible configurations for the controller. For example, communication with trailer auxiliary components or with the tractor CAN bus are not necessary to control the hitch, so they can be excluded for simpler configurations of the controller. The controller illustrated above is most closely based on the test setup for this research, and includes the extra safety systems and supplementary measurements.

5.1.4 Test track

The full scale testing of the active hitch is conducted primarily at driver training track for the Waterloo Region Emergency Services. A satellite image of the test track, with dimensions, is shown in Figure 5.7:

Figure 5.7: Satellite image of test track

The track is primarily concrete, with a 70x15m patch of smooth asphalt, which is used to simulate lower road friction. A fire hydrant is also installed on the perimeter of the track, so wet road conditions can also be created when desired. Due to its relatively small size, the track is most useful for maneuvers under 90km/h. While sway behavior is more likely at higher speed, the inertial settings of the trailer can be adjusted such that sway occurs at speeds that suit the track. The maneuvers used to test the hitch on this track are steer impulse, double lane change, steady-state steer. Some of the maneuvers simulated in chapter 3 could not be replicated at the track. The nature of the trailer oscillations are similar enough between types of maneuvers that the missing maneuvers can be validated by simulation if the track maneuvers match the corresponding simulations with enough accuracy.

5.2 Results

This section comprises all the work done towards full scale testing of the active hitch prototype. This includes the bench-testing of the hardware and its integration with the vehicle hardware.

5.2.1 Dynamic model validation

Since the Equinox is equipped with a variety of sensors that may not present on a production vehicle, it is possible to validate the dynamic model from chapter 3 by recreating physical test conditions in the simulator. Before integrating the active hitch controller into physical testing,

the trailer was driven in different maneuvers, while maintaining a consistent longitudinal speed. The steering inputs from the physical test, along with the trailer properties, were added to the state space model and simulated. A fairly stable trailer configuration was used initially, which had a mass of approximately 650kg, with a tongue weight close to the recommended 10%. Results for the comparison are shown in Figure 5.8:

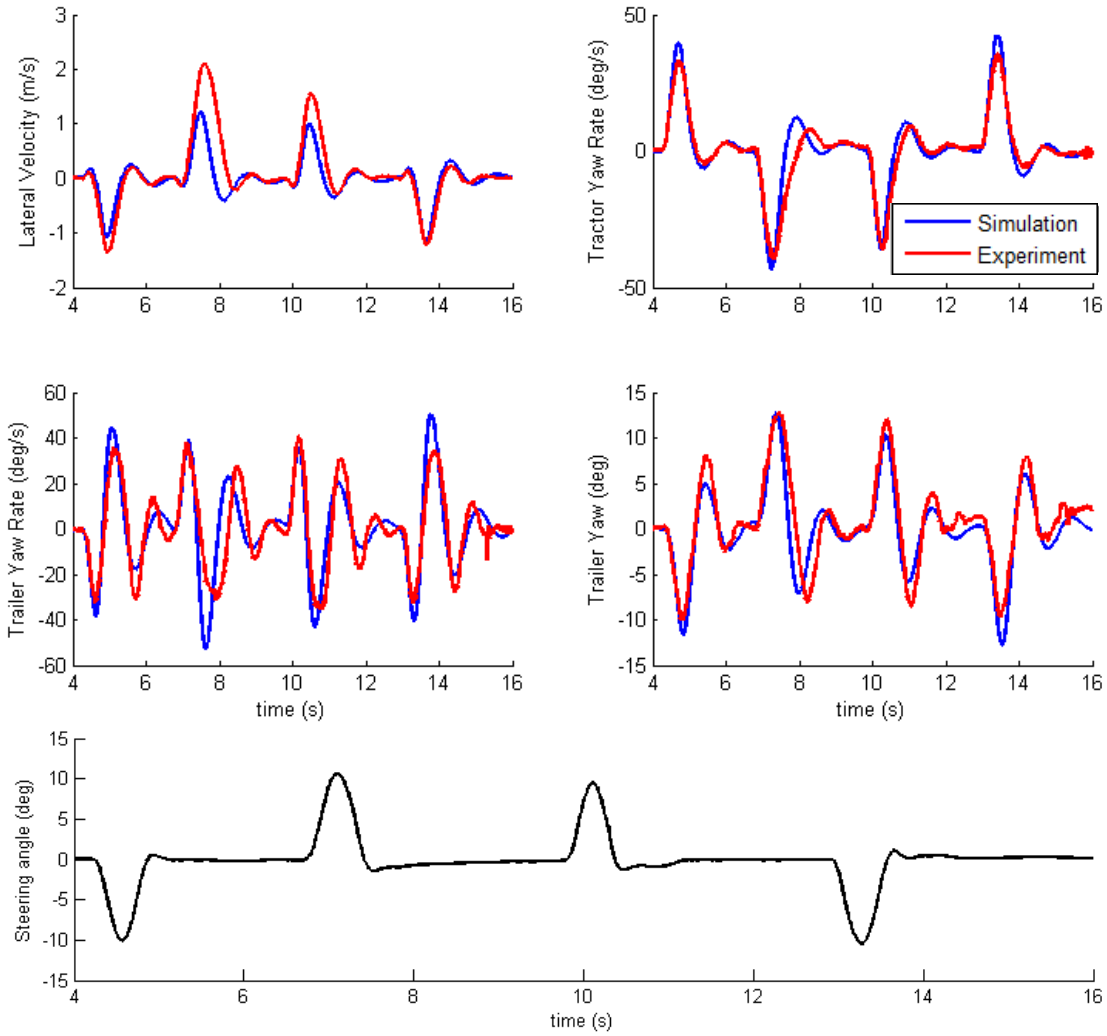

Figure 5.8: Comparison of simulation and experimental results, steering impulses at 60km/h

Considering the assumptions made when constructing the model, the simulations match with the experiment very closely. The only notable difference is the increased lateral velocity experienced by the tractor during experiment, due to the tires saturating and causing the tractor to drift. Since the trailer tires are still at reasonably small slip angles, the decaying oscillations resemble the pure sinusoids from the simulation.

To test higher slip angles and more unstable dynamics, the trailer was changed to the approximate properties listed in TABLE 5.I:

TABLE 5.I: TEST TRAILER CONFIGURATIONS

Property	Stable trailer	Unstable trailer
Mass (kg)	650	700
Yaw inertia (kgm^2)	900	1200
Wheelbase (m)	2.1	1.7
Tongue weight (%)	10	-10

A single steering impulse of 8.5 degrees was applied to the system at a longitudinal speed of 65km/h, resulting in the comparison in Figure 5.9:

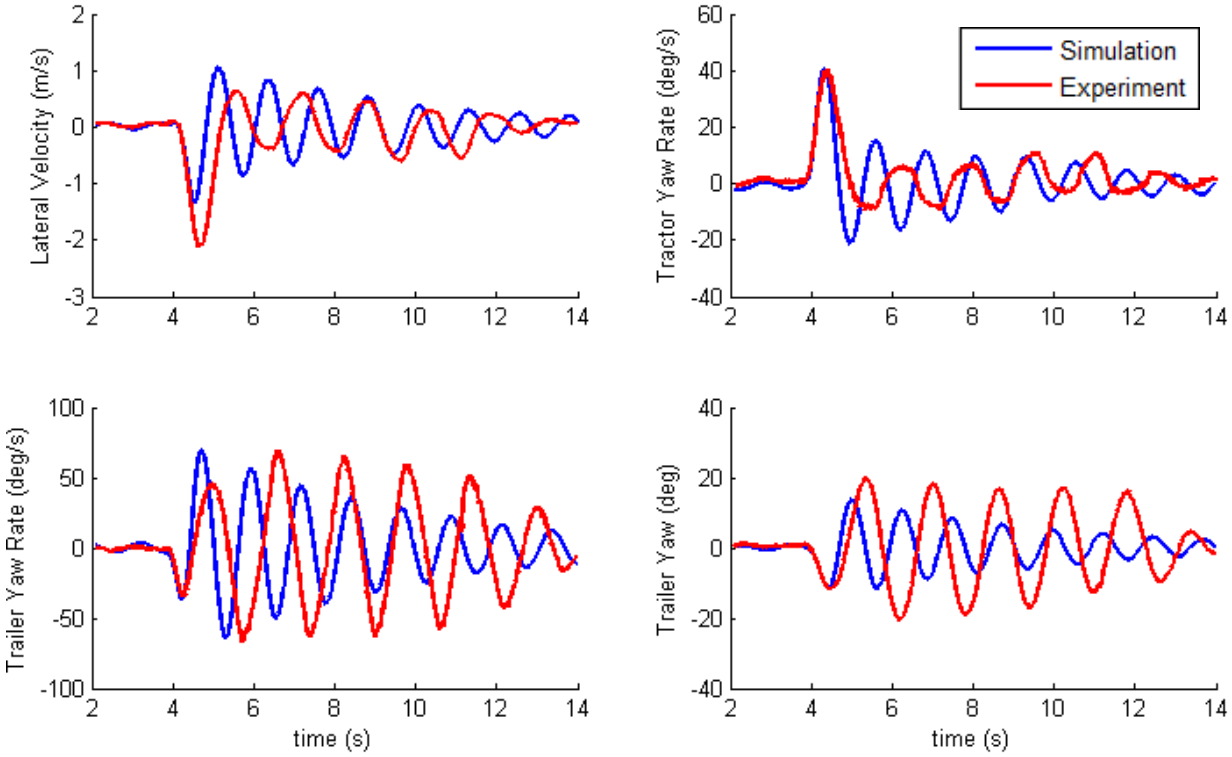

Figure 5.9: Comparison, impulse steer of unstable trailer at 65km/h

There is a more pronounced difference between the experiment and the bicycle model in this case. The experiment shows tire saturation through the saw-tooth appearance of the trailer yaw oscillations, similar to those observed in the MapleSim results. The tractor dynamics match fairly well, which also suggests that the trailer is sliding more than predicted by the linear model, since trailer with saturated tires would not transfer as much force to the tractor through the hitch.

5.2.2 Controller implementation and tuning

The controller design was implemented through a Simulink build of the test vehicle, and was loaded onto the memory of the AutoBox. The I/O on the AutoBox are routed into the Simulink model through proprietary routing blocks. The Simulink build was made as simple as possible, to reduce the time required to rebuild the model when implementing changes. The active hitch module contains three sub-controllers: the main active hitch feedback controller, the low-level stepper motor controller, and the trailer brake controller.

The trailer brake controller is a safety precaution for the track, where differential braking will be applied to the trailer if the trailer angle reaches a threshold value, originally set at 45°. It will also apply differential trailer braking if the driver depresses the brake pedal past a certain threshold. The brakes act through a relay block, so the brakes do not release until the trailer has settled.

Standard filtering techniques are used to extract a cleaner signal from the trailer sensors. The global refresh rate of the Equinox is set to 200Hz, so several time steps can be used simultaneously without causing significant delays. The 200Hz refresh rate is chosen because it is twice the rate of a standard production vehicle, so it has additional information for research purposes, but is still suited for commercial sensors and controllers. Low-pass filter designs were originally considered specifically to block the EM noise produced by the Equinox powertrain motors, but they were unable to outperform simple moving average filters. For numerical differentiation, signal noise is significantly increased, so more time steps need to be used on filtering of signal derivatives. Differentiation was implemented using an FIR filter that calculates the slope of the line running through a set of points by least squares regression. Least squares creates a better fit to the data than simply taking an average. Based on a derivation in [60], the slope of the line in a least squares regression can be formulated in the form of an FIR filter. Since the dependent variable (time) is increasing evenly, significant algebraic simplifications can take place, which removes the nonlinear terms from the least squares formulation and leaves a weighted sum of the time steps, where the weights are given by:

$$\beta_i = \frac{12i - 6(N-1)}{N(N^2-1)} \tag{5.1}$$

And where N is the chosen number of time steps used in the filter. The weights are negative symmetric, which means that the earlier time steps will be weighed negatively.

Attempts to drive the hitch at high speeds initially resulted in stalling of the motor. The stepper motor controller had to be tuned in software and in hardware to ensure that the hitch could move the required load at a reasonable speed. The stepper motor has 200 permanent magnet poles, but the motor driver allows for microstepping, where the drive sends interfering signals that make the motor behave as though it has more poles. This is useful for smoothing the motion of the hitch, specifically in reaction to measurement noise on the kinematics sensors. There is a compromise to be made, since the use of microstepping introduces some hysteresis which results in a small loss in motor torque. Additionally, the high mircostepping signal require high frequency signalling from the ECU, and will cause a stall if the AutoBox cannot consistently produce the frequency content. A microstep setting of 6400 pulses/rev was found to be the best balance of noise reduction, speed, and torque handling.

In addition to the hardware settings on the motor driver, the motor controller requires additional regulation from the Simulink model. A saturation block is used to prevent the controller from requesting frequency content that is too high for the AutoBox to deliver. A slew rate limiter also sets acceleration and deceleration limits on the hitch to prevent damaging the components. These acceleration limits offered some improvement to the hitch performance in bench tests, but the added inertia of the trailer combined with the acceleration limits resulted in a resonance between the main controller and the stepper motor controller, so the acceleration limits had to be discarded.

The stepper motor is driven by its own feedback controller, which acts on the difference between the actual hitch position and the position requested by the main controller. Since the requested position is constantly changing, a certain tracking error will develop, where the hitch will lag behind its required position. As discussed in section 3.2.5, the active hitch controller is unstable for delays of greater than 0.25s. Simply increasing the gain on the low-level stepper controller will cause excessive noise and controller resonances, so some compensating techniques are required to minimize the tracking error.

Feedforward control can be used to compensate for disturbances in a system, or to eliminate tracking error. In this case, it anticipates future hitch value requests by taking the derivative of the hitch request and applying a gain as shown in Figure 5.10:

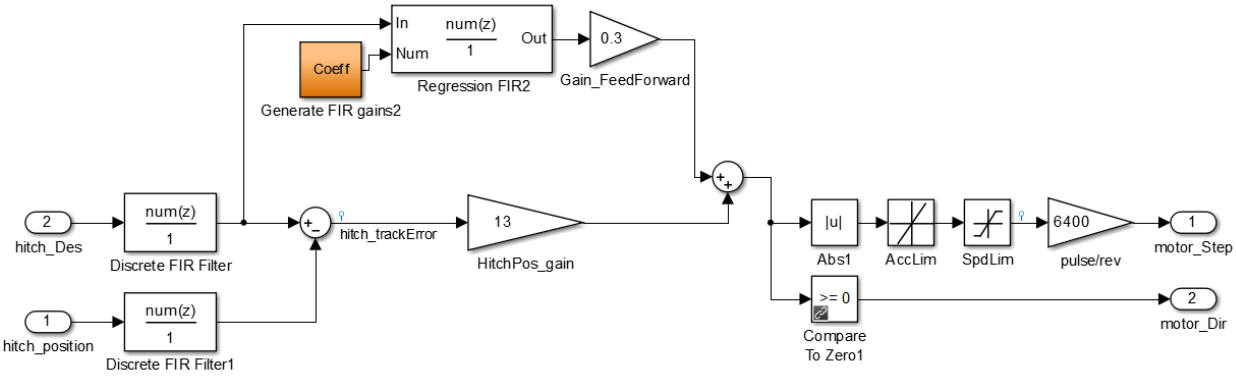

Figure 5.10: Simulink diagram of low-level stepper motor control

The feedforward compensator uses the linear regression filter to calculate the rate of change of the hitch request. Since numerical differentiation is noisy even when filtered, the feedforward gain must be set modestly. The selection of 0.3 for the feedforward gain resulted in a 50% reduction in peak tracking error over sinusoidal hitch requests, which is also reflected in the full scale test results.

As predicted in simulation, the addition of derivative action on the main controller was not effective, since the noise content of the differentiated signal is larger than the expected range of the signal. More extreme filtering on the signal simply results in non-trivial delays in measurement, which are more detrimental than neglecting the derivative action.

5.2.3 Anti-sway control testing

This section examines the feasibility of the active hitch prototype by performing a combination of maneuvers at the track. Multiple runs for each maneuver were performed, so that the set of speed and steering inputs are as similar as possible between open and closed loop runs. To make the influence of the controller more obvious, the unstable trailer configuration described in TABLE 5.I was used for the majority of the tests.

Initial tests were performed using derivative action on the trailer yaw rate. As with the MATLAB and MapleSim simulation results, derivative action had very low effectiveness at stabilizing the hitch. The baseline value for the proportional gain was set at 0.3 inches per degree of trailer

angle, which is equivalent to setting the gain to 0.68m/rad in the MATLAB and MapleSim models. A steer impulse was performed at 65km/h and at 75km/h in open and closed cases, as presented below:

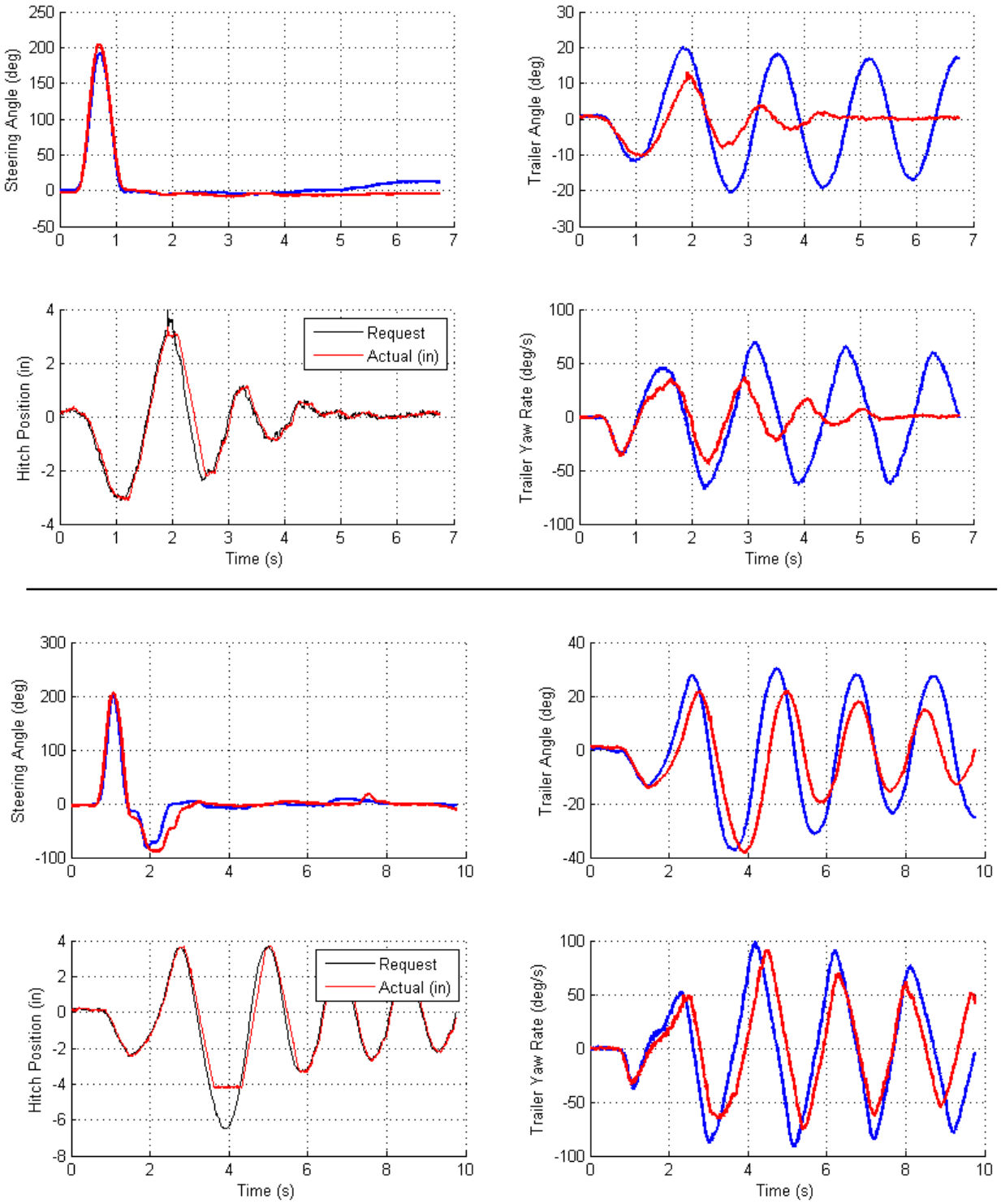

Figure 5.11: Responses at 65km/h and 75km/h for no feedback (blue), and for K=0.3in/deg (red)

In both cases, the active hitch controller is able to reduce sway. The effect of the active hitch is more pronounced in the first figure, where the tires are still in a somewhat linear region. At 65km/h, the active hitch can damp out oscillations in 4 seconds, where the open loop response would have continued to oscillate indefinitely. This effect would be more pronounced for an unskilled driver, where attempting to compensate with steering would likely result in increased instability. There is a region where the tracking error increases due to the motor controller reaching a speed limit. These tests were performed without feedforward compensation, and without the final tuning setting for the microstep driver. Subsequent tests showed significant improvements in the top speed and the tracking error of the controller.

At 75km/h, the hitch is still able to reduce the sway behavior, but over a longer time scale. It should be noted that the 75km/h speed could not be maintained in the open loop case, where the high trailer angle and yaw rate caused the vehicle to decelerate due to the extra friction introduced. So the active hitch allowed the vehicle to maintain a higher speed, while still reducing sway. The controller requested a hitch value that was higher than the physical limit of the hitch. The hitch holding at its maximum value does not have a significant effect on the sway reduction, since the trailer yaw rate is low at the peaks of trailer angle.

After controller improvements as described in section 5.2.2, the steering impulse was repeated at 70km/h, with a reduction in feedback gain to 0.2in/deg to reduce the risk of stalling. The comparison between system responses is shown in Figure 5.12:

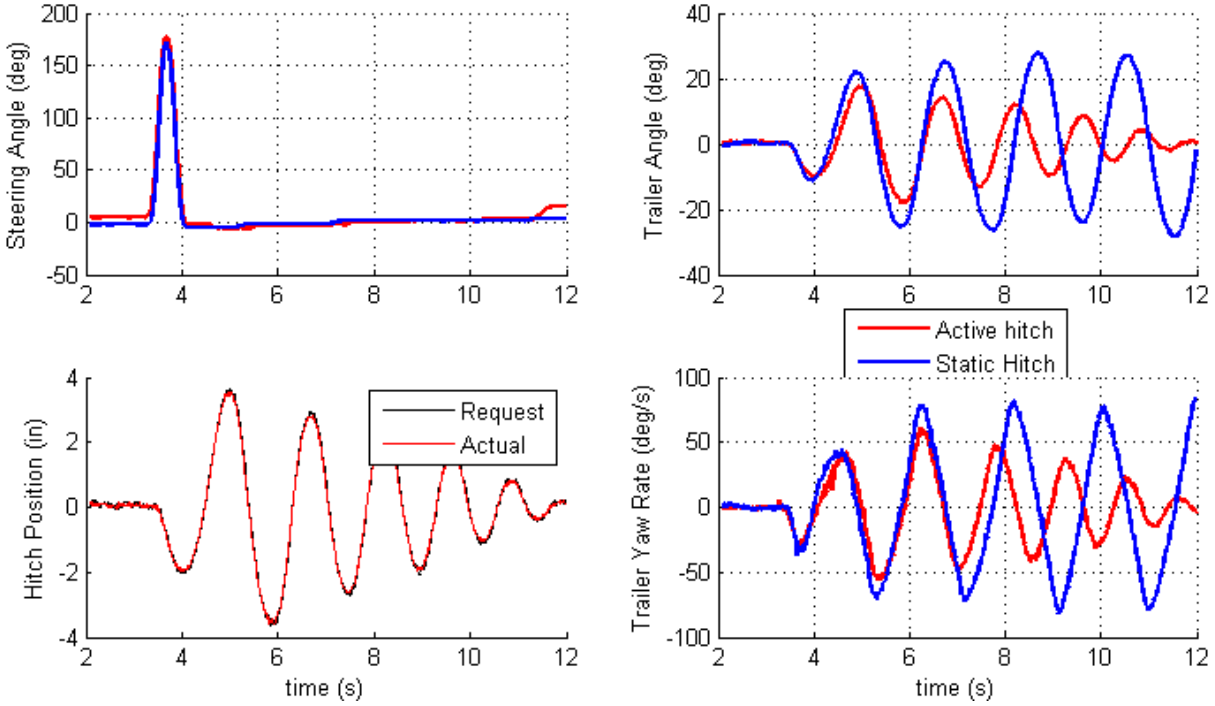

Figure 5.12: Steer impulse response with improved controller, 70km/h, K=0.2in/deg

The tracking error on the hitch is significantly lower, and the hitch does not experience stalling, despite the harsh maneuver. The improvements to the controller allow it to reduce sway with a lower required actuation effort.

For double lane change maneuvers, the starting speed of the vehicle was reduced to 45km/h due to the instability of the trailer configuration. Higher speeds caused jackknifing of the trailer and required the intervention of the trailer brake controller. At the speeds where jackknifing does not immediately occur, the active hitch produces improvements in the system response, as presented in Figure 5.13:

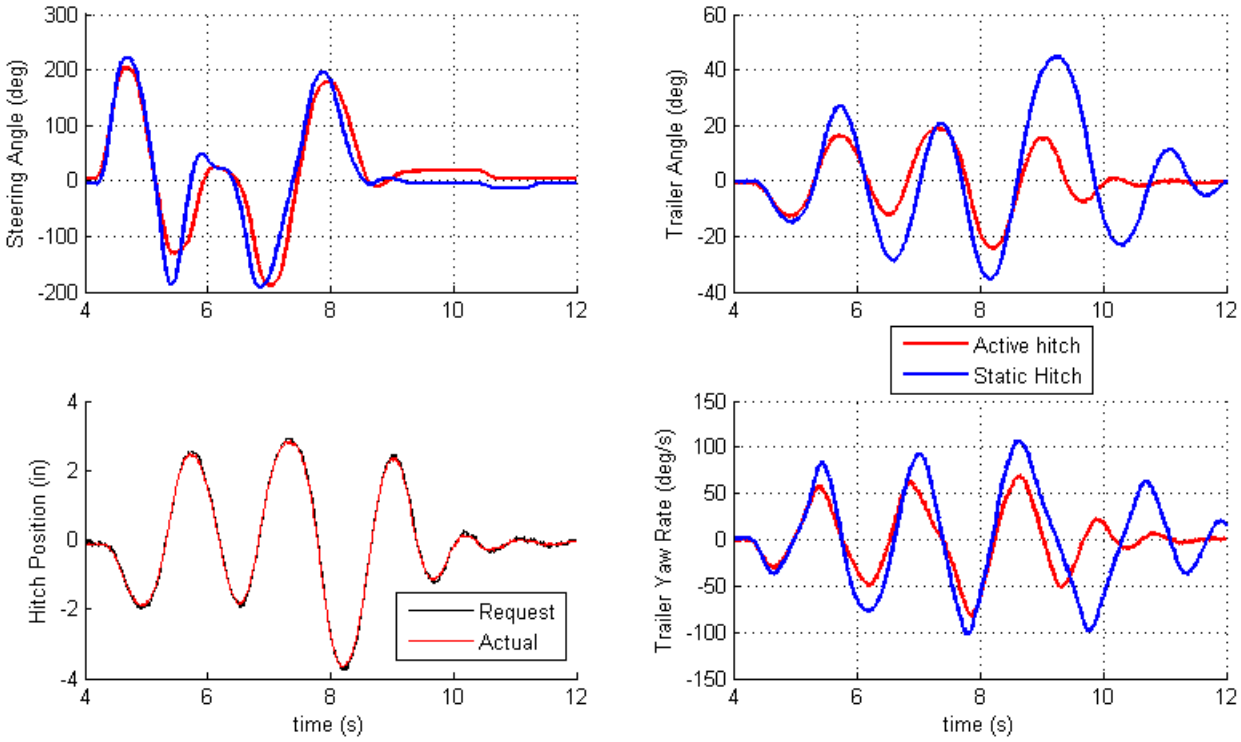

Figure 5.13: Double lane change at 45km/h, K=0.15in/deg

The feedback gain was reduced in proportion to the reduction in speed, as was recommended by the speed gain tuning study presented in section 3.2.6. By reducing the amplitude of oscillation at the start of the maneuver, the active hitch was able to prevent the large swing that occurred at 9 seconds in the open loop test. The test shows that even in the nonlinear region of the tires, the simple active hitch controller can improve stability so long as there are oscillations in the trailer angle.

A brake-in-turn maneuver was performed to test the limitations of the controller in high slip scenarios. At 45km/h, the trailer will have limited transient oscillations, but the unstable configuration will still create handling issues and potential for crashes. While entering a turn, the brakes are applied until the tires are nearly locked, which creates a combined slip condition that is detrimental to cornering forces.

The comparison between a static hitch and the active hitch response to the maneuver is presented below:

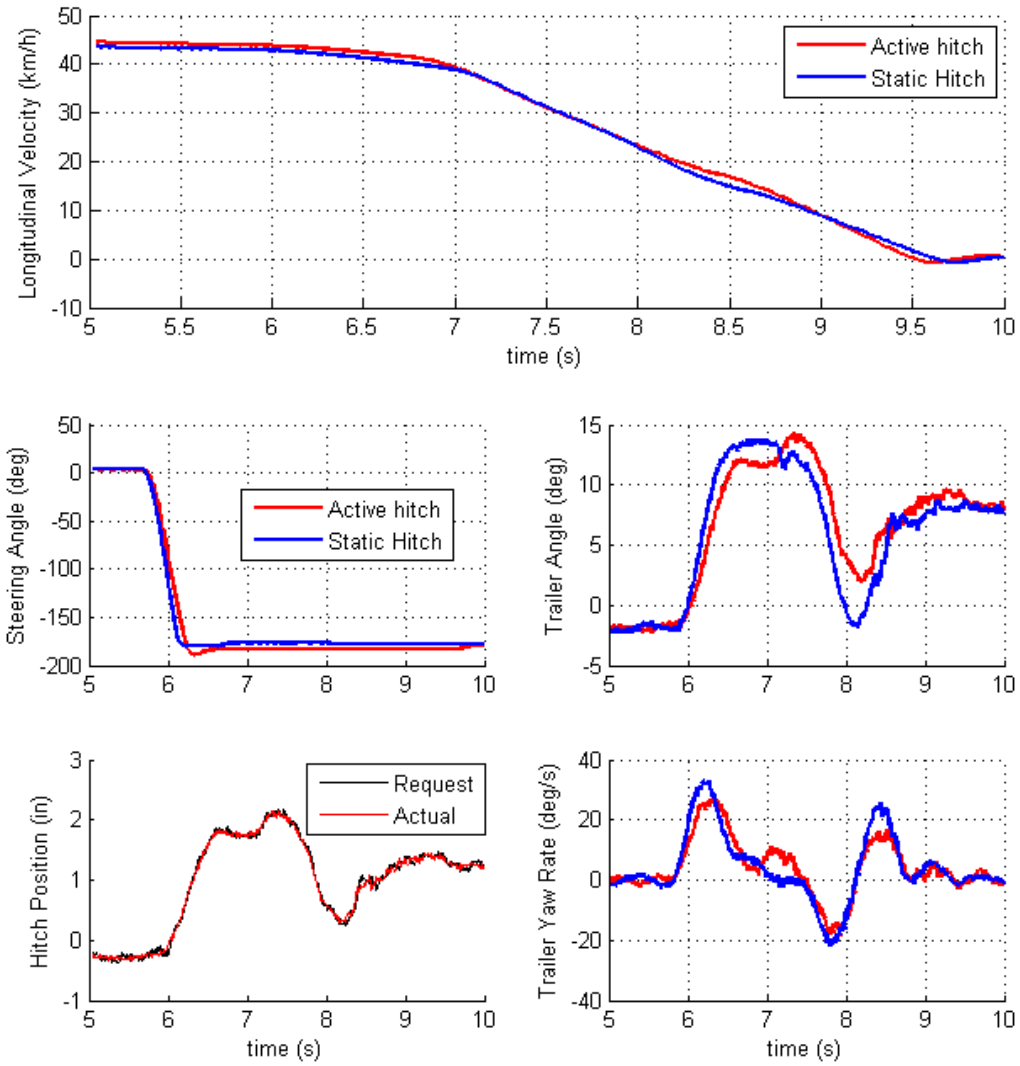

Figure 5.14: Brake in turn at 45km/h, 0.5g deceleration, K=0.15in/deg

There is a negligible difference between the open and closed loop tests. When attempting this test at higher speeds, the trailer very quickly jackknifed, putting it out of the useful range of the active hitch. The maneuver is limited by the size of the test track, where a more typical brake-in-

turn would involve traveling at highway speed and applying a much smaller steering step before applying brakes. MapleSim studies of this type or maneuver indicate that the active hitch can keep the trailer tires within their linear range, thereby providing enough lateral force that the vehicle can come to a stop. These results are analogous with the behavior of an active steering controller; the controllers can greatly reduce yaw instability with relatively small actuation, provided that the tires are not saturated with tractive forces or with high sideslip.

Conclusions and Recommendations

As demonstrated by testing of the prototype active hitch, it is possible to significantly reduce sway behavior in unstable trailer configurations. The effectiveness of the controller is limited by the linear working region of the trailer tires, which is typical of controllers that require tire lateral forces to apply yaw moments to the system. The control action is achieved using only kinematic measurement of the trailer angle relative to the tractor, although additional measurements could be used to assess the required control gains based on the trailer configuration. Even without extra measurements, the hitch controller is robust to changes in the tractor and trailer parameters, despite its simplicity.

The sway reduction can be achieved within a small physical envelope, and can be powered by auxiliary vehicle power at a roughly estimated average power consumption of 500W, which indicates its applicability as a commercial product. However, the current placement of the trailer yaw sensors are not ideal for versatile commercial use, and the use of a hydraulic power pack is not ideal for packaging. Initial research into purely electric versions of the active hitch indicate that a ball screw linear actuator may be able to replace the current hydraulic setup.

The dynamic model derived in chapter 3 was found to accurately predict the tractor-trailer system response when the slip angles of the trailer are reasonably low. When the linear region of the tires is exceeded, the dynamic model is still useful for predicting the effectiveness of the active hitch control action. The vehicle modules developed for use in MapleSim are effective at bridging the gap between the linear model and the actual system, accounting for nonlinearities in the tire lateral forces, weight transfer, driver responses, etc.

Future work

The following are the suggestions for next steps to take when reviewing or iterating the design of the active hitch prototype, as well as some areas for improvement.

As indicated by the small structural damage sustained in by the linkage arm, the current prototype is not suited for the original range of trailer sizes. For heavier tractor-trailer combinations, the structural design of the components should be revisited to ensure that the hitch is applicable for heavy-duty applications, which can be most easily attained by thickening the

sheet metal elements of the structure. The design of the power pack suggests that the current actuation system can handle increased loading, although the selection of a servo-type motor to drive the hydraulics may be better suited to consistent performance at higher loads. The finite element analysis performed on the structural elements only considered single loadings and impacts. Although all fasteners and bushing/bearing elements were rated well above the expected loading, a fatigue analysis on the pivot points should be considered.

For future research on trailer stability in the MVSL, it would be beneficial to modify the test trailer to accommodate a wider variety of tests. Specifically, the track width of the trailer could be increased without having to replace the majority of the trailer components. The current track width was chosen for transportability and rigidity. A wider trailer could be retrofit as a tow trailer for transporting vehicles to and from the test track, or could be used for situations where the roll dynamics of the trailer are more prominent, like an enclosed trailer experiencing sway behavior due to aerodynamic loads. Additionally, a wider track width would generate greater yaw moments from the trailer brake controller, so a wider trailer would be more useful in DYC research.

The majority of the testing of the active hitch occurred on dry pavement. Since low friction surfaces are detrimental to steering-type controllers, it would be beneficial to repeat the test maneuvers on wet ground or on sloped ground. At lower friction, the cornering stiffness of tires is approximately the same, but the linear working region is decreased. Since the controller can still provide stability in the nonlinear tire region, it is reasonable to assume that the controller is less effective on wet ground, but can still be useful.

Although it is out of the scope of this thesis, the active hitch design is amenable to assisting in backing up trailers at low speed as described in chapter 2. A simple backing controller for the active hitch was developed for straight line and constant radius backup. This controller was only successful in simulation, since the disturbances from an actual road hindered performance in testing. Future iterations of the backing controller should use heuristic rules and fuzzy inference based controllers, since they have seen the most success in literature.

References

[1] J. Darling, D. Tilley and B. Gao, "An experimental investigation of car-trailer high speed stability," *IMechE Part D: Journal of Automobile Engineering,* vol. 223, pp. 471-484, 2009.

[2] R. Jazar, Vehicle Dynamics: Theory and Applications, New York: Springer, 2008.

[3] A. Khajepour, S. Fallah and A. Goodarzi, Electric and Hybrid Vehicles Technologies, Modeling and Control: A Mechatronic Approach, West Sussex: Wiley, 2014.

[4] P. Falcone, F. Borrelli, J. Asgari, H. Tseng and D. Hrovat, "Predictive Active Steering Control for Autonomous Vehicle Systems," *IEEE TRANSACTIONS ON CONTROL SYSTEMS TECHNOLOGY,* vol. 15, no. 3, pp. 566-580, 2007.

[5] H. Pacejka, Tire and Vehicle Dynamics, Second Edition, Oxford: Butterworth-Hienemann, 2006.

[6] T. D. Gillespie, Fundamentals of Vehicle Dynamics, Warrendale, PA: Society of Automotive Engineers, 1992.

[7] J. R. Ellis, Vehicle Dynamics, London: Business Books Limited, 1969.

[8] A. Hac, D. Fulk and H. Chen, "Stability and Control Considerations of Vehicle-Trailer Combination," *SAE International Part J: Passenger Cars - Mechatronic Systems,* vol. 1, no. 1, pp. 925-937, 2008.

[9] A. Bostrom, "Rigid Body Dynamics," July 2012. [Online]. Available: http://www.am.chalmers.se/~paja/RBD/Handouts/Compendium.pdf.

[10] P. Nilsson and K. Tagesson, "Single-track models of an A-double heavy vehicle combination," Chalmers University of Technology, Goteborg, 2013.

[11] P. Fancher, "The Static Stability of Articulated Commercial Vehicles," *Vehicle System Dynamics,* vol. 14, no. 4-6, pp. 201-227, 1985.

[12] L. De Novellis and A. Sorniotto, "Direct yaw moment control actuated through electric drivetrains and friction brakes: Theoretical design and experimental assessment," *Mechatronics,* vol. 26, no. March 2015, pp. 1-15, 2015.

[13] C. Zong, T. Zhu, C. Wang and H. Liu, "Multi-objective Stability Control Algorithm of Heavy Tractor Semi-trailer Based on Differential Braking," *CHINESE JOURNAL OF MECHANICAL ENGINEERING,* vol. 25, no. 1, pp. 88-97, 2012.

[14] G. Fisher, R. Heyken and A. Trachter, "Active Stabilisation of the Car/Trailer Combination for the BMW X5," *ATZ Worldwide,* vol. 104, no. 4, pp. 7-10, 2002.

[15] A. Goodarzi, *class notes for ME 780,* Dept. of Mechanical Engineering, University of Waterloo, 2015.

[16] Hayes Towing Electronics, "Sway Master Electronic Sway Control," Hayes Towing Electronics, [Online]. Available: http://www.hayesbc.com/products/controllers/sway-master/.

[17] Curt Manufactuing, "Sway Control Units," Curt Manufacturing, 2015. [Online]. Available: https://www.curtmfg.com/masterlibrary/17200/installsheet/CM_17200_INS.PDF.

[18] F. Sorge, "On the sway stability improvement of car–caravan systems by articulated connections," *International Journal of Vehicle Mechanics and Mobility,* vol. 53, no. 9, pp. 1349-1372, 2015.

[19] A. Percy and I. Spark, "A numerical control algorithm for a B-double truck-trailer with steerable trailer wheels and active hitch angles," *IMechE,* vol. 226, no. D, pp. 289-300, 2011.

[20] A. Odhams, R. Roebuck and B. Jujnovich, "Active steering of a tractor–semi-trailer," *Institution of Mechanical Engineers, Part D: Journal of Automobile Engineering,* vol. 225, no. 7, pp. 847-869, 2011.

[21] S. C. Baslamish, I. E. Kose and G. Anlas, "Design of active steering and intelligent braking systems for road vehicle handling improvement: A robust control approach," in *2006 IEEE International Conference on Control Applications*, Munich, 2006.

[22] Y. Bin, T. Shim, N. Feng and D. Zhou, "Path Tracking Control for Backing-up Tractor-Trailer System via Model Predictive Control," in *24th Chinese Control and Descision Conference*, Taiyuan, China, 2012.

[23] H. Kinjo, M. Maeshiro, E. Uezato and T. Yamamoto, "Adaptive Genetic Algorithm Observer and its Application to a Trailer Truck Control System," in *SICE-ICASE International Joint Conference*, Bexco, Busan, Korea, 2006.

[24] G. Siamantas and S. Manesis, "Backing-up Fuzzy Control of a Truck-trailer Equipped with a Kingpin Sliding Mechanism," in *Artificial Intelligence Applications and Innovations III*, Boston, Springer, 2009, pp. 373-378.

[25] Ford Motor Company, "2017 F-150 Trailer Backup Assist QUICK START GUIDE," 2016. [Online]. Available: http://www.fordservicecontent.com/Ford_Content/Catalog/owner_information/2017-F150-TBA-QSG-Version-1_QG_EN-US_08_2016.pdf.

[26] N. T. K. a. G. N. D. S. Manesis, "On the Suppression of Off-tracking in Multi-articulated Vehicles through a Movable Junction Technique," *Journal of Intelligent and Robotic Systems,* vol. 37, pp. 399-414, 2003.

[27] H. Kinjo, M. Maeshiro, E. Uezato and T. Yamamoto, "Adaptive Genetic Algorithm Observer and its Application to a Trailer Truck Control System," in *SICE-ICASE International Joint Conference*, Bexco, Korea, 2006.

[28] M. Best, A. Newton and S. Tuplin, "The identifying extended Kalman filter: parametric system identification of a vehicle handling model," *Proceedings of the Institution of Mechanical Engineers, Part K: Journal of Multi-body Dynamics,* vol. 221, no. 1, pp. 87-98, 2007.

[29] M. Bolhasani and S. Azadi, "Parameter Estimation of Vehicle Handling Model Using Genetic Algorithm," *Scientia Iranica,* vol. 11, no. 1-2, pp. 121-127, 2004.

[30] J. Jordan, N. Hirsenkorn, F. Klanner and M. Kleinsteuber, "Vehicle Mass Estimation Based on Vehicle Vertical Dynamics Using a Multi-Model Filter," in *IEEE 17th International Conference on Intelligent Transportation Systems*, Qingdao, China, 2014.

[31] W. Kober and W. Hirschberg, "On-Board Payload Identification for Commercial Vehicles," in *IEEE International Conference on Mechatronics*, Budapest, 2006.

[32] P. Breedveld, "Elimination of time derivative of source inputs," 2005. [Online]. Available: doc.utwente.nl/75691/.

[33] T. Zhu and C. Zong, "Modelling and Active Safe Control of Heavy Tractor Semi-Trailer," in *2009 Second International Conference on Intelligent Computation Technology and Automation*, Changsha, 2009.

[34] "Chevrolet 2015 Equinox Options and Specifications," Chevrolet, 2015. [Online]. Available: http://www.gm.ca/gm/english/vehicles-2015/chevrolet/equinox/compare-options-and-specifications#mechanical.

[35] G. Heydinger, R. Bixel and W. Garrott, "Measured Vehicle Parameters - NHTSA's Data Through November 1998," *Society of Automotive Engineers, Inc.,* vol. 1, 1999.

[36] N. Nise, Control Systems Engineering, Sixth Edition, Jefferson City: Wiley, 2011.

[37] Z. Zhao, M. Tomizuka and S. Isaka, "Fuzzy gain scheduling of PID controllers," in *First IEEE Conference on Control Applications*, 1992.

[38] Mechanical Simulation, "CarSim," 2017. [Online]. Available: https://www.carsim.com/.

[39] MapleSoft, "MapleSim," 2017. [Online]. Available: http://www.maplesoft.com/products/maplesim/.

[40] E. Fiala, "Seitenkraefte am Rollenden Luftreifen," *VDI Zeitschrift,* vol. 96, 1954.

[41] "CURT Class 3 Trailer Hitch #13591," Curt Manufacturing, [Online]. Available: http://www.curtmfg.com/part/13591.

[42] Dassault Systems, "Solidworks Simulation Packages," Dassault Systems, 2017. [Online]. Available: http://www.solidworks.com/sw/products/simulation/packages.htm.

[43] M. Bauccio, ASM Metals Reference Book, Materials Park, OH: ASM International, 1993.

[44] F. Beer, E. R. Johnston, J. DeWolf and D. Mazurek, Mechanics of Materials, Sixth Edition, New York: McGraw-Hill, 2012.

[45] D. Hutton, Fundamentals of Finite Element Analysis, McGraw-Hill, 2004.

[46] A. Abel and H. Muir, "The nature of microyielding," *Acta Metallurgica,* vol. 21, no. 2, pp. 99-105, 1973.

[47] Delphi, "Non-Contact Rotary Position Sensor," [Online]. Available: http://www.delphi.com/manufacturers/auto/sensors/chassis/noncontact/.

[48] J. M. McCarthy, "UC Irvine Machine Theory: Four-Bar Linkage Analysis," [Online]. Available: https://synthetica.eng.uci.edu/mechanicaldesign101/McCarthyNotes-2.pdf.

[49] "Optima Yellowtop Deep Cycle Batteries," [Online]. Available: https://www.optimabatteries.com/en-us/yellowtop-deep-cycle-battery.

[50] "H-1500 Series High Pressure Cylinders," Cylinders & Valves, Inc, [Online]. Available: http://www.cylval.com/bore-high-pressure-cylinder-1500-series-clevis-mount-p-321-l-en.html?cPath=1_15_18.

[51] Danfoss, "OSPM Mini-Steering Unit," [Online].

[52] Stepper Online, "42HS59-6004S," [Online]. Available: http://www.omc-stepperonline.com/nema-42-cnc-stepper-motor-60a-22nm3115ozin-42hs596004s-p-174.html.

[53] "D116 12V Pump Motor," [Online]. Available: http://www.hydro-tek.com/product/power_park_parts.html.

[54] "32oz Piston Accumulator," [Online]. Available: https://www.mcmaster.com/#6716k42/=17wc283.

[55] I. Society of Automotive Engineers, "Recommended Practice for the Design of Tubing Installations for Aerospace and Fluid Power Systems," [Online]. Available: https://saemobilus.sae.org/content/arp994.

[56] "Cerka Online Trailer Parts," [Online]. Available: http://www.cerka.ca/.

[57] "Race Grade IMU Manual," [Online]. Available: http://racegrade.com/downloads/RG_SPEC-0027%20IMU%20V2.pdf.

[58] dSpace, "dSpace MicroAutoBox II Product Infiroamtion," [Online]. Available: https://www.dspace.com/shared/data/pdf/2017/dSPACE_MicroAutoBoxII_Product_information_03-2017_English.pdf.

[59] Oxford Technical Solutions, "RT2000 Family," [Online]. Available: http://www.oxts.com/products/rt2000-family/.

[60] C. Turner, "Slope Filtering: An FIR Approach to Linear Regression," *IEEE Signal Processing Magazine*, pp. 159-163, 2008.